SYNTHESIS OF CORNCOB BASED CARBON ACID CATALYST BY ARYLATION OF 4-BENZENEDIAZONIUM SULFONATE FOR BIODIESEL PRODUCTION

TANG ZO EE

MASTER OF ENGINEERING SCIENCE

LEE KONG CHIAN FACULTY OF ENGINEERING & SCIENCE
UNIVERSITI TUNKU ABDUL RAHMAN
JANUARY 2019

SYNTHESIS OF CORNCOB BASED CARBON ACID CATALYST BY ARYLATION OF 4-BENZENEDIAZONIUM SULFONATE FOR BIODIESEL PRODUCTION

By

TANG ZO EE

A dissertation submitted to the Department of Chemical Engineering,
Lee Kong Chian Faculty of Engineering & Science,
Universiti Tunku Abdul Rahman,
in partial fulfillment of the requirements for the degree of
Master of Engineering Science
January 2019

ABSTRACT

The utilisation of low cost feedstock such as palm fatty acid distillate (PFAD) in biodiesel product has significantly reduced the biodiesel raw material cost. Carbon acid catalyst that is low cost, non-toxic, biodegradable and highly reusable is able to convert the high free fatty acid (FFA) content in the low cost feedstock into biodiesel (FAME). In this study, corncob derived carbon acid catalyst was synthesised through arylation of 4-benzenediazonium sulfonate (4-BDS) sulfonation method and the synthesised catalyst was used in the esterification reaction of PFAD and methanol. SEM micrographs showed that the activated carbon (AC) had porous structure and the AC obtained had exhibited large BET surface area of 972.66 m^2/g. Besides that, EDX and FT-IR had confirmed the successful attachment of $–SO_3H$ groups onto the activated carbon. TGA result showed that the catalyst was thermally stable up to the temperature of 230 ˚C. The optimum catalyst synthesis condition obtained was at 900 ˚C carbonisation temperature, 1.5 hours sulfonation time and 11: 1 sulfanilic acid to AC weight ratio. The optimum catalyst, Cat_900h possessed the total acid density of 2.48 mmol/g and had achieved FAME yield of 72.09% and conversion of 93.49% in the esterification reaction. In addition, the optimum esterification reaction obtained from RSM was at reaction temperature 89.24 ˚C, reaction time of 6.48 hours, 11 wt.% catalyst loading and 21.94:1 methanol to oil molar ratio with maximum FAME yield of 83.48%. Kinetic studies had proven that the esterification reaction of PFAD and methanol in the presence of corncob based carbon acid catalyst followed the pseudo-homogeneous first order reaction model with activation energy of 23.36 kJ/mol.

ACKNOWLEGDEMENT

I would like to express my utmost gratitude to everyone who had contributed to the successful completion of this research. As the most important person, I would like to thank my research supervisor Dr. Steven Lim and co-supervisor Dr. Pang Yean Ling for their invaluable advice, guidance and their enormous patience throughout the development of the research.

Next, I would like to express my deepest thanks to University Tunku Abdul Rahman (UTAR) for providing scholarship and research funding (UTARRF/2017-CI/S06) for this project. In addition, I sincerely thanks to all Assistant Laboratory Managers of Department of Laboratory Management, Safety and Administration for the helping hand during my laboratory work.

Finally, I must express my very profound gratitude to my family for giving me unfailing support and encouragement throughout the years of my studies. Not to forget all my friends who had helped me unconditionally throughout the process of my research and thesis writing. This accomplishment would not have been possible without them. Thank you.

APPROVAL SHEET

This dissertation entitled "**SYNTHESIS OF CORNCOB BASED CARBON ACID CATALYST BY ARYLATION OF 4-BENZENEDIAZONIUM SULFONATE FOR BIODIESEL PRODUCTION**" was prepared by TANG ZO EE and submitted as partial fulfillment of the requirements for the degree of Master of Engineering Science at Universiti Tunku Abdul Rahman.

Approved by:

____
(Dr. STEVEN LIM) Date:…………………..
Assistant Professor/Supervisor
Department of Chemical Engineering
Lee Kong Chian Faculty of Engineering & Science
Universiti Tunku Abdul Rahman

____
(Dr. PANG YEAN LING) Date:…………………..
Assistant Professor/Co-supervisor
Department of Chemical Engineering
Lee Kong Chian Faculty of Engineering & Science
Universiti Tunku Abdul Rahman

LEE KONG CHIAN FACULTY OF ENGINEERING & SCIENCE

UNIVERSITI TUNKU ABDUL RAHMAN

Date: ________________

SUBMISSION OF FINAL YEAR PROJECT /DISSERTATION/THESIS

It is hereby certified that ***TANG ZO EE*** (ID No: ***16UEM06196***) has completed this dissertation entitled "_SYNTHESIS OF CORNCOB BASED CARBON ACID CATALYST BY ARYLATION OF 4-BENZENEDIAZONIUM SULFONATE FOR BIODIESEL PRODUCTION" under the supervision of Dr. STEVEN LIM (Supervisor) from the Department of Chemical Engineering, Lee Kong Chian Faculty of Engineering & Science , and Dr. PANG YEAN LING (Co-Supervisor) from the Department of Chemical Engineering, Lee Kong Chian Faculty of Engineering & Science.

I understand that University will upload softcopy of my dissertation in pdf format into UTAR Institutional Repository, which may be made accessible to UTAR community and public.

Yours truly,

____
(*TANG ZO EE*)

DECLARATION

I hereby declare that the dissertation is based on my original work except for quotations and citations which have been duly acknowledged. I also declare that it has not been previously or concurrently submitted for any other degree at UTAR or other institutions.

Name TANG ZO EE

Date 1st JANUARY 2019

TABLE OF CONTENTS

LIST OF TABLES

LIST OF FIGURES

Figure **Page**

LIST OF ABBREVIATIONS

AC	Activated Carbon
AV	Acid Value
BET	Brunauer-Emmet-Teller
EDX	Energy Dispersive X-ray
FAME	Fatty Acid Methyl Esters
FFA	Free Fatty Acid
FT-IR	Fourier-transform Infrared
GC-FID	Gas Chromatography – Flame Ionisation Detector
PFAD	Palm Fatty Acid Distillate
SEM	Scanning Electron Microscope
TG	Triglyceride
TGA	Thermogravimetric Analysis
XRD	X-ray Diffractometer
4-BDS	4-Benzenediazonium Sulfonate

LIST OF APPENDICES

CHAPTER 1

INTRODUCTION

1.1 World Energy Overview

Energy is essential and necessary for human to perform work in their daily life. It is originally existed in the form of motion, gravitational, light, sound, chemical, thermal and electrical. Since 2014, world energy consumption has increased by 1 % every year (B.P., 2017). However, the increment of energy consumption does not solely due to the increase of population. The main factor which drives the current trend is the development of world economy especially in China and India since they had recorded energy consumption increment of 1.6 % and 5.4 % in their respective country (B.P., 2017). By 2040, it is estimated that world energy consumption will increase by 28% compare to 2015 (EIA, 2017a).

As shown in Figure 1.1, industrial, buildings, transportation and residential are the four main energy end-use sectors. In 2017, industrial sector contributes the highest energy consumption at 32% among all the other sectors, followed by 29% of energy consumption by transportation sector (EIA, 2017b). Although industrial sector consumed the most energy, it was predicted that the energy demand in transportation sector will grow faster at 1 %/year than the industrial sector at 0.7 %/year in the next 35 years (EIA, 2017a).

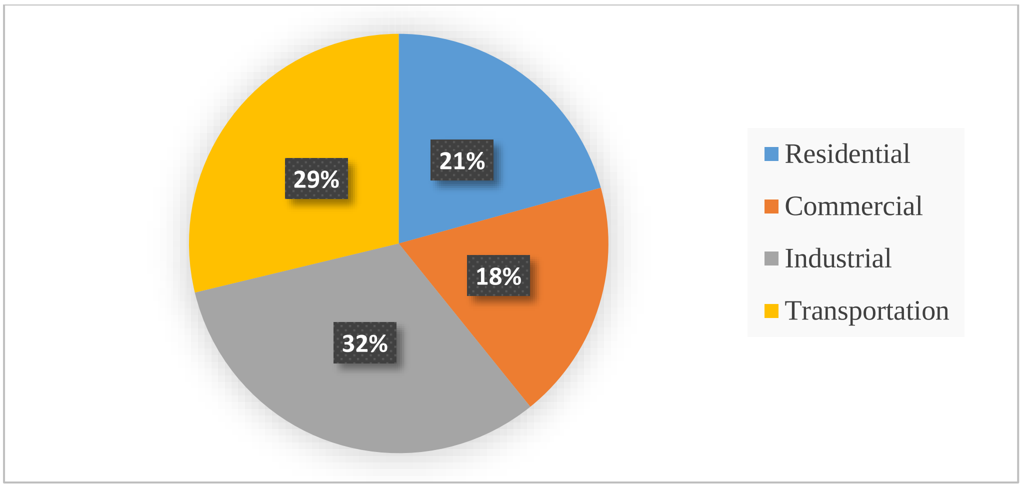

Figure 1.1: World energy consumption by sector in 2017 (EIA, 2017b).

Energy can be obtained from either renewable or non-renewable sources. Renewable energy is defined as infinite source of energy that can be harnessed and will replenish rapidly within reasonable human timescale. Currently, renewable energies such as hydro power, solar energy technology, wind energy technology, geothermal energy, biomass conversion and many more are developing rapidly. On the other hand, non-renewable energy cannot be replenished at sufficient rate to compensate the consumption demand. Nuclear fuels and fossil fuels such as coal, petroleum and natural gas are examples of non-renewable fuels.

Majority of energy sources in transportation sector are dependent on non-renewable petroleum and natural gas as they produce high amount of energy through simple combustion. According to EIA (2017a), about 92.63% of energy consumed by transportation sector is sourced from petroleum. The invention of combustion engine vehicles had led to high amount of petroleum consumption daily and it had become the main pillar of the industry sectors especially in developing countries' economics.

However, the usage of non-renewable energy such as fossil fuels is facing two major problems. Combustion of fossil fuels will lead to the emission of greenhouse gases (GHG) and other harmful gases leading to global warming and health threatening. It was reported that transportation sector accounts for about 18% of the anthropogenic GHG emission (Bilgen, 2014).

In addition, continuous usage of non-renewable energy is causing the rapid depletion of the fossil fuels. B.P. (2017) had reported that the world oil reserves could only be sustained for another 50.6 years where oil reserves represents the oil remaining in all the discovered oil reservoir. Although there are possibilities for undiscovered oil reservoirs in the Arctic, the drilling of oil still remains a big challenge due to high cost incurred, unpredictable weather conditions and disruption of ecosystem.

Figure 1.2 shows that the renewable energy consumption at different regions had gradually increased from 1996 to 2016. In 2016, the usage of renewable energy (excluding hydro energy) in power generation has risen by 14.1% (B.P., 2017). Biofuels is considered as a renewable energy as it can be regenerated in a short time frame. Nevertheless, the amount of carbon dioxide produced can be compensated by the carbon dioxide intake by plants for photosynthesis, resulting in net zero production of carbon dioxide.

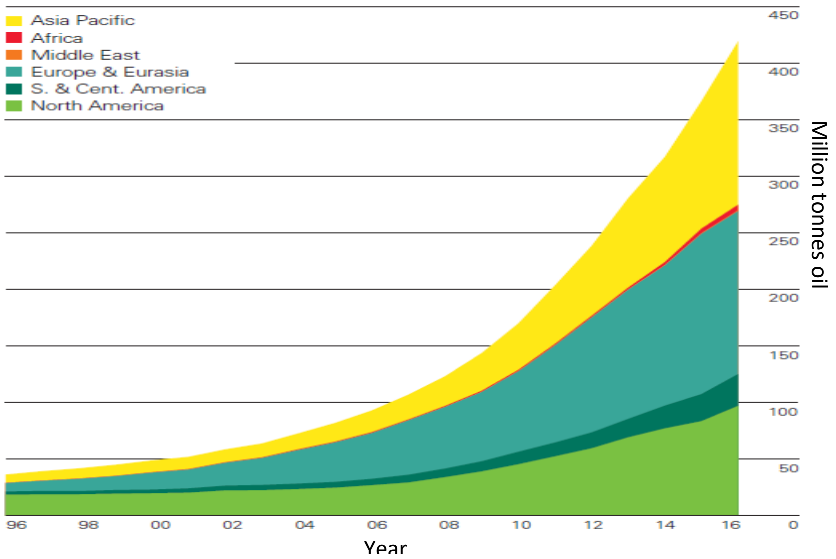

Figure 1.2: Renewable energy consumption at different region (B.P., 2017).

1.2 Biofuels

Combustible fuels that are derived from biomass such as agricultural waste and animal dung are known as biofuels. One of the main differences between biofuels and fossil fuels is that fossil fuels are formed through the geological process that requires hundred over millions of years. In contrary, biofuels source can be obtained through biological processes such as agriculture or reproduction which take a shorter time to be regenerated.

Biofuels can be categorised into primary and secondary biofuels. Primary biofuel can be used directly in raw form such as fuelwood and municipal waste. On the other hand, secondary biofuels are fuels that have been processed from primary biofuels, for example, bioethanol, biodiesel and biogas. Biofuels can be separated into solid, liquid and gaseous biofuel according to their phase.

Liquid biofuel is the secondary biofuel that is derived from organic matter through several different reactions. Biodiesel and bioethanol are the two most common liquid biofuels in the biofuel industry to serve as the transportation fuels. Compared to solid biofuel and biogas, liquid biofuels has a more dominant market share and focused in a number of large industries. United States and Brazil had dominated the liquid biofuel production at 46% and 24% of 2015 global production respectively. During that year, bioethanol occupied 74% of the global biofuels production, 22% for biodiesel and the remaining 4% was contributed by the hydrotreated vegetable oil (HVO) (REN21, 2016).

Liquid biofuels have gained the most attention due to their potential in replacing fossil fuels in the transportation sector. The evolution of first to fourth generation of biofuels is to find cost effective solutions to resolve the problems associated with biofuel production in order to expand biofuel industry in the future market. Since secondary biofuel is converted directly from the raw solid biomass, the types of biomass used will play an important role in determining the future development of the biofuels. The main difference between the first to fourth generations of biofuel depends on the different sources of biomass feed used for biofuel production (Alaswad et al., 2015).

First generation biofuel is produced by using mainly edible food crops. Most of the current biofuel industry produces the first generation biofuels by using food crops such as palm oil in Malaysia, corn in United States, rapeseed oil in Germany and sugarcane in Brazil. However, the utilisation of edible food crops as the feedstock for biofuel production has led to the food vs. fuel competition which resulting in the increment of food price. On the other hand, their biofuel production also incurred high production cost without considering the subsidies from government. Their limited reduction rate render this generation of biofuels an expensive way to reduce the GHG (Bioenergy, 2008).

Next, second generation biofuel is able to resolve the food versus fuel competition problem which occurs in first generation biofuels by employing non-edible biomass or biomass waste as the feedstock such as agricultural waste, forest residue, non-edible energy crops and industrial by-product for biofuels production. These biofuels are also known as the advanced biofuels. Energy crops are non-edible specialty crops that are planted for the purpose of energy production and can be planted on semi-arable land while still achieving higher energy and oil yield compare to food crops. However, the production cost still remains relatively high as the oil yield can hardly be maintained without adequate amount of nutrient replenished at the same land in long run (Sims et al., 2010).

Third generation biofuel derived its feedstock mainly from marine or aqua biomass such as microalgae and seaweed that has very high growth rate. The usage of marine biomass is able to mitigate the food and land competition problems in second generation biofuel. However, cultivation and harvesting of marine biomass such as microalgae is energy intensive while extraction of biofuels from the biomass is also challenging (Dutta et al., 2014; Alaswad et al., 2015).

As for fourth generation biofuel, it uses similar biomass feedstock as the third generation biofuel which are marine biomass and also microbes. Fourth generation biofuel focuses on the metabolic engineering and genetic modification of the marine biomass to improve their carbon dioxide sequestration abilities, increase oil content in the algae and also to boost up the growth rate. Although fourth generation biofuel requires high investment cost and is still at the initial research stage, it has a high potential to be developed as a sustainable and clean energy. (Dutta et al., 2014).

As mentioned previously, bioethanol is one of the most common liquid biofuels which consisted of 74% of the total production in 2015. It is usually produced from biomass feedstock with high sugar content such as starch and sugarcane through fermentation of simple sugar materials. However, other complex biomass material require to be broken down into fermentable sugars first before undergo fermentation process to produce bioethanol. Therefore, bioethanol production process usually involves pre-treatment, hydrolysis to form simple sugar and lastly fermentation. Bioethanol can be blended with gasoline in transportation vehicle to improve combustion performance and to reduce emission of carbon monoxide (Mohd Azhar et al., 2017).

Besides bioethanol, biodiesel is the second largest biofuel which accounts for 22% of the total liquid biofuels produced in 2015. Commonly, biodiesel can be produced through transesterification of vegetable oil or animal fat in the presence of alcohol. In transportation sector, biodiesel is usually mixed with conventional fossil fuels derived diesel to reduce carbon monoxide emissions. On the other hand, it was reported that biodiesel yields 93% more net energy output over energy input for its production life cycle (Hill et al., 2006).

1.3 Biodiesel

Diesel is a well-known fuel that is being used every day especially in trucks, cars or other diesel engine powered vehicles. Petroleum diesel is one of the most common types of diesel that is derived from petroleum. In contrary, biodiesel, also known as fatty acid methyl ester (FAME), is a non-petroleum based diesel which can be obtained from vegetable oil or animal fats. It is the esters of vegetable oil that consist of long chain alkyl esters produced from chemical reaction with alcohol such as methanol. In addition, biodiesel is a renewable fuel energy with continuous supply and high sustainability. These render it to passes the largest advantage over non-renewable petroleum diesel that is facing the depletion crisis.

Diesel engine, which is also known as compression-ignition engine was invented by a German inventor, Dr. Rudolf Diesel in year 1890s. It was powered by self-ignition of fuel at elevated temperature and pressure conditions. Originally, the diesel engine designed to be powered by coal dust and was later tested by Dr. Rudolf with other fuel types including vegetable oil. Later in 1920s, several literatures had reported the application of vegetable oil in the diesel engine and found that the high viscosity of vegetable oil had brought several operating problems such as development of engine deposit. In 1980s, the first reported usage of vegetable oil esters on the diesel engine was able to resolve the operational issue associated with the high viscosity of vegetable oil. However, it was noted that transesterification of vegetable oil to produce alkyl esters had started in year 1853 long before the invention of diesel engine (Knothe and Razon, 2017).

In 20th century, massive refinery of crude oil to petroleum had left with excess distillate which could serve as an excellent fuel for the compression ignition engine. This distillate is later known as diesel. Although petroleum derived diesel is more favourable in the current transportation sector, its supply is still finite. Biodiesel as a potential alternative has numerous advantages over the non-renewable petroleum based diesel. Biodiesel is produced from non-toxic renewable sources such as biomass, it is able to reduced emission of hazardous gases, has high flash point at 150 – 180 ºC which renders safer handling and storage, miscible with petroleum based diesel at all blend ratios and also compatible with the current energy infrastructure (Saluja et al., 2016; Knothe and Razon, 2017)

In 2016, global biodiesel production has risen by 6.5% since 2006 (B.P., 2017). This shows that the demand of biodiesel in the world has been gradually increasing and leaving a big potential for further expansion of biodiesel industry. Currently, Costa Rica has the highest biodiesel blend mandates of B20 where 20% of biodiesel is blended into 80% of petroleum diesel to be used in ignition-compression engine powered vehicles. On the other hand, Brazil has also implemented B7 mandates and this has stimulated the demand for biodiesel.

Other countries such as South African and Philippines are running on the B5 biodiesel blend mandates, which helps to expand the biodiesel market (REN21, 2016).

In Malaysia, the pioneer biodiesel production plant was established in 2006 by Malaysia Palm Oil Board (MPOB) to produce palm oil derived biodiesel. As shown in Figure 1.3 the supply and demand of biodiesel had gradually increased over the year. During the initial stage, the biodiesel produced in Malaysia was usually exported out to other countries in Asia, Europe and United States to support B5 biodiesel blend mandates in those countries. Locally, biodiesel blend only started to ramp up in 2011 at 1.3% blend and was only available in Selangor and Negeri Sembilan states. The availability of biodiesel was then spread to Melaka and Johor states at 2.0% of biodiesel blend. Later in 2014, B5 biodiesel blend was available nationwide in Malaysia and B7 was then implemented in 2015 (Wahab, 2016). The implementation of B7 mandate in Malaysia has led to a leap in the biodiesel production by 40% due to the increase of demand (REN21, 2016).

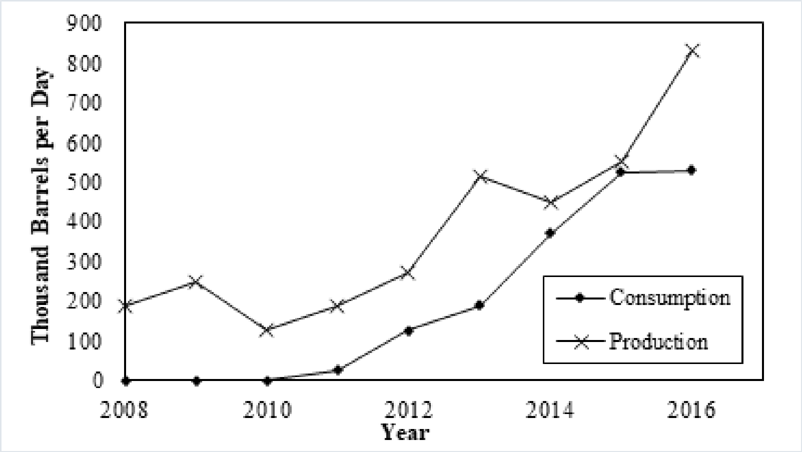

Figure 1.3: Production and consumption of biodiesel in Malaysia (Wahab, 2016).

1.4 Production Pathways of Biodiesel

The usage of high viscosity vegetable oil in the diesel engine can cause operational problems and damage to the engine. Therefore, upgrading of vegetable oil into high quality biofuel such as biodiesel is necessary to improve the functionality of biodiesel in diesel engine. The production of biodiesel can be carried out in several different pathways, for example, direct use or blending, micro-emulsion, thermal or catalytic cracking and transesterification. Table 1.1 listed several the merits and demerits of the different biodiesel production pathways.

Table 1.1: Comparison of various biodiesel production pathways.

Routes	Advantages	Disadvantages
Direct use/ Blending	• Reduce viscosity • Phase separation easily occur	• Coke formation • Carbon deposit • Gelling of lubricant oil
Micro-emulsion Process	• Reduce viscosity • Fuel with reduced emissions	• Deposit of heavy carbon • Increase lubricant oil viscosity • Fuel release lower energy
Thermal/ Catalytic Cracking (Pyrolysis)	• Lower cloud point • Product has similar chemical properties with diesel	• Expensive processing equipment • Require distillation equipment
Transesterification	• Fuel has higher combustion efficiency	• Long reaction time • Require high heat energy • Require purification step

In the early research stage on the diesel engine fuel, direct usage of vegetable oil without any prior modification has been investigated. It was discovered that vegetable oil has high viscosity and thus not suitable to be used directly. However, diesel engine can be operated for short term by using vegetable oil blends with petroleum diesel in the ratio of 1:10 or 1:20 to reduce the viscosity (Gashaw et al., 2015).

On the other hand, investigation of micro-emulsion process had been carried out since 1980-1990s. This is a process where non-polar oil and polar phase solvents are mixed together with the aid of non-ionic or ionic amphiphile surface agent. Surface agent, or also known as surfactant and co-surfactants helps in reducing the interfacial tension between two non-miscible phases of oil and polar liquid. (Arpornpong et al., 2014; Bora et al., 2016).

Furthermore, thermal cracking is the application of heat treatment towards long chain saturated substance, for example, biomass and vegetable oil in an inert environment to chemically modify the structure to form shorter chain compound in solid, liquid and gaseous form. Cracking process consisted of two consecutive stages namely the primary and secondary stage. For primary stage, the C-O bond of the triglycerides compound in the vegetable oil will be broken down into short chain acid species. During the secondary stage, the acid compounds will be further degraded to form biofuel with similar properties with the petroleum diesel (Prado and Antoniosi Filho, 2009).

As for transesterification, it is the most common biodiesel production pathway adopted by the industry. It is the reaction between vegetable oil and alcohol (usually methanol) at above room temperature to form esters (biodiesel) and glycerol as the by-product. Transesterification can either be carried out in the presence of acidic or basic catalyst at lower temperature or without the presence of catalyst at higher temperature and pressure. This process will be further discussed in Chapter 2.

1.5 Problem Statement

In most of the current biodiesel production industry, homogeneous base catalysed transesterification reaction was employed to produce biodiesel. However, the base catalysed transesterification process usually requires the usage of high quality refined oil with low free fatty acid (FFA) content as the oil feedstock to avoid saponification between FFA and base catalyst and this has incurred high raw material cost in the production.

In addition, the usage of homogeneous catalyst has also created separation problem since the final product appears in the same phase with the catalyst. In order to remove the catalyst from the final product, washing of the final product is required and this will generate a large amount of waste water which requires extra treatment process. Since the homogeneous catalyst will be washed off from the product, it then cannot be reused after reaction.

In this case, heterogeneous acid catalyst is a promising catalyst for the biodiesel production process. The utilisation of heterogeneous catalyst in biodiesel production is still under intensive research. The catalytic activity, reusability and the reaction kinetics of the catalyst are the main focus of the researchers as these are the key factors to commercialise the catalyst in biodiesel production industry in the future.

Biomass derived heterogeneous acid catalyst is able to outperform other commercial heterogeneous catalysts due to its sustainable framework and ability to add higher values to the low value waste. Nevertheless, the feasibility of different sources of biomass for the synthesis of catalyst varied with the types of biomass used. It also has a close relationship with the synthesizing method and the conditions of synthesis process. In addition, the operating conditions in biodiesel production reaction may also vary with the types of catalyst used. Therefore, more researches should be conducted to study the suitability of the selected biomass to be synthesised as the catalyst and also to find out the optimum operating conditions for this catalyst.

1.6 Scope of Study

In this study, corncob waste was chosen as the raw material to synthesise the carbon support for the biomass based heterogeneous acid catalyst. Plantation of corn as food crop is one of the main agricultural activities in Malaysia. However, the harvesters are only interested on the edible corn kernels. The left over biomass such as corncob after the extraction of corn kernel are usually disposed as waste. Therefore, corncob waste was selected as the raw material for catalyst synthesis in this study as this was able to fully utilise the waste by converting it into high value product.

This catalyst was synthesised by carbonisation of corncob followed by sulfonation through arylation of 4-benzenediazonium sulfonate (4-BDS). During the catalyst synthesising process, the parameters of carbonisation and sulfonation were varied to study the effects towards the performance of the catalyst based on their catalytic activity in transesterification and esterification reaction for the biodiesel production by using palm fatty acid distillate (PFAD), a by-product from palm oil refinery as the feedstock. The optimum operating conditions for biodiesel production were also investigated.

Catalyst characterisation was subsequently carried out to study the physical and chemical properties of the catalyst synthesised. In addition, the synthesised catalyst with optimised synthesising condition was subjected to the study of biodiesel production operating conditions by using the Response Surface Methodology (RSM). The reusability of the catalyst will also be investigated. Lastly, reaction kinetics of the biodiesel production reaction by using the synthesised catalyst were also postulated.

1.7 Research Objective

This research project focuses on discovering better alternative of fuels for the future transportation sector by aiming to discover a simple and cost effective biodiesel production pathway. The objectives of this study include:

a. To synthesise and characterise corncob based carbon acid catalyst through arylation of 4-benzenediazonium sulfonate.
b. To study the effect of catalysts synthesising condition towards the FAME yield and FFA conversion.
c. To investigate the effect of esterification reaction parameters for biodiesel production employing the self-synthesised catalyst synthesised by using Response Surface Methodology.
d. To study the reusability of catalyst and the reaction kinetics of the catalytic esterification reaction.

CHAPTER 2

LITERATURE REVIEW

2.1 Transesterification and Esterification for Biodiesel Production

In biodiesel production process, transesterification can be defined as the reversible reaction between alcohol (usually methanol) and triglycerides (TGs) in vegetable oil and animal fats in the presence of homogeneous or heterogeneous base catalyst to form FAME and glycerol as the by-product. Figure 2.1 shows the overall and three-step transesterification reaction pathways. In the first stage, triglyceride will react with alcohol to form diglyceride and one mole of ester followed by the reaction of diglyceride and alcohol to form monoglyceride and another one mole of ester. At the third step, monoglyceride will continue to react with alcohol to form glycerol and one mole of ester. In overall, one mole of triglyceride will react with three moles of methanol to form three moles of esters and one mole of glycerol.

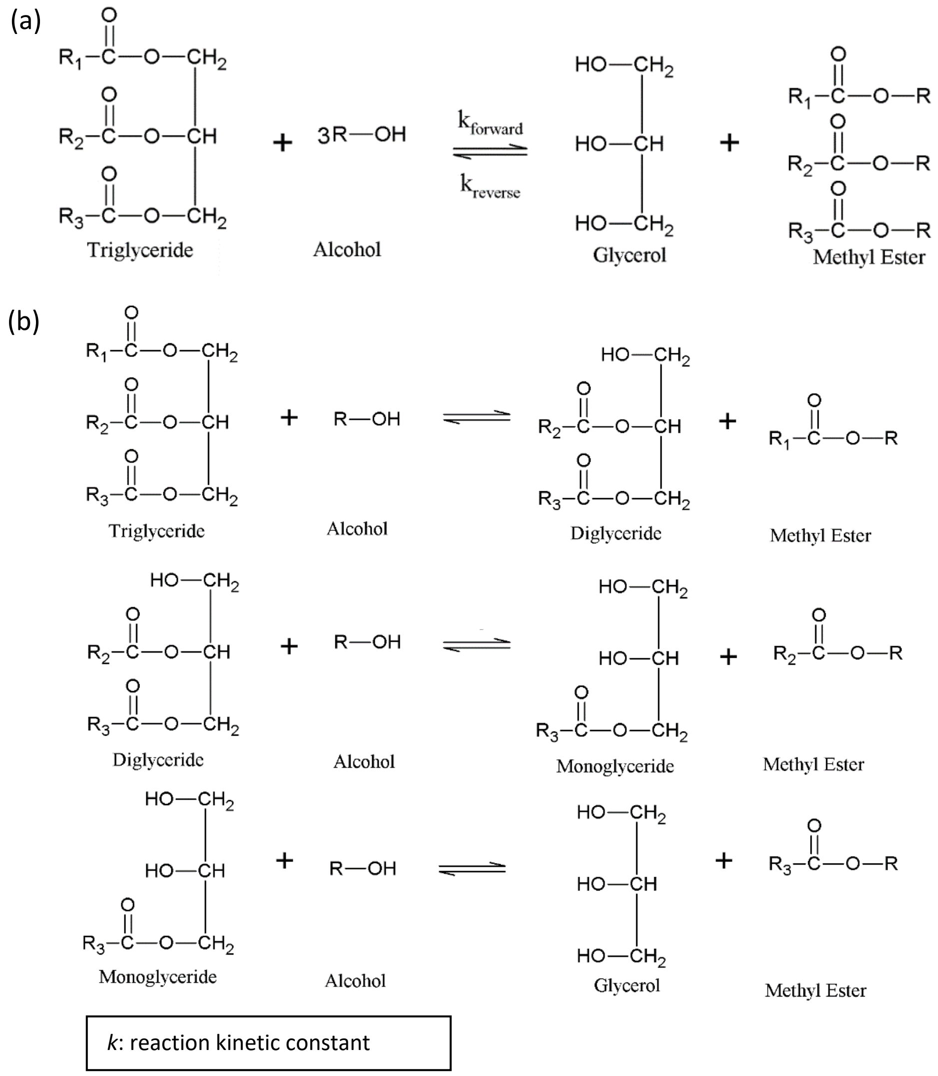

Figure 2.1: (a) Overall (b) Three-step transesterification reaction of triglyceride and alcohol.

Commercialised homogeneous base catalysts such as NaOH and KOH are commonly used in the current biodiesel production industry. Base catalyst is being used extensively in the industry because base catalysed transesterification reaction has higher catalytic activity, requires milder reaction conditions and lower operating cost. However, expansion of biodiesel industry still remains extremely slow due to the high feedstock cost. The oil feedstock of the raw material for biodiesel production can contribute up to 70% of the total production cost and this has become one of the major obstacles hindering the commercialisation of biodiesel industry (Dehkhoda and Ellis, 2013). Base catalysed transesterification reaction requires the usage of expensive refined oil as the feedstock with less than 1% of FFA (Zhou et al., 2016). The FFA content presents in oil composes of different acid compositions as shown in Table 2.1 that have the potential to be used in biodiesel production. The presence of FFA can cause saponification when base catalyst reacts with FFA leading to the following consequences:

i. Formation of soap and water that will deactivate the catalyst
ii. Water hydrolyses triglyceride to form more FFAs
iii. Soap hinders the reaction and reduces biodiesel yield
iv. Amount of catalyst required increases which contributes to the increment of production cost.

Table 2.1: FFA composition in different types of oil. (Robles et al., 2009)

Plant Oil and Fats	**Free Fatty Acid (FFA) Composition, % by weight**						
	Lauric 12:00	**Myristic 14:00**	**Palmitic 16:00**	**Stearic 18:00**	**Oleic 18:1**	**Linoleic 18:2**	**Linolenic 18:3**
Soybean	0.1	0.1	10.2	3.7	22.8	53.7	8.6
Cottonseed	0.1	0.7	20.1	2.6	19.2	55.2	0.6
Palm	0.1	1.0	42.8	4.5	40.5	10.1	0.2
Lard	0.1	1.4	23.6	14.2	44.2	10.7	0.4
Tallow	0.1	2.8	23.3	19.4	42.4	2.9	0.9
J. curcas	0.0	0.0	12.8	6.2	35.58	45.4	0.0

The utilisation of unrefined plant oil or wastes oil as feedstock to produce biodiesel is more favourable since they have lower cost. This is able to mitigate the extremely high production cost incurred by the usage of expensive refined oil feedstock. Therefore, esterification reaction was introduced whereby the FFA content in the feedstock will react with alcohol in the presence of acid catalyst to form esters and water as shown in Figure 2.2. In a two-stage biodiesel production process, esterification will first be carried out to eliminate the FFA content in the feedstock prior to base catalysed transesterification. However, two-step production requires higher operating cost and larger product loss due to the multiple processing stages (Ayodele and Dawodu, 2014). Therefore, several researchers had demonstrated simultaneous esterification and transesterification reaction at higher temperature (>60 ºC) as a more straightforward one-step production (Lien et al., 2010; Dehkhoda and Ellis, 2013).

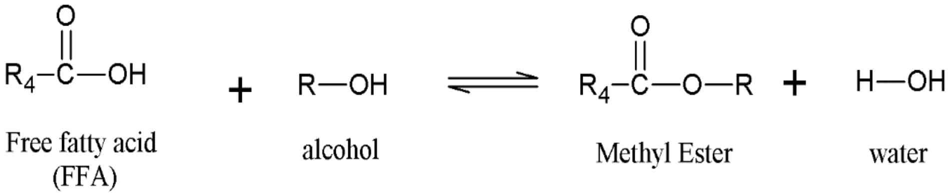

Figure 2.2: Esterification reaction of FFA and alcohol.

2.2 Catalytic Biodiesel Production Process

There were numerous types of catalyst that have been investigated for the biodiesel production reactions such as transesterification and esterification reaction. These include the homogeneous base catalyst, heterogeneous base catalyst, homogeneous acid catalyst and heterogeneous acid catalyst and also the enzymatic catalyst. Compared to homogeneous catalysts, heterogeneous catalysts and enzymatic catalysts are more favourable due to the ease of separation after reaction and have better reusability characteristic. The application of these catalysts on biodiesel production will be discussed in Section 2.2.1 to 2.2.3.

2.2.1 Heterogeneous Base Catalyst

Transesterification in the presence of base catalyst is the most common biodiesel production method. In a three-step transesterification, one mole of ester will form in each step when one mole methanol reacts with one mole of triglyceride in the first step, diglyceride in the second step and monoglyceride in the third step. Figure 2.3 shows the reaction mechanism of base catalysed transesterification reaction to produce esters (biodiesel). Initially, the hydroxyl ions of base catalyst will react with the –OH group of alcohol, forming strong nucleophiles alkoxide ions, RO^- in step (1). It then follows by the attack of alkoxide ions towards the carbonyl group of triglycerides to form a tetrahedral intermediate in step (2). In step (3), the breakdown of tetrahedral intermediate occurs and one mole of ester will be formed. At the last stage of the reaction in step (4), the catalyst will be regenerated and formed diglycerides. This process will then be repeated with the attack of alkoxide to diglyceride and monoglyceride to form the remaining two moles of esters (Lotero et al., 2005).

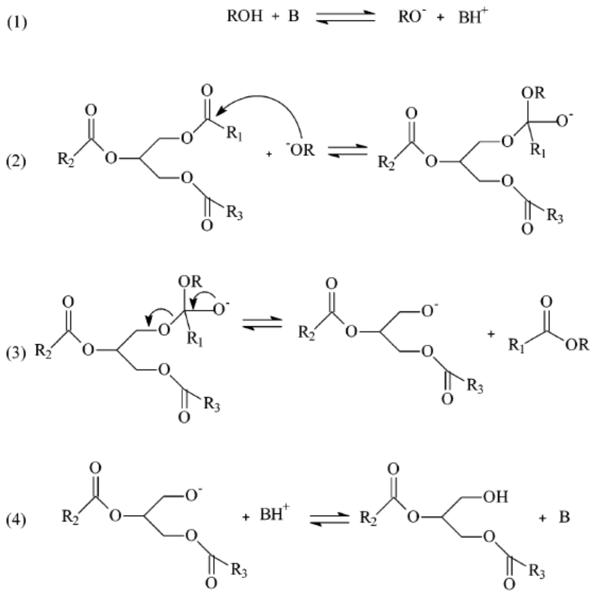

B: base catalyst

R$_1$, R$_2$, R$_3$: carbon chain of fatty acid

R: alkyl group of alcohol (normally CH$_3$)

Figure 2.3: Esterification reaction of FFA and alcohol (Lotero et al., 2005).

Easy separation, high reusability and non-corrosive are the main highlights of heterogeneous base catalyst compared to homogeneous catalyst. Metal oxides such as calcium oxide (CaO) are the most common and widely studied heterogeneous catalyst at the early development stage of heterogeneous base catalysed transesterification to produce biodiesel. Liu et al. (2008b) had successfully demonstrated transesterification reaction catalysed by CaO with biodiesel yield more than 95% at 65 ºC for 1.5 hour with 12:1 methanol to oil molar ratio at 8 wt.% catalyst loading. On the other hand, Zhu et al. (2006) had reported on an enhanced CaO catalyst known as solid super base which was synthesised by dipping CaO into ammonium carbonate solution followed by calcination. Zinc oxide (ZnO), was also being studied and has been proven to be a metal oxide catalyst that provides good performance in transesterification. ZnO was prepared by the calcination of zinc hydroxide at 800 ºC and gave biodiesel yield of 95% at the transesterification of rapeseed oil and supercritical methanol at 250 ºC, 105 bar for 10 minutes at 1.0 wt.% catalyst loading (Yoo et al., 2010).

Lately, researchers had also investigated on the mixed oxide heterogeneous catalysts such as calcium-magnesium oxide (CaO-MgO) and calcium-zinc oxide (CaO-ZnO) for the biodiesel production. It was proven that CaO based mixed oxides has about 60% higher BET surface area compared to the CaO catalyst (Taufiq-Yap et al., 2011). On the other hand, the co-existence of different oxides was able to improve the base catalytic performance in transesterification reaction. Taufiq-Yap et al. (2014) successfully prepared calcium-lanthanium oxide ($CaO-La_2O_3$) by using co-precipitation method. $CaO-La_2O_3$ had catalysed transesterification reaction of *Jatropha* oil and methanol and provided 86.51% of biodiesel yield.

The raw materials of the catalyst mentioned previously are conventionally applied for catalyst synthesis. There are also heterogeneous base catalyst that can be synthesised from biomass. Figure 2.4 summarises different synthesis pathways of base heterogeneous catalyst by using biomass as starting material. Biomass can either be directly converted into base catalyst through thermal decomposition process or be converted into supporting material for the alkali active sites.

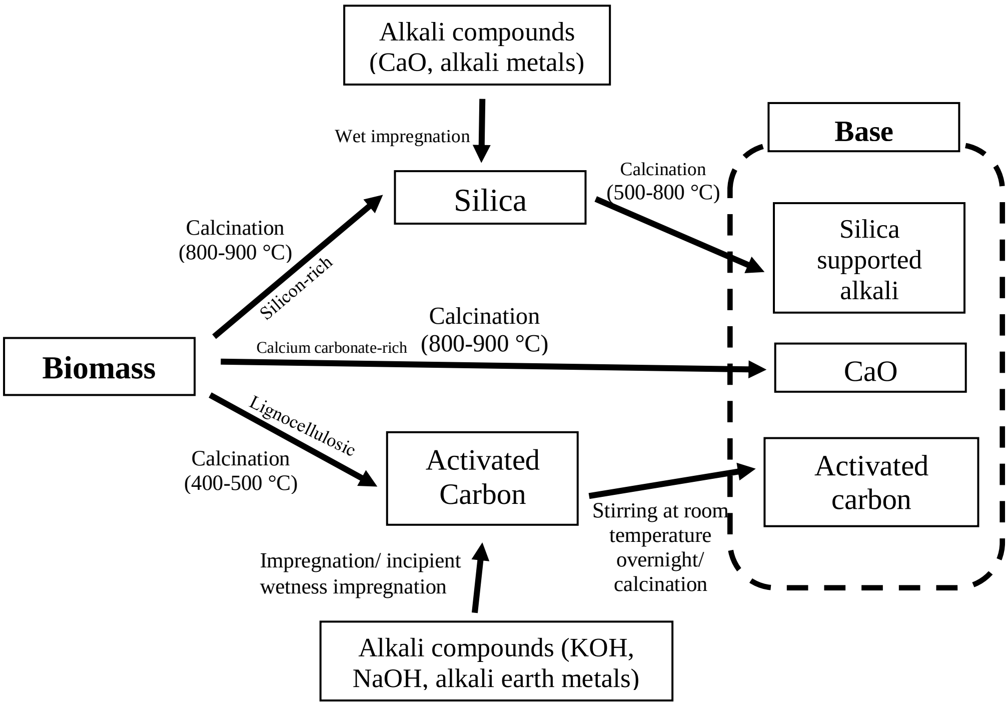

Figure 2.4: Synthesis routes of biomass derived solid base catalyst.

Most of the time, biomass with high calcium carbonate ($CaCO_3$) content is more favourable for the synthesis of base catalyst where the $CaCO_3$ in the biomass will be decomposed into CaO and CO_2 under high temperature (800-900 ºC) as shown in Equation 2.1. Mucino et al. (2014) had investigated on the sea sand derived CaO catalyst. A white solid with more than 98% of CaO was formed by calcinating sea sand at 800 ºC. This CaO catalyst had achieved biodiesel yield of 95.4%. Later on, it was found that doping of metal ions such as barium, molybdenum and zirconium into the synthesised CaO was able to improve the performance and characteristic of catalyst in terms of the basicity and reusability of catalyst (Boro et al., 2014; Mansir et al., 2018).

$$CaCO_3 \rightarrow CaO + CO_2 \qquad (2.1)$$

Nonetheless, the usage of CaO in the stand alone form may suffer from several limitations such as sensitive to moisture and low surface area. Therefore, attachment of the CaO onto supporting material helps to mitigate the problems. Fly ash and rice husk ash are examples of base catalyst supporting materials which had been studied by the researchers. Chen et al. (2015) had produced base catalyst from rice husk ash loaded with 30% of egg shell derived CaO and a biodiesel yield of 91.5% was successfully obtained. In addition, biomass can also be converted into activated carbon support and functionalised with base solution such as KOH to form heterogeneous base catalyst (Dhawane et al., 2016). The synthesis of activated carbon from biomass will be explained in detail in Section 2.3.1.

Table 2.2 summarises the different types of heterogeneous base catalyst employed in the biodiesel production reaction. Most of the heterogeneous base catalysts were able to achieve a convincing biodiesel yield of above 80%. As compared to the conventional base catalyst, biomass derived catalysts had shown comparable performance in the transesterification reaction. It is worth to note that biomass derived catalyst has a big advantage over conventional catalyst since it is able to be synthesised from low cost raw materials which are usually available in abundance.

Table 2.2: Transesterification reactions by using heterogeneous base catalyst for biodiesel production.

Biomass	Catalyst	Reaction Conditions					Yield (%)	Ref.
		Feedstock/ Alcohol	Temperature (°C)	Alcohol to oil molar ratio	Reaction Time (h)	Catalyst Loading (wt. %)		
-	Conventional CaO	Refined soybean oil/ methanol	65	12:1	1.5	8	95	(Liu et al., 2008b)
-	Conventional Cao-MgO	Refined *Jatropha curcas* oil/ methanol	65	15:1	6	4	80	(Taufiq-Yap et al., 2011)
-	Conventional CaO-La_2O_3	Refined *Jatropha curcas* oil/ methanol	65	24:1	6	4	86.51	(Taufiq-Yap et al., 2014)
Sea sand	CaO	Pre-treated used cooking oil/ methanol	60	12:1	6	7.5	95.4	(Muciño et al., 2014)
Turbonilla Striatula waste shell	Barium doped CaO	Pre-treated waste cooking oil/ methanol	60	6:1	8	1% Ba loading	Complete conversion	(Boro et al., 2014)
Waste *Gallus domesticus* shell	Mo-Zr doped CaO	Waste cooking palm oil/ methanol	80	15:1	3	3	90.1%	(Mansir et al., 2018)
Rice husk ash, egg shell	Rice husk ash supported CaO	Refined palm oil/ methanol	65	9:1	4	7	91.5	(Chen et al., 2015)
Flamboyant pods	Activated carbon supported KOH	Refined *Hevea Brasiliensis* oil (rubber seed oil) / methanol	55	15:1	1	3.5	89.81	(Dhawane et al., 2016)

2.2.2 Biocatalyst

Enzyme, which is also known as the biocatalyst is able to help in catalysing chemical reaction. One of the most common types of enzyme, lipase is well known in the biodiesel research as it is able to act as biocatalyst to produce biodiesel from oil feedstock similar to the base catalyst. Biocatalyst is superior among other catalysts since it is operational friendly as it requires only mild reaction conditions (25-50 °C), less energy consumption and less waste water produced (Tran et al., 2016). In addition, the largest advantage of biocatalyst over base catalyst is the ability of biocatalyst to convert unrefined raw oil or waste oil with high FFA content into biodiesel (Guldhe et al., 2015).

Figure 2.5 shows the reaction mechanism of converting oil to biodiesel catalysed by the biocatalyst. The whole reaction mechanism can be separated into two steps where the first step is the hydrolysis reaction to breakdown the large ester (triglyceride) into FFA and glycerol, then followed by methanolysis of FFA to form smaller ester (biodiesel) in the second step. Firstly, the enzyme will attached with the oil substrate to form enzyme-oil substrate (E.S) complex. Next, an enzyme-fatty acid (E.FA) will be formed after the protonation occurs. Later on, alcohol will be introduced, forming enzyme-fatty acid-alcohol (E.FA.A) complex and then forming enzyme-biodiesel-glycerol (E.Bd.G) after the reaction. Finally, biodiesel will be detached from the enzyme and the enzyme is ready for the next reaction (Paiva et al., 2000).

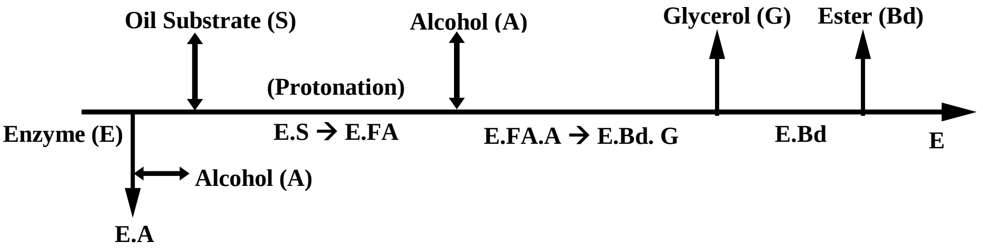

Figure 2.5: Reaction mechanism of enzyme catalysed reaction (Paiva et al., 2000)

Many researches had been done on the investigation of lipase as the biocatalyst used in the biodiesel production. Lipase used in the reaction may be immobilised on inert carriers to enhance the stability and resistance of the catalyst against the environmental changes. Immobilisation is able to reduce the production cost as it is easily separated and the immobilised lipase is reusable (Guldhe et al., 2015). Immobilisation can be done through several methods such as cross-linking, micro-encapsulation and covalent bonding (Mardhiah et al., 2017).

Nelson et al. was one of the first researchers reported on the usage of lipase as catalyst in the biodiesel production reaction. It was found that lipase obtained from *Mucor meihei* gave the best catalytic activity in the reaction of tallow and methanol with the reaction condition of 10 wt.% lipase loading, 8 hours and 45 °C by using hexane as solvent (Nelson et al., 1996).

Huang et al. (2015) had investigated on the recombinant *P. pastoris* strain expressed *Rhizomucor miehei* lipase (GH2) with unique properties as a more suitable lipase for conversion of microalgae oil into biodiesel. Under the reaction of methanol and microalgae oil in the presence of GH2, 95% FAME conversion was achieved at 30 °C for 24 hours with 3:1 methanol to oil ratio and 160 U/g of enzyme loading. Recently, Guldhe et al. (2015) had demonstrated successful biodiesel production by using *P. fluorescens* lipase with biodiesel conversion of 90.81% was obtained. On the other hand, Navarro et al. (2016) had also studied on *Rhizopus oryzae* lipase and obtained the highest FAME conversion of 83% at 35 °C for 72 hours.

As a whole, enzyme catalysts were able to obtain high biodiesel yield above 80%. However, it can be seen that the reaction time required was relatively long at up to 72 hours despite the lower reaction temperature and methanol loading required. *P. pastoris* strain expressed *Rhizomucor miehei* lipase recorded the highest biodiesel yield at 95% compared to the other species.

2.2.3 Heterogeneous Acid Catalyst

Due to the high production cost incurred from the requirement of expensive refined oil feedstock with low FFA content in base transesterification process, esterification reaction of FFA to form biodiesel catalysed by biocatalyst and acid catalyst was introduced. However, the usage of biocatalyst and several drawbacks such as less cost effective and requires longer reaction time. Therefore, esterification of FFA in the presence of acid catalyst is more favourable.

The reaction mechanism of acid catalysed esterification reaction is as shown in Figure 2.6. Initially, carbonium ion will be formed from the protonation of the carbonyl carbon in FFA by the protons of the acid catalyst. Next, a tetrahedral intermediate will be formed from the nucleophilic attack of the alcohol towards the carbonium ion. The tetrahedral intermediate will then be broken down when the proton migrated to form water and fatty acid esters. The proton from the acid catalyst will then be reformed for the protonation of other FFAs (Guo and Fang, 2011).

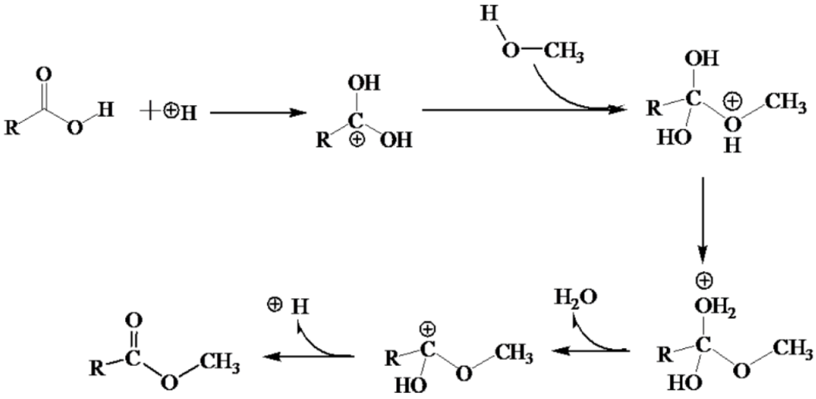

Figure 2.6: Reaction mechanism of acid catalysed esterification (Guo and Fang, 2011).

Compared to homogeneous acid catalyst such as sulfuric acid (H_2SO_4), heterogeneous acid catalysts possess several advantages as they are easily separable, reusable and non-corrosive. Many researches on several types of supported heterogeneous acid catalyst had been carried out. Fu et al. (2015) had reported on the synthesis of sulfonated macroporous cation exchange resins solid catalyst. The resin ball was produced by using styrene and divinyl benzene as the raw materials and sulfonated with 93% H_2SO_4. It gave good catalytic activity at mild reaction condition of rapeseed oil (acid value 64.9mg KOH/g) at methanol to oil molar ratio of 15:1, 100 ˚C with 10 wt.% catalyst loading for 3 hours, the maximum biodiesel conversion obtained was 97.8%. However, this catalyst was sensitive to water as it will be easily deactivated by water which presence in large amount in low cost feedstock.

On the other hand, Carvalho et al. (2017) reported that the Keggin heteropolyacid (HPA) 12-molybdophosphoric acid ($H_3PMo_{12}O_{40}$) supported on alumina was able to give promising result in the esterification reaction of high moisture feedstock noting that Keggin HPA is a stronger Bronsted acid than H_2SO_4. Other than alumina, tungstophosphoic HPA can also be immobilised on zirconia as reported by Alcañiz-Monge et al. (2018) obtaining biodiesel conversion above 90% at reaction temperature 60 ˚C for 6 hours with methanol to oil molar ratio 94.9:1 and 30 wt. % catalyst loading by using palmitic acid as feedstock. Despite the high conversion achieved, this catalyst suffered from fouling after reaction due to the blockage of organic matter on the pore structure.

Nevertheless, Zuo et al. (2013) had investigated on the synthesis of arene sulfonic acid functionalised mesoporous SBA-15 catalyst which provides good access for the large and long alkyl chains molecules to the active site to reduce the diffusion resistance. It was able to obtain biodiesel yield of 80% in the reaction of soybean oil (20% FFA) and 1-butanol at 190 ˚C for 30 minutes with 5 wt. % catalyst loading and 6:1 alcohol to oil molar ratio. However, the arene sulfonic acid functionalised catalyst involved a series of complex and long synthesis steps including 20 hours of pre-hydrolysis, followed by 24 hours of aging at 100 ˚C and another 24 hours of refluxing with methanol.

Besides that, there were also researches carried out on the carbon supported acid catalyst with several advantages which render it more superior as compared to other heterogeneous acid catalysts. Carbon supported acid catalyst is usually low cost as they can be produced from biomass waste while at the same time has high surface area and high density of mesopores (Liu et al., 2010). In addition, carbon supported acid catalyst also possesses amphiphilic properties that favours esterification reaction. The hydrophilic functional group attracts the polar reactant while the hydrophobic carbon hinders the adsorption of water which will poison the catalyst (De et al., 2015). The researches done on the carbon based acid catalyst will be discussed in detailed Section 2.3.

The different types of heterogeneous acid catalysts employed in the biodiesel production and the operating conditions are summarised in Table 2.3. It shows that Keggin HPA $H_3PMo_{12}O_{40}$ supported on alumina had achieved the highest biodiesel yield among other heterogeneous acid catalysts at 97%. However, the operating conditions required were quite severe since reaction temperature of 200 °C was used and high methanol to oil molar ratio of 120:1 was required. Although sulfonated carbon catalyst obtained a relatively low biodiesel yield, the operating conditions required were milder than the reactions catalysed by other conventional catalysts. Nevertheless, the performance of a carbon based catalysts is also dependant on the biomass source used for the synthesis of the carbon support. Therefore, carbon based catalyst still possesses a very large potential and high research value to seek for suitable biomass sources for the synthesis of carbon acid catalyst. More researches on the carbon based acid catalyst will be further discussed in Section 2.3.

Table 2.3: **Transesterification and esterification reactions by using heterogeneous acid catalysts.**

Catalyst	**Reaction Conditions**					**Yield, Y/ Conversion, C (%)**	**Ref.**
	Feedstock/ Alcohol	**Temperature (°C)**	**Alcohol to oil molar ratio**	**Reaction Time (h)**	**Catalyst Loading (wt. %)**		
Sulfonated cation exchange resins	Rapeseed oil/ methanol	100	15:1	3	10	C=97.8	(Fu et al., 2015)
Keggin HPA $H_3PMo_{12}O_{40}$ supported on alumina	*Mucor circinelloides/ ethanol*	200	120:1	4	10	Y=97	(Carvalho et al., 2017)
HPA supported on zirconia	Palmitic acid/ methanol	60	94.9:1	6	30	Y=90	(Alcañiz-Monge et al., 2018)
Arene sulfonic acid functionalised SBA-15	Soybean oil (20% FFA)/ 1-butanol	190	6:1	0.5	5	Y=80	(Zuo et al., 2013)
Sulfonated carbon material	Acetic acid/ methanol	70	10:1	10	3.33	Y=78%	(Liu et al., 2010)

2.3 Carbon Based Heterogeneous Acid Catalyst

Many researches had been carried out to study the conversion of lignocellulosic biomass into carbon based solid acid catalyst with the application of catalysing the biodiesel production reactions. The synthesis pathway of the carbon based acidic catalyst is shown in Figure 2.7. Basically, the lignocellulosic biomass will first be converted into carbon materials through thermal treatment or carbonisation at high temperature to remove the volatiles material in the biomass. After that, the carbon material formed will be functionalised with sulfonic group, SO_3H as the active site for reaction through sulfonation process to form carbon acid catalyst. The detailed carbonisation and sulfonation process of carbon acid catalyst will be discussed in Section 2.3.1 and 2.3.2.

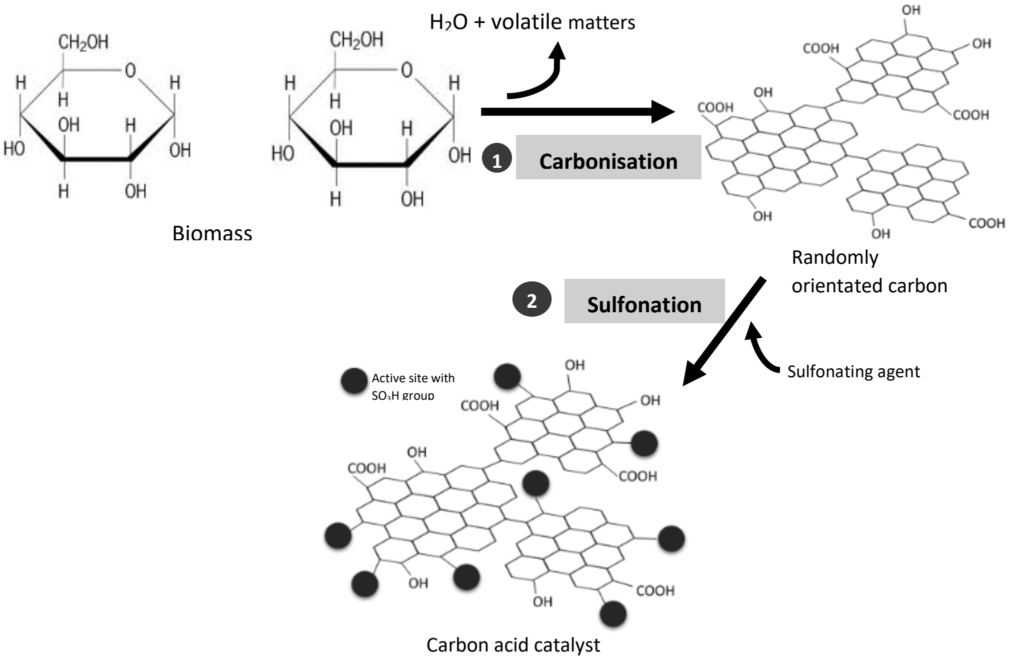

Figure 2.7: Synthesis pathway of carbon based heterogeneous acid catalyst.

2.3.1 Synthesis of Carbon from Biomass

Anthropogenic agricultural activities had generated massive amount of biomass residue which requires post handling process before disposal. Previously, these waste biomass has no market value and their potential in the future market was neglected. Biomass is composed of cellulose, hemicellulose and lignin with high carbon content favouring the formation of high performing carbon materials. Recently, researches had been carried out on converting low cost biomass into high quality carbon materials that can be utilised in various applications.

Biomass has a large potential to create a sustainable framework in biodiesel market. Catalysts derived from biomass have several advantages over conventional catalysts as they are biodegradable, non-toxic and have higher surface area (Liu et al., 2010). Shu et al. (2009) had reported a pioneer carbon based catalyst synthesised from biomass by using vegetable oil asphalt as raw material for biodiesel production. Since then, many researches on the carbon acid catalyst had been carried out by using different types of biomass sources.

There are several pathways available for the synthesis of carbon material from biomass as illustrated in Figure 2.8. Basically, carbon material can be synthesised through three main processes which include hydrothermal carbonisation (HTC), templated directed method and also direct carbonisation. On the other hand, carbon material can also be synthesised with or without activation. Commonly, the carbon synthesised without undergoing activation is known as biochar and carbon synthesised with activation process is known as activated carbon.

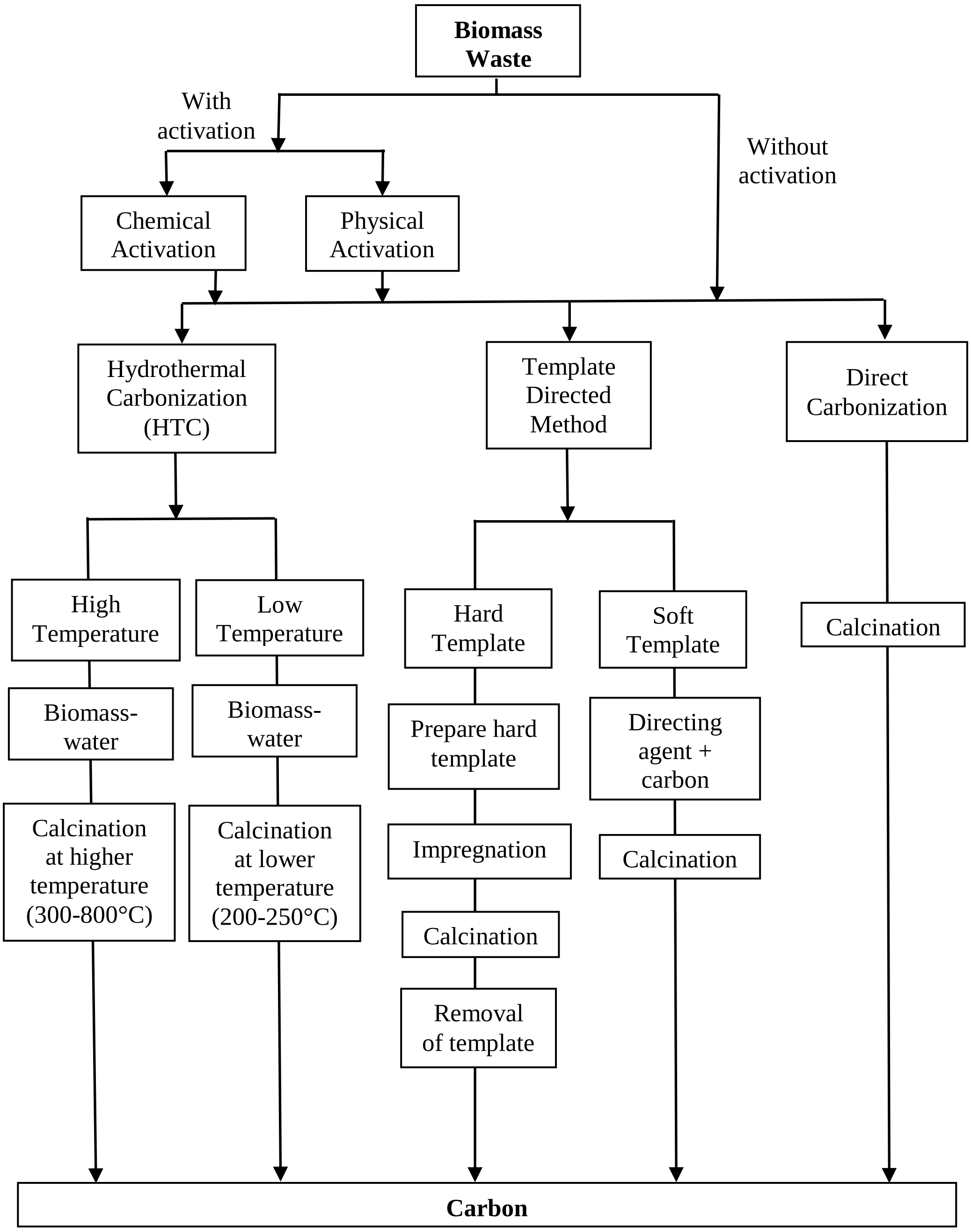

Figure 2.8: Overview of carbon synthesis pathway.

2.3.1.1 Hydrothermal Carbonisation

HTC is a thermochemical process that is usually been carried out in the presence of water with a series of reactions including hydrolysis, dehydration, decarboxylation, condensation and aromatization in liquid phase. In HTC, water helps to hydrolyse the cellulose and hemicellulose in the biomass to produce a highly porous carbon product known as hydrochar (Reza et al., 2014). HTC process is usually being carried out at elevated pressure to suppress the water molecules and prevent them from escaping from the system. Solid hydrochar, bio-oil and gaseous products are the three main products produced from HTC process (Liu et al., 2013b).

This process can be categorised into high and low temperature HTC. Sadaka et al. (2014) was able to synthesis hydrochar with 49% of fixed carbon compound from switchgrass through high temperature HTC process. On the other hand, it was reported that the fixed carbon content increased with the increase of temperature from 300 to 400 ˚C and 3 hours residence time since the volatiles materials has been efficiently removed at this operating conditions. After all, high temperature HTC is less favourable as compared to low temperature HTC that is less hazardous due to less chemical transformation involved and requires lower operating conditions.

Smith and Ross (2016) had successfully synthesised hydrochar with improved combustion properties by using high ash content macroalgae *L. hyperborea* as the raw material. This had proven that biomass material with high water and ash content such as macroalgae was able to significantly enhance the hydrothermal treatment process with increased carbon content and reduced oxygen content. The results showed that low temperature HTC is a feasible method in producing carbon material from biomass.

2.3.1.2 Template Directed Carbonisation

Template directed method possesses several advantages whereby this method allows the synthesis of carbon material with tuneable pore size according to the types of template used to achieve the desired carbon structure can be achieved. Currently, researchers have been focussing on the soft template and hard template method in synthesising carbon material.

The synthesis of carbon material through hard template method usually uses the artificial silica template such as halloysite nanotube or silica template. Normally, hard template method will firstly be carried out by impregnation of hard template and biomass solution then followed by carbonisation of the template-biomass mixture. The template will then be removed by washing the product with solvent such as hydrogen fluoride after carbonisation process. Xie et al. (2016) had demonstrated the synthesis of hierarchical porous carbon through hard template directed method from sodium lignin sulfonate by using halloysite nanotube as the hard template. On the other hand, Janaun and Ellis (2011) had also successfully synthesised a randomly ordered mesoporous carbon from glucose by using silica template.

For soft template method, surfactants, block copolymer and organic compounds are several examples of the soft template usually employed in the synthesis process. Soft template directed method requires low temperature during operation as soft template such as surfactant is inherently unstable at high temperature. However, at low operating temperature, efficient interaction between soft template and carbon precursor is difficult to be achieved. Therefore, screening of suitable template is paramount to improve the interaction between the soft template and carbon precursor (De et al., 2015).

Several researches had been carried out on the dual template method which combines the hard and soft template during the synthesis process whereby soft template helps in the mesopores formation on the carbon product while hard template favours the macropores formation with high pore volume and surface area (De et al., 2015). Liu et al. (2014) had demonstrated the synthesis of porous carbon from banana peel as precursor through dual template directed method by using Al (III) based metal organic framework as the hard template and Pluronis F127 as the soft template. The duration of this process was very long including 7 days of impregnation in hard template, 24 hours impregnation in soft template and 24 hours of thermal polymerisation despite the desirable properties of the end carbon product.

2.3.1.3 Direct Carbonisation

Most of the studies reported on the carbon support of the carbon acid catalyst used in the biodiesel production usually synthesised through direct carbonisation as this method is simple and straightforward. Unlike HTC that uses water or template directed method that requires the usage of template as scaffold, direct carbonisation method does not requires additional material to be carried out. Usually, direct carbonisation is done by direct thermal treatment on the biomass to form biochar by removing and decomposing the volatile material on the biomass and other non-carbon elements such as oxygen, hydrogen and nitrogen to form a rigid skeleton-like aromatic carbon structure carbon (Mohamad Nor et al., 2013).

Toda et al. (2005) had introduced the synthesis of biochar derived from sugar using incomplete carbonisation to form amorphous carbon material with randomly orientated aromatic carbon sheets. The biochar formed was then functionalised with concentrated H_2SO_4 to form carbon acid catalyst which was successfully applied in the esterification reaction of oleic acid and methanol to produce biodiesel.

However, biochar produced from direct carbonisation method usually had surface area lower than 600 m^2/g depending on the raw material and carbonisation conditions (Iqbaldin et al., 2013; Härmas et al., 2016). In this context, the surface area of the carbon material can be improved through activation process to facilitate better pore formation during the carbon synthesis process. The carbon material produced after activation process is also known as the activated carbon.

2.3.1.4 Activation Method

Activation process plays an important role in enlarging the pore volume, increasing pore diameter and also improving the pore formation of the carbon material. On the other hand, activation can also significantly boost up the specific surface area of the carbon material formed by 4 to 50 times, allowing more surface area for the reaction to occur (Härmas et al., 2016). Activation method can be carried out by either chemical activation with chemical activating agent or physical activation by using gaseous activating agent. The selection of activation method and the choice of activating agents are important as they may influence the properties of the activated carbon formed (Sun et al., 2016).

In chemical activation, the biomass will first be treated with chemical activating agent prior subjected to carbonisation at elevated temperature to form activated carbon. As compared to physical activation, chemical activation is able to produce activated carbon with higher pore density, higher carbon content and shorter carbonisation time required (Härmas et al., 2016). The commonly used activating agents as reported were phosphoric acid (H_3PO_4), potassium hydroxide (KOH), sodium hydroxide (NaOH) zinc chloride ($ZnCl_2$) and iron (III) chloride ($FeCl_3$) (Somasundaram et al., 2013; Sahira et al., 2013; Anis et al., 2014; Härmas et al., 2016; Sun et al., 2016,).

Jain et al. (2015) had demonstrated chemical activation by using $ZnCl_2$ on coconut shell. Coconut shell derived activated carbon with mesopores (2-50nm) was obtained and it showed that the surface area was increased by 100%. In this study, H_2O_2 was also added as oxidizing agent to improve the effectiveness of the chemical activation process.

H_3PO_4, $ZnCl_2$ and KOH are several examples of the commonly used chemical activating agents as they are able to effectively enhance the pore development with higher surface area (Sahira et al., 2013). A study conducted by Harmas et al. (2016) showed that both KOH and $ZnCl_2$ could produce glucose derived activated carbon with the same specific surface area at 2150 m^2/g. However, for the case of activated carbon produced from rubber seed pericarp, KOH gave far lower specific surface area at 392 m^2/g as compared to H_3PO_4 and $ZnCl_2$ that gave the activated carbon with specific surface area of 1589 m^2/g and 1686 m^2/g, respectively (Anis et al., 2014; Sun et al., 2016).

Although the activated carbon produced from KOH exhibited low specific surface area, a well-developed and organised pore structure was observed. As for H_3PO_4, it has advantage over other activating agents since that it is less corrosive to the process equipment as compared to the hydroxide activating agent (Sahira et al., 2013; Sun et al., 2016)

In contrast, the activated carbon synthesis step for physical activation is the reverse of chemical activation. Physical activation with gaseous activation through gasification will be carried out only after the synthesis of biochar through pyrolysis. Steam and carbon dioxide (CO_2) are the most commonly employed gaseous activating agents. Some studies shows that steam has superior performance compared to CO_2 because steam has smaller molecule size and is able to have good access into the biochar structure which will then result in higher surface area and wider pore size distribution (Maneerung et al., 2016; Smets et al., 2016).

Compared to chemical activation, physical activation is more cost effective due to the cheaper activating agents (Härmas et al., 2016). However, it produces activated carbon with narrower pore size distribution which mainly composes of micropores (Prauchner and Rodríguez-Reinoso, 2012). In addition, it was found that physical activated carbon had lesser specific surface area increment compared to chemical activation (Yacob et al., 2015). On the other hand, chemical activation can produce activated carbon with wider pore size distribution ranging from micro- to mesopores and can highly increase the specific surface area of the carbon material (Somasundaram et al., 2013).

2.3.2 Sulfonation Methods

The carbon material produced from carbonisation will be functionalised through sulfonation to form carbon based acid catalyst. The sulfonation process of carbon is usually done through direct sulfonation with acid under thermal treatment or through arylation reaction. The most common sulfonation method is through direct sulfonation by using H_2SO_4 at elevated temperature. Sulfonation of carbon can be done by using different methods with various types of sulfonating agents such as H_2SO_4, p-toluenesulfonic acid (PTSA), fuming sulfuric acid and 4-benzenediazonium sulfonate (4-BDS)

2.3.2.1 Direct Sulfonation with Acid

Functionalisation of carbon by direct sulfonation is usually being carried out by direct grafting of the $–SO_3H$ functional group onto the carbon structure under heat treatment of the activating agent and carbon. Most of the researches on synthesis of carbon acid catalyst focuses on direct sulfonation by using H_2SO_4. This sulfonation method was carried out by heating the mixture of carbon impregnated with concentrated H_2SO_4 at 150 ˚C (Ezebor et al., 2014a; Akinfalabi et al., 2017).

Direct sulfonation approach with concentrated H_2SO_4 was conducted by Ezebor et al. (2014a) by using sugarcane bagasse and oil palm trunk as the raw material for carbon material to synthesise carbon acid catalyst for biodiesel production. The anchoring of $–SO_3H$ functional group in the catalyst was confirmed by the peak at wavelength 1160 cm^{-1} and 1030 cm^{-1} in FT-IR representing the asymmetric S-O and O=S=O stretching from the –SO_3H group. The catalyst produced had shown promising result with 94.43% and 93.36% of biodiesel yield achieved by sugarcane bagasse and oil palm trunk derived carbon catalyst, respectively. In this study, the catalysts were proven to be comparable with the conventional zirconia catalyst that gave 90% biodiesel yield in the esterification reaction between methanol and palmitic acid (Saravanan et al., 2016). Besides that, numerous researches were carried with other biomass wastes such as *C.inophyllum* seed cake, coffee residue, coconut shell, *jatropha curca*s and coconut meal residue (Dawodu et al., 2014; Ngaosuwan et al., 2016; Haziratul et al., 2017; Endut et al., 2017; Thushari and Babel, 2018).

A study was conducted by Ngaosuwan et al. (2016) to investigate the effect of temperature on the catalytic performance of the carbon acid catalyst synthesised. It was found that as sulfonation temperature increased, the –SO_3H density in the catalyst would eventually decreases. Nonetheless, the amount of weak acid –COOH group increased with the increment of temperature. It was mentioned that a balance amount of –SO_3H group and weak acid was needed to optimise the catalytic performance as –SO_3H group acts as the active site for reaction to occur and weak acid played a role in dispersing the catalyst to minimise mass transfer limitation (Hara, 2010). In addition, it was reported that the sulfonation reaction was favourable at the optimum temperature of 100-105 ˚C and extremely high sulfonation temperature would lead to the production of undesired sulfone groups (Zhou et al., 2016; Endut et al., 2017).

On the other hand, sulfonation time will also give a significant effect towards the catalytic activity. Ezebor et al. (2014a) had reported on sulfonation with concentrated H_2SO_4 by varying the sulfonation time. The sulfonation of bagasse derived biochar was carried out at 150 ˚C for 2 to 10 hours demonstrated positive effect to the total acid density of the catalyst and the sulfonation time increased from 2 to 6 hours. Further increasing the time showed insignificant change. Similar trend was observed in the study conducted by Zhou et al. (2016) that the increase of sulfonation time would increase the biodiesel conversion and achieved optimum sulfonation time of 2 hours by using the bamboo derived carbon catalyst.

Most of the time, direct sulfonation with concentrated H_2SO_4 will be carried out in two steps whereby the carbon will first be synthesised before sulfonation to functionalise the carbon. However, there were also researches carried out in a single step with *in-situ* carbonisation and sulfonation from several types of biomass. Fu et al. (2013) has conducted the single step sulfonation by hydrothermally carbonised the mixture of microalgae and H_2SO_4 simultaneously at 120 ˚C. The microalgae derived catalyst was able to achieve higher biodiesel conversion of 98% as compared to the Amberlyst-15 with only 82% conversion due to the porous structure that provide better access for the reactants to reach active sites.

Since then, one-step sulfonation with simultaneous carbonisation and sulfonation was being studied by several other researchers since it is cost effective and time saving. Liu et al. (2017) had performed the one step sulfonation at room temperature in order to reduce the energy consumption. In this study, distiller grains was mixed with concentrated H_2SO_4 and maintained at 20 ˚C for 1.4 hours. The catalyst was able to give promising result with 97% of conversion but the catalyst synthesised from this method had low reusability whereby the conversion dropped to 50.7% at the fifth esterification cycle due to leaching problem.

Other than concentrated H_2SO_4 as the most commonly used sulfonating agent, researchers had also investigated on several other sulfonating agents to seek for more alternatives. Fuming H_2SO_4 is one of the sulfonating agents used in the sulfonation of biomass derived carbon material as reported by Liu et al. (2013a) with fuming H_2SO_4 with 50 wt.% SO_3 on carbonised corn straw and Janaun et al. (2013) with fuming H_2SO_4 20 wt.% SO_3 on seaweed derived carbon to synthesise acid catalyst. Fuming H_2SO_4 or Oleum is made up of H_2SO_4 dissolves with varying composition of free sulfur trioxide. According to Liu et al. (2013a), the catalyst synthesised was able to produce 92% of optimum FAME conversion in esterification reaction between oleic acid and methanol at methanol to oil molar ratio 3:1 at 60 ˚C for 4 hours with 3 wt. % catalyst loading.

Besides dissolving in concentrated H_2SO_4 as fuming H_2SO_4, sulfur trioxide was also able to be used as the sulfonating agent in stand-alone gaseous form. Kastner et al. (2012) had performed sulfonation using gaseous sulfur trioxide by exposing the wood chip derived biochar to the sulfur trioxide in a glass jar sealed air-tight for 6 days at room temperature. The catalyst synthesised through this method had achieved biodiesel conversion of 97% at 55-60 ˚C at reaction time of 5 hours with methanol to palmitic acid molar ratio of 6:1 and 6 wt.% catalyst loading.

Other than concentrated H_2SO_4, fuming H_2SO_4 and sulfur trioxide, *p*-toluenesulfonic acid (PTSA) was also being investigated as another potential option for sulfonation to synthesise the carbon acid catalyst. The usage of PTSA as the sulfonating agent to sulfonate sawdust derived biochar into catalyst was studied by Wang et al. (2013). The carbon acid catalyst synthesised gave 86.6% of FAME conversion in the esterification reaction of high acetic acid contented bio-oil with alcohol. In addition, Dawodu et al. (2014) had also synthesised *C. inophyllum* seed cake derived catalyst through sulfonation using PTSA and obtained FAME conversion of 76.7%.

2.3.2.2 Sulfonation by Arylation or Reduction

The sulfonation methods mentioned previously in Section 2.3.2.1 mostly involved the usage of corrosive chemicals which will still cause corrosion to the equipment in the industry. Besides direct sulfonation by using acid, sulfonation of carbon material through chemical reduction or arylation process was also being studied extensively by many researchers as it does not involve highly corrosive chemicals and can be easily handled. The overall sulfonation process through chemical reduction and arylation is shown in Figure 2.9.

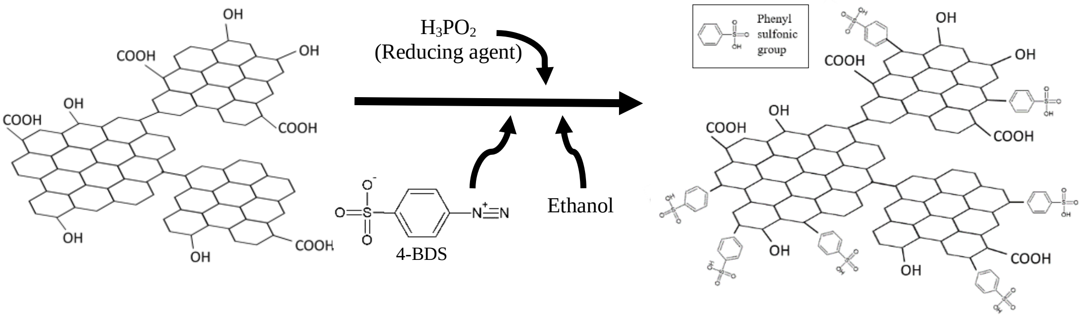

Figure 2.9: Arylation reaction of 4-BDS and carbon material.

Liu et al. (2010) had first demonstrated sulfonation of activated carbon through arylation of 4-benzenediazonium sulfonate (4-BDS) in the presence of hypophosphorus acid (H_3PO_2) as the reducing agent. In this chemical reaction, the ethanol reacted with the 4-BDS to form the H-terminated benzenesulfonic acid as shown in Figure 2.10. On the other hand, the reducing agent H_3PO_2 aided in the formation of radicals on the carbon ring through reduction or arylation process (Abiman, Wildgoose and Compton, 2008). Then, the activated carbon was grafted with the phenyl sulfonic group in a strong covalent bond between the carbon surface and sulfonic group (Wang et al., 2007).

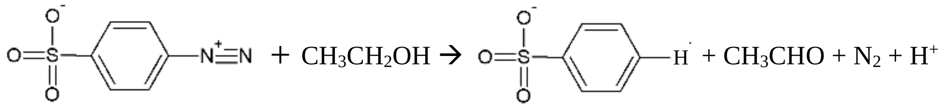

Figure 2.10: Formation of H-terminated benzenesulfonic acid

Later, Konwar et al. (2015) had carried out similar approach by using biomass waste generated after vegetable oil extraction process. In this study, the researcher had converted de-oiled waste cake of *P. Pinnata* into carbon material. It was then functionalised through sulfonation by arylation of 4-BDS in a series of steps. In this sulfonation process, sulfanilic acid was acidified by first dispersing into hydrochloric acid solution followed by the addition of sodium nitrite solution in dropwise manner in order to avoid temperature rise and ensure well mixing of the solution. This step was to synthesise the 4-BDS as the sulfonating agent and the whole system was maintained at 3 – 5 ˚C in an ice bath. Next, the synthesised 4-BDS was mixed with ethanol, carbon material and H_3PO_2 and continued to stir at 3 – 5 ˚C. The *P. Pinnata* seed cake derived catalyst recorded the sulfonic group density of 0.84 mmol/g and successfully obtained 95% conversion of FAME from oleic acid.

Compared to direct sulfonation by using H_2SO_4, it was claimed that sulfonation by arylation of 4-BDS did not induce the formation of weak acid from side reaction. On the other hand, arylation of 4-BDS produces sulfonic group with the presence of phenyl group in the form of phenyl sulfonic, –$PhSO_3H$, which is a bulkier group as compare to the –SO_3H group attached from direct sulfonation method. As a result, carbon material occupied with the bulkier –$PhSO_3H$ group would show a more significant reduction in surface area and pore volume as compare to being occupied with the smaller –SO_3H group. Also, Konwar et al. (2015) had demonstrated that in the esterification reaction of oleic acid with methanol, catalyst produced from arylation of 4-BDS method obtained higher FAME conversion at 90% as compared to H_2SO_4 sulfonated catalyst with FAME conversion of only 50%.

In addition, Malins et al. (2015) had demonstrated a modified arylation process by eliminating the usage of reducing agent. For this study, the arylation reaction of activated carbon grain and 4-BDS was carried out without using H_3PO_2 at higher temperature (50-70 ˚C). The catalyst synthesised through this modified method recorded $PhSO_3H$ acid density of 0.72 mmol/g and achieved FAME conversion of 95% in the esterification reaction of rapeseed oil fatty acids and methanol.

2.3.2.3 Other Sulfonation Methods

Besides direct sulfonation with acid or arylation reaction of diazonium salts, there were also several other sulfonation methods being studied by other researchers to seek for more alternatives in this process. Suwanwong et al. (2008) had performed sulfonation of activated carbon by using non acidic aqueous solution of ferric sulfate to synthesise heterogeneous acid catalyst for biodiesel production. This sulfonation was carried out by incipient wet impregnation of activated carbon by using ferric sulfate solution of different weight percent concentrations whereby the activated carbon was loaded with the solution according to the wetness point (0.55 ml/g). This catalyst loaded with 20 wt.% ferric sulfate solution had successfully converted FAME up to 98.22% in the esterification reaction of PFAD and methanol at 95 ˚C, catalyst loading of 40 wt.% and 12:1 methanol to oil molar ratio for 6 hours of reaction time.

Nonetheless, Shuit and Tan (2014) had compared several different sulfonation methods in their study by using conventional carbon material, multi-walled carbon nanotube (MWCNT) as the catalyst support. The sulfonation reported were *in situ* polymerization of poly(sodium4-styrenesulfonate) (PSS), in situ polymerization of acetic anhydride and H_2SO_4 and also sulfonation by thermal decomposition of ammonium sulfate. The catalysts derived from all these methods exhibited high FAME yields at the range of 85 – 95%. Amongst, catalyst sulfonated from *in situ* polymerization of PSS gave the highest FAME yield in the esterification of PFAD but it required a very long sulfonation duration of 4 days with a series of complicated steps. On the other hand, sulfonation by thermal decomposition of ammonium sulfate synthesised catalyst achieved FAME yield of 88% in esterification reaction. Although the FAME yield was lower, this method did not involve the usage of corrosive chemicals and also required much shorter sulfonation duration of 30 minutes.

The performance of carbon based solid acid catalyst on the biodiesel production reaction by using a variety of feedstock and optimum reaction conditions was summarised in Table 2.4. Most of the catalyst showed promising result with biodiesel yield or conversion above 80% which prove that they have a large potential to be further developed and being utilised in the industrial scaled production. Based on the comparison, catalyst synthesised from direct sulfonation by using H_2SO_4 gave the best result compared to the other catalysts. However, this method still involve the usage of highly corrosive concentrated H_2SO_4 which will corrode the operating equipment and this does not resolve the problem incurred by using the homogeneous acid catalyst. In this case, sulfonation through arylation or reduction of diazonium salt is shown to possess advantages as it does not involve highly corrosive chemicals while able to give comparable biodiesel yield. Thus, more comprehensive researches should be carried out to improve and to optimise the catalytic performance in biodiesel production.

Table 2.4: Transesterification and esterification reactions by biomass derived solid acid catalyst for biodiesel production.

Biomass	Sulfonation method/ agent	Reaction Conditions					Yield, Y/ Conversion, C (%)	Ref.
		Feedstock/ Alcohol	Temperature (°C)	Alcohol to oil molar ratio	Reaction Time (h)	Catalyst Loading (wt. %)		
Sugarcane bagasse	Direct sulfonation/ conc. H_2SO_4	Waste oil	130	1.17 mL/min	4	12	Y = 83.2	(Ezebor et al., 2014a)
Oil palm trunk	Direct sulfonation/ conc. H_2SO_4	Waste oil	130	1.17 mL/min	4	12	Y = 80.6	(Ezebor et al., 2014a)
Bamboo	Direct sulfonation/ conc. H_2SO_4	Oleic acid/ ethanol	90	7:1	2	6	C = 98.4	(Zhou et al., 2016)
Coffee residue	Direct sulfonation/ conc. H_2SO_4	Caprylic acid/ methanol	60	3:1	4	5	C=71.5	(Ngaosuwan et al., 2016)
C. inophyllum cake	Direct sulfonation/ conc. H_2SO_4	*C. inophyllum* oil/ methanol	150	5g :5.5g	5	6	C=84.2 Y=36.4	(Dawodu et al., 2014)
De-oiled *jatropha curcas* seed	Direct sulfonation/ conc. H_2SO_4	*jatropha curcas* oil/ methanol	60	12:1	1	7.5	C=99.13	(Haziratul Mardhiah et al., 2017)
Coconut shell	Direct sulfonation/ conc. H_2SO_4	Palm oil/ methanol	60	30:1	6	6	C=88.25	(Endut et al., 2017)
Coconut meal residue	Direct sulfonation/ conc. H_2SO_4	Waste palm oil/ methanol	65-70	12:1	10	5	Y=92.7	(Thushari and Babel, 2018)

Table 2.4 (continued): Transesterification and esterification reactions by biomass derived solid acid catalyst for biodiesel production.

Biomass	**Sulfonation method/ agent**	**Reaction Conditions**					**Yield, Y/ Conversion, C (%)**	**Ref.**
		Feedstock/ Alcohol	**Temperature** (°C)	**Alcohol to oil molar ratio**	**Reaction Time (h)**	**Catalyst Loading (wt. %)**		
Microalgae residue	*In situ* partial hydrothermal carbonization with sulfonation/ conc. H_2SO_4	Oleic acid, triolein/ methanol	80	-	12	5	C = 98 (oleic acid) Y = 24 (triolein)	(Fu et al., 2013)
Corn straw	Direct sulfonation/fuming sulfuric acid (50wt% SO_3)	Oleic acid/methanol	60	3:1	4	3	Y=92	(Liu et al., 2013a)
Biochar	Direct sulfonation/fuming sulfuric acid (>20wt% SO_3)	Canola oil + oleic acid/methanol	315	30:1	3	5	Y = 48	(Janaun et al., 2013)
Pine chip char	Direct sulfonation/Sulfur trioxide	Palmitic acid/methanol	55-60	6:1	6	-	C = 97	(Kastner et al., 2012)
Sawdust pellet	Direct sulfonation/ *p*-toluenesulfonic acid	Acetic acid/methanol	-	2.8:1	2	0.5	C = 86.6	(Wang et al., 2013)

Table 2.4(continued): Transesterification and esterification reactions by biomass derived solid acid catalyst for biodiesel production.

Biomass	Sulfonation method/ agent	Reaction Conditions					Yield, Y/ Conversion, C (%)	Ref.
		Feedstock/ Alcohol	**Temperature** (°C)	**Alcohol to oil molar ratio**	**Reaction Time (h)**	**Catalyst Loading (wt. %)**		
Activated carbon	Arylation/4-benzene-diazonium sulfonate	Aliphatic acid ethanol	70	10:1	10	1.2	C = 52	(Liu et al., 2010)
De-oiled waste cake	Arylation/4-benzene-diazonium sulfonate	Oleic acid/ methanol	64	20:1	10	3	C = 97	(Konwar et al., 2015)
Activated carbon	Arylation/4-benzene-diazonium sulfonate	Rapeseed oil/ methanol	65	20:1	7	10	C = 95	(Malins et al., 2015)
Activated carbon	Ferric sulfate	PFAD/ methanol	95	12:1	6	40	C = 98.22	(Suwanwong et al.)
MWCNT	Polymerization of PSS	PFAD/ methanol	170	20:1	3	2	Y = 93.4	(Shuit and Tan, 2014)
MWCNT	Polymerization of acetic anhydride and H_2SO_4	PFAD/ methanol	170	20:1	3	2	Y = 85.8	(Shuit and Tan, 2014)
MWCNT	Thermal decomposition of ammonium sulfate	PFAD/ methanol	170	20:1	3	2	Y = 88	(Shuit and Tan, 2014)

2.4 Process Optimisation

It is important to obtain a catalyst with good catalytic performance that is feasible to carry out the esterification and transesterification reaction to produce biodiesel. However, the tuning of operating conditions during the esterification and transesterification reaction are also crucial in order to maximise the biodiesel yield obtained with the most cost effective operating conditions. The optimisation of the reaction conditions can be carried out either by using the one variable at a time (OVAT) method or with design of experiment (DOE) method.

2.4.1 One Variable at a Time

In optimisation study when OVAT is employed, the variables are being studied one factor at a time. It is carried out by varying one variable at a time while the other factors are kept constant. After obtaining the optimum point of the first variable, the optimised first variable will be carried forward to study the second variable and so on.

Dawodu et al. (2014) had demonstrated OVAT in optimising the methanol to oil molar ratio (12: 1 to 45: 1), catalyst concentration (1.5 to 7.5 wt.%), temperature (100 to 200 ˚C) and time (1 to 5 hours) in the transesterification reaction to produce biodiesel. Figure 2.11 shows the results from the optimisation of reaction conditions based on the biodiesel yield obtained. It was carried out by first obtaining the optimum methanol to oil molar ratio of 30: 1 while keeping other conditions constant. Then, it is followed by obtaining the optimised catalyst concentration (7.5 wt.%), temperature (180 ˚C) and time (5 hours) while the optimised condition was used for the study of next variable.

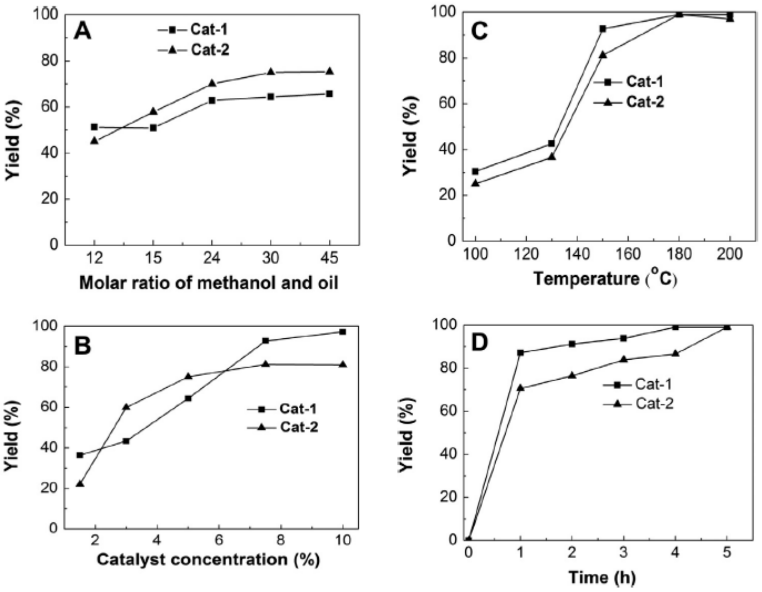

Figure 2.11: Results for (a) effect of methanol to oil molar ratio at 5 wt.% catalyst concentration, 150 ˚C and 5 hours reaction time (b) effect of catalyst concentration at 30: 1 methanol to oil molar ratio, 150 ˚C and 5 hours reaction time (c) effect of temperature at 30: 1 methanol to oil molar ratio, catalyst concentration of 7.5 wt.% and 5 hours reaction time (d) effect of time at 30: 1 methanol to oil molar ratio, catalyst concentration of 7.5 wt.% and 180 ˚C (Dawodu et al., 2014).

2.4.2 Design of Experiment

Optimisation by using statistically designed experiment is one of the popular methodologies used by many researchers. It is very useful in studying the effect of multiple factors as it is able to vary several factors simultaneously. Conducting process optimisation by using design of experiment (DOE) method possesses several advantages over the OVAT method since DOE method requires lesser time and lower cost to obtain the equivalent amount of information. Besides that, it is also able to estimate the effect of factors towards the response more precisely and able to study the interaction effect between the factors studied (Czitrom, 1999).

DOE by using response surface methodology (RSM) is one of the most common mathematical and statistical methods to form empirical models whereby the mathematics models will be used to optimise the response of the study that is dependent on the independent variables studied. Optimisation by using RSM is usually been carried out by first choosing the statistical model for the study, followed by running the experiment designed in random order and finally perform the analysis of variance (ANOVA) and obtaining the optimised condition (Ferreira et al., 2007). Box-Behnken and Central Composite Design (CCD) were the most commonly used methods in optimisation and variable effect studies.

Box-Behnken design is a second order and incomplete full factorial design that requires lesser number of runs. Dharma et al. (2016) had demonstrated the optimisation of biodiesel production by using the Box-Behnken design with three levels. The variables included in this study were methanol to oil molar ratio (30: 1 to 70: 1), catalyst concentration (0.5 to 2.0 wt.%) and agitation speed (800 to 1800 rpm) consisted of 17 experiment runs with biodiesel yield as the response. It was found that the results were fitted well into the model since the R-squared obtained was 0.9958.

On the other hand, CCD is also a second order design but with more design points and with full factorial design. Regalado et al. (2017) had employed the three factors and five level CCD consisted of 15 experiment runs. The independent variables set was the catalyst weight (0.1 to 0.2 g), methanol to oil molar ratio (3: 1 to 7: 1) and temperature (20 to 40 ˚C) and the response was the FAME yield. The R-squared of 0.943 indicated that 94.3 % of the variables studied can be explained by the model. Besides that, Anand et al. (2016) also had carried out optimisation study using three factors five levels CCD with 20 sets of experiment. The variables studied were base catalyst loading (0.4 to 1.2 gm), acid catalyst loading (1.25 to 1.75 mL) and methanol to oil molar ratio (7: 1 to 11: 1). This model had a R-squared value of 0.9040.

Moreover, Ali et al. (2017) had performed a four factors five levels CCD consisted of 30 experiment runs. The independent variables set included the temperature (35 to 50 ˚C), methanol to oil molar ratio (2: 1 to 4: 1), loading of lipase (0.5 to 2 gm) and agitation speed (150 to 200 rpm) with biodiesel yield as the response. The R-squared obtained was 0.9907 indicating that the predicted and actual values were very close. This indicated that the model was feasible to describe the relationship between the variables and the response.

2.5 Factors Affecting Biodiesel Production Reactions

In a heterogeneous acid catalysed reaction, there are several factors that will give a big impact towards the achievable biodiesel yield and conversion. According to Table 2.4, the four main factors affecting the final biodiesel yield and conversion are the reaction time, reaction temperature, catalyst loading and alcohol to oil molar ratio. The influence of the mentioned parameters to the biodiesel production reaction will be explained in Section 2.5.1 to 2.5.4.

2.5.1 Reaction Time

The duration of the whole reaction is one of the important factors that will influence the final outcome. An appropriate reaction duration is necessary to ensure a sufficient mass transfer between the reactant mixtures and catalyst throughout the reaction. As shown in Table 2.4, the range of optimum reaction time for esterification and transesterification reaction was from 1 to 12 hours. The optimum reaction time for the reaction varied with the types of catalyst used and the setting of other operating conditions.

Ayodele and Dawodu (2014) had investigated the reaction of *C. inopyllum* oil and methanol at reaction time range of 1 to 5 hours and reached optimum biodiesel conversion above 99% at reaction time of 4 hours . It was found that that a prolonged reaction time was required to achieve substantial conversion of oil to biodiesel since the reaction should have sufficient retention time to occur on the catalyst surface between the reactants and active sites.

On the other hand, Haziratul et al.(2017) had studied the reaction time from 30 to 120 minutes and obtained optimum conversion of 99.13% at reaction time of 60 minutes. The conversion of biodiesel started to drop after exceeding the optimum reaction time. This might be due to the accumulation of by-product over the duration which had the potential to deactivate the catalyst and affacted the catalytic activity. Sometimes, the biodiesel yield would also show insignificant changes at longer reaction time (Dawodu et al., 2014).

2.5.2 Reaction Temperature

The temperature of the reaction system is also one of the crucial factors manipulating the yield or conversion of FAME in biodiesel production reactions. According to Table 2.4, many researchers had reported the reaction temperature of 60 – 70 ˚C to obtain biodiesel conversion of above 80%. This had indicated that biodiesel production was achievable with only mild operating temperature. Nevertheless, there were also researches which recorded the reaction temperature of 100 – 200 ˚C to achieve the biodiesel yield of above 80%.

Buasri et al. (2012) studied the reaction temperature of 50 – 70 ˚C and obtained the optimum reaction temperature of 60 ˚C. They found that the increment of reaction temperature would give positive effect to the biodiesel yield due to the endothermic nature of the reaction. Since transesterification and esterification are reversible reactions, increasing the reaction temperature is able to drive the equilibrium of the endothermic reaction towards the product side (Niu et al., 2018). On the other hand, the reaction temperature also should be high enough to provide sufficient energy for the activation and protonation of the carbonyl group from the oil feedstock (Ayodele and Dawodu, 2014).

Nevertheless, it was claimed that excessive high reaction temperature exceeding the optimum temperature would cause reverse reaction leading to the decrement of FAME yield (Tao et al., 2015). This was because extremely high temperature in an open system would also intensify the rate of evaporation of the alcohol and subsequently reduce the amount of alcohol in the reactant mixture. Subsequently, the contact rate was also reduced between the reactants which retarded the FAME conversion (Buasri et al., 2012; Haziratul Mardhiah et al., 2017).

2.5.3 Catalyst Loading

In the transesterification or esterification reaction between oil and alcohol, these two reactants will usually form two immiscible layers whereby the contact surface is very small. Therefore, catalyst is playing an important role in providing sufficient contact surface for the reactants in order for reaction to occur. As shown in Table 2.4, the catalyst loading required for most of the biodiesel production reactions catalysed by carbon based catalyst were only less than 10 wt.%.

Haziratul et al. (2017) had carried out the study on effect of catalyst loading at 2.5 to 10 wt.% towards the biodiesel conversion and recorded the optimum catalyst loading of 7.5% with biodiesel conversion above 98%. It was reported that the increment of catalyst loading in the reaction system would give positive effect to the FAME yield and conversion since the catalyst played an important role in lowering the activation energy of the reactions which in return speed up the rate of reaction as compared to non-catalytic reaction (Dawodu et al., 2014). Moreover, the presence of catalyst in the reaction system will also promote the occurrence of reaction by providing active sites whereby increasing the catalyst amount will drive the equilibrium of the reaction towards the product side (Zhou et al., 2016).

Increasing the amount of catalyst loaded into the reaction will raise the FAME production but excessive loading of catalyst will cause adverse effect. When catalyst is added into the reactant mixture beyond its optimum amount, the viscosity of the reaction system will increase leading to mixing problem which will hinder the mass transfer of the reactants and in return, reducing the FAME yield achieved (Ayodele and Dawodu, 2014).

2.5.4 Alcohol to Oil Molar Ratio

In reversible transesterification and esterification reaction, alcohol (usually methanol) will be added in excess molar ratio in order to push the equilibrium of the reaction towards the product side to favour the formation of desired product at the end of reaction. As listed in Table 2.4, methanol to oil molar ratio applied in the reaction was usually in the range of 10: 1 to 30: 1 instead of the stoichiometric molar ratio of 3: 1.

Increasing methanol to oil molar ratio will usually increase the formation of biodiesel in the reaction (Ali et al., 2017). Meanwhile, the presence of alcohol in the reaction system also acts as a co-solvent to promote the collision rate between the catalyst and reactants to minimise the mass transfer limitation (Niu et al., 2018).

Thushari et al. (2018) had studied the effect of molar ratio from 6:1 to 16:1 to the biodiesel yield. It was found that the biodiesel increased to the optimum of 77.3% when the molar ratio increased to 12: 1. Further increasing the methanol to oil molar ratio had led to the fall of biodiesel yield obtained. In addition, Niu et al. (2018) and Dawodu et al. (2014) had also reported on the similar trend for the effect of methanol to oil molar ratio towards biodiesel yield with optimum molar ratio of 1: 7 and 1: 15 respectively.

Studies showed that addition of methanol beyond the optimum molar ratio would give negative effect to the biodiesel yield because it would result in the reduction of biodiesel formation. Too much amount of alcohol will dilute the reaction system and causes flooding to the active sites. These can prevent the reactants to get in contact with each other and thus reducing the collision frequency (Zhou et al., 2016).

CHAPTER 3

METHODOLOGY

3.1 Overall Research Methodology

This research was carried out to synthesise corncob derived heterogeneous acid catalyst for biodiesel production. The research methodology of the whole study is summarised in Figure 3.1.

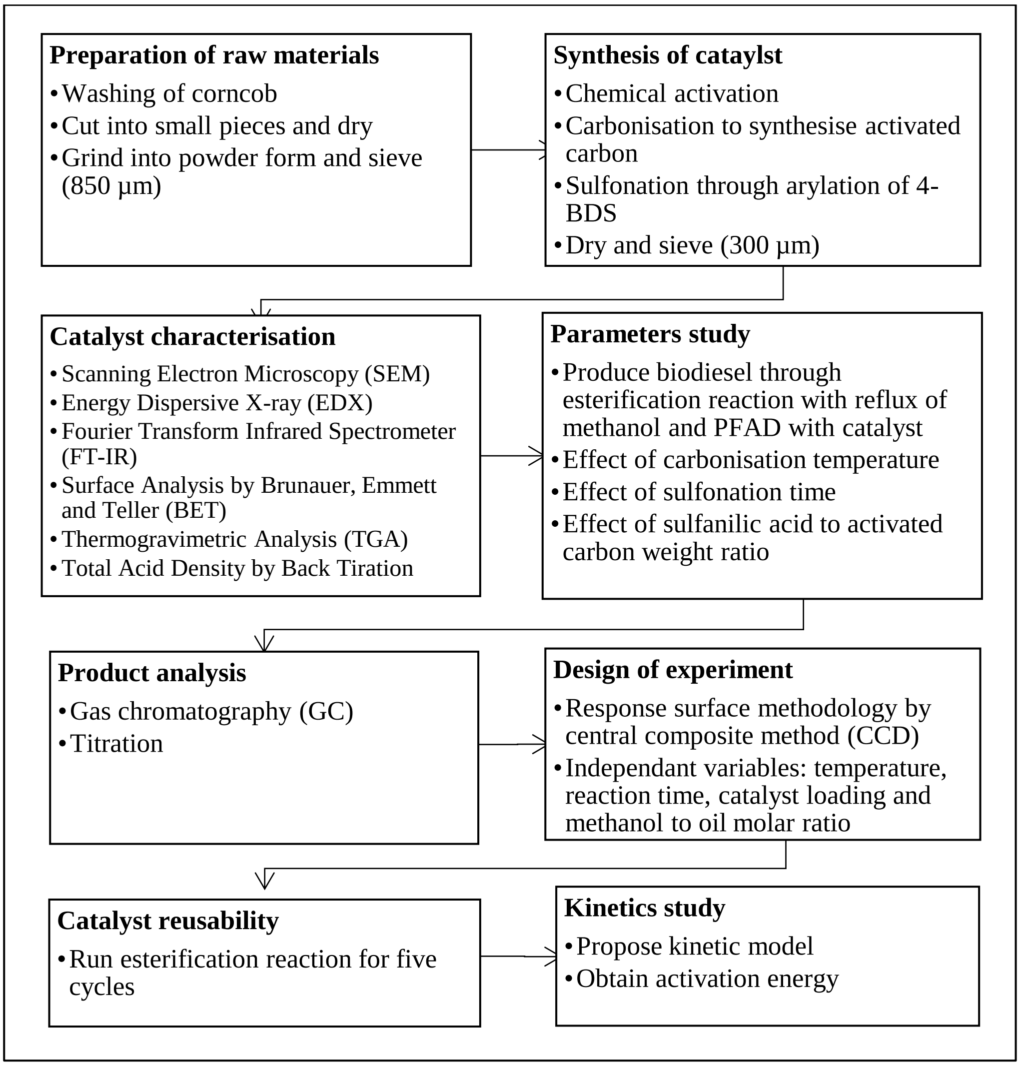

Figure 3.1: Overall flow of research methodology.

3.2 Materials and Apparatus

3.2.1 Materials and Chemicals

Numerous types of raw materials and chemicals had to be prepared to ensure the experiment can be carried out efficiently. Corncob (de-kernelled) was selected as the raw materials in this study for the synthesis of heterogeneous acid catalyst. The usage and source of all materials and chemicals needed in this study are listed in Table 3.1.

Table 3.1: List of materials and chemicals required for this research.

Materials/ Chemicals	Source	Quantity	Usage
Corncob	Local night market	10 kg	• Raw material for activated carbon
Palm Fatty Acid Distillate(PFAD)	Local palm oil mill	2 kg	• Raw material for biodiesel
Phosphoric acid, 85%	Merck	5 L	• For chemical activation • For sulfonation
Sulfanilic acid, >99%	Merck	1 kg	• To produce 4-BDS as sulfonating agent
Sodium Nitrate, 98.5%	Thermo Fisher	500 g	• To produce 4-BDS as sulfonating agent
Ethanol, 99%	Merck	1 L	• For sulfonation
Methanol, 99%	Merck	1 L	• Reactant for esterification

Table 3.1(continued): List of materials and chemicals required for this research.

Materials/ Chemicals	Source	Quantity	Usage
Hydrochloric acid, 37%	Merck	500 mL	• To produce 4-BDS as sulfonating agent and for total acid density titration
Potassium Hydroxide	Merck	100 g	• For acid value titration
Sodium Hydroxide	Merck	100 g	• For total acid density titration
Hexane	Merck	1 L	• Solvent for biodiesel
Isopropanol	Merck	1 L	• Solvent for biodiesel
Methyl Heptadecanoate	Sigma-Aldrich	1 g	• Standard for GC
Methyl Palmitate	Sigma-Aldrich	1 g	• Standard for GC
Methyl Stearate	Sigma-Aldrich	1 g	• Standard for GC
Methyl Oleate	Sigma-Aldrich	1 g	• Standard for GC
Methyl Linoleate	Sigma-Aldrich	1 g	• Standard for GC

3.2.2 Apparatus and Instrument

The research experiments involved the experimental set-up with the specification and usage of apparatus and equipment required listed in Table 3.2. In addition, Table 3.3 shows the specification and usage of instruments required for the products analysis.

Table 3.2: List of apparatus and equipment required for this research.

Apparatus/ Equipment	Specification	Usage
Air convection oven	Memmert	Drying of samples
Furnace	Carbolite, RHF 15/8	Carbonisation of corncob
Vacuum pump	Rocker 300	For filtration processes
Heating mantle	Digital Heating Mantle HM-11	To heat and stir reaction mixture
Stirring hotplate	IKA RCT Basic	To heat and stir reaction mixture
Grinder	Berjaya BJY-CB2LN	To grind corncob into powder form
Pestle and mortar	320 mL, Porcelein	To grind activated carbon into powder form
Test sieve	300 µm, 850 µm	To screen corncob powder and catalyst into desired size
Ice bath	Ice cubes in 2L beaker	To maintain temperature in sulfonation process
Coiled condenser	300 mm, 24/40	To reflux methanol during reaction
Round bottom flask	500 mL, 24/29	To contain reaction mixture

Table 3.3: List of instruments required for this research.

Instrument	Specification	Usage
Scanning Electron Microscope (SEM)	Hitachi Model S-3400N	To study the surface morphology of samples
Energy Dispersive X-ray Spectroscopy (EDX)	Hitachi Model S-3400N	To study elemental composition of samples
Fourier Transform-Infrared (FT-IR)	Perkin Elmer, Spectrum RX1	To study functional groups attached on samples
Thermogravimetric Analysis (TGA)	Perkin Elmer, STA 8000	To study weight loss profile and thermal stability of catalyst
Surface Analyser	Micrometrics, ASAP 2020	To study surface properties of samples
Gas Chromatography (GC-FID)	Perkin Elmer Clarus 500	To determine compound present in biodiesel product

3.3 Preliminary Study

Preliminary study was carried out prior to the selection of biomass as raw material for this research. The catalytic performance and properties of non-edible macroalgae (wild seaweed) and corncob (de-kernelled) derived carbon based catalyst were compared.

In this study, both of the biomass were carbonised at temperature of 200 to 500 ˚C following the methodology described in Section 3.4.2. It was then followed by the sulfonation of the synthesised activated carbon to transform them into –SO_3H groups loaded catalyst. The total acid density of the catalyst synthesised was determined and compared. The determination of total acid density was described in Section 3.6.5. The synthesised catalysts were then applied in esterification of PFAD and methanol for biodiesel production and the catalyst that gave higher would be subjected to further studies.

3.4 Synthesis of Catalyst

3.4.1 Preparation of Raw Materials

In this study, corncob was selected as the raw material to be used for the synthesis of activated carbon (AC) as catalyst support. Corncob (de-kernelled) was collected from a local night market stall. As shown in Figure 3.2, the collected corncob was washed with tap water to clean and remove physical impurities. It was then manually cut into smaller pieces for the ease of grinding later and dried overnight in the oven at 80 ˚C. The dried corncob pieces were then grinded into powder form and sieved to mesh size of 850 µm for further treatments.

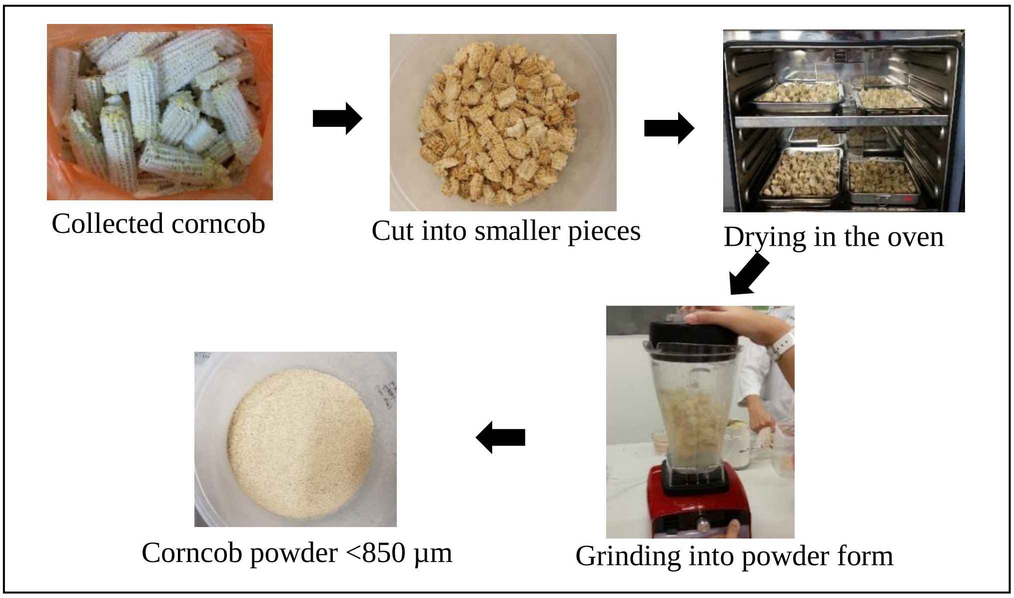

Figure 3.2: Overall process flow for raw material preparation.

3.4.2 Synthesis of Activated Carbon

The activated carbon was synthesised through a series of steps by using corncob powder as the starting material as illustrated in Figure 3.3. Firstly, corncob powder was impregnated with 30 v/v% phosphoric acid (H_3PO_4) for 24 hours at room temperature with the corncob to H_3PO_4 weight ratio of 1:7. The impregnated corncob powder was then rinsed with distilled water and dried overnight in the oven at 80 ˚C. The dried and impregnated corncob powder was then subjected to carbonisation at temperature 600, 700, 800, 900 and 1000 ˚C for 2 hours with the ramping rate of 5 ˚C/min from room temperature by using Carbolite furnace. The produced activated carbon was then grinded with pestle and mortar into finer form and screened with sieve of mesh size 300 µm to control the size of activated carbon produced. The activated carbon produced was annotated as CCAC600, CCAC700, CCAC800, CCAC900 and CCAC1000 according to the carbonisation temperature

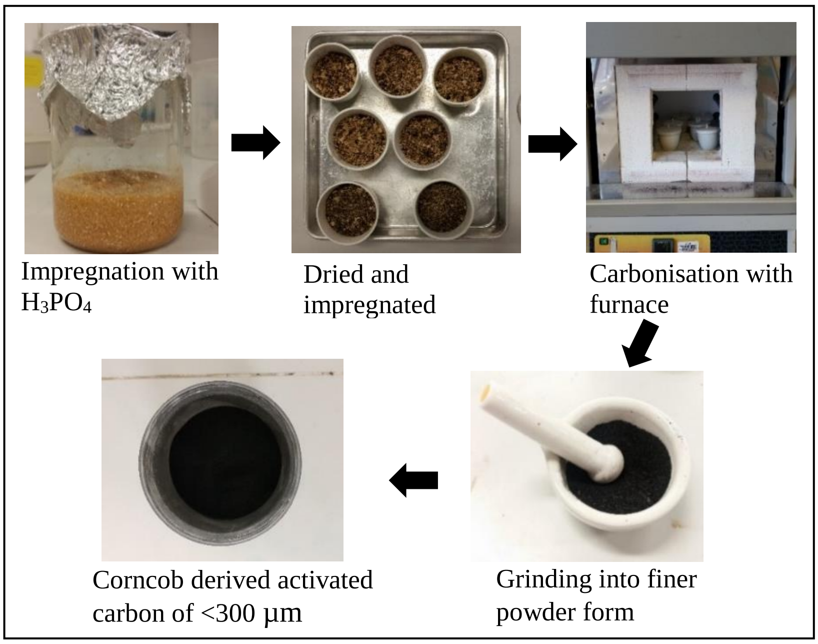

Figure 3.3: Overall process flow for the synthesis of corncob derived activated carbon.

3.4.3 Synthesis of Heterogeneous Acid Catalyst

Corncob derived carbon acid catalyst was synthesised through arylation reaction of 4-BDS with activated carbon. The sulfonation process was divided into two stages whereby the first stage was to synthesise the 4-BDS and second stage was the sulfonation of the activated carbon by using 4-BDS. The sulfonation method was similar to the method as reported by Konwar et al. (2015).

Firstly, sulfanilic acid (sulfanilic acid to AC weight ratio: 3:1, 5:1, 7:1, 9:1, 11:1, 13:1) was dispersed into 300 mL of 1M HCl in a 500 mL round bottom flask and stirred continuously, followed by the dropwise addition of 90 mL 1M sodium nitrite. The mixture was then stirred for 1 hour and maintained at temperature 0 – 5 °C in an ice bath. Next, the solution was filtered to collect the 4-BDS formed. 4-BDS was then added into a mixture of 60 mL ethanol and 200 mL of deionised water followed by addition of 3 g AC and 100 mL 30 v/v% phosphoric acid and stirred for 30 minutes. Next, 50 mL of phosphoric acid was added into the mixture and stirred for another 0.5, 1, 1.5, 2 and 2.5 hour(s). The catalyst was washed with deionised water and dried overnight in the drying oven at 80 ˚C. The experiment set up was shown in Figure 3.4.

Figure 3.4: Apparatus set-up for sulfonation process.

3.4.4 Process Parameters Study

There were several parameters being studied throughout the catalyst synthesis process including the carbonisation temperature, sulfonation duration and sulfanilic acid to AC weight ratio. This parameters study was carried out with one-variable-at-a-time (OVAT) method. The optimum point of the study was determined according to the highest FAME yield achieved. The operating conditions and annotations of the catalyst produced are as listed in Table 3.4.

Table 3.4: List of annotations for catalysts and the varied parameters.

Sample	Carbonisation	Sulfonation	
	Temperature (˚C)	Time (hour)	Sulfanilic acid to AC weight ratio
Cat_600	600	1	5:1
Cat_700	700	1	5:1
Cat_800	800	1	5:1
Cat_900	900	1	5:1
Cat_1000	1000	1	5:1
Cat_900a	900	0.5	5:1
Cat_900b	900	1.5	5:1
Cat_900c	900	2	5:1
Cat_900d	900	2.5	5:1
Cat_900e	900	1.5	3:1
Cat_900f	900	1.5	7:1
Cat_900g	900	1.5	9:1
Cat_900h	900	1.5	11:1
Cat_900i	900	1.5	13:1

3.5 Esterification Reaction

Esterification reaction was carried out by using PFAD and methanol as the reactants. Figure 3.5 shows the apparatus set up for biodiesel production including a 500 mL round bottom flask fitted to a 300 mm coiled condenser for the reflux of methanol. The mixture of PFAD, methanol and catalyst was added into the round bottom flask for reaction. In the study of effect of carbonisation and sulfonation conditions, reaction was carried out at fixed reaction conditions at reaction temperature of 100 °C, reaction time 4 hours, catalyst loading of 5 wt.% and 30:1 methanol to oil molar ratio. The esterification reaction follows the reaction chemical equation as shown in Figure 2.2 whereby the FFA in PFAD will react with methanol (alcohol) to form biodiesel (FAME) and water according to the reaction mechanism as shown in Figure 2.6.

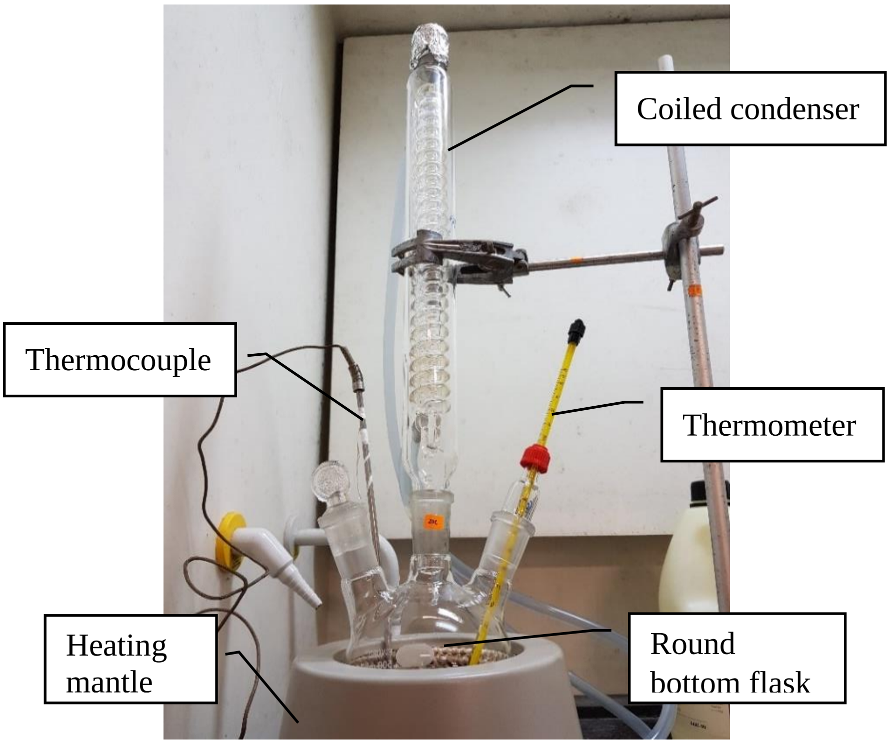

Figure 3.5: Apparatus set-for esterification reaction.

3.6 Catalyst Characterisation

There were several analytical instruments used for the characterisation of activated carbon and catalyst synthesised in the study. The instruments and methodologies involved in this study include scanning electron microscopy (SEM), energy dispersive x-ray (EDX), fourier transform infrared spectroscopy (FT-IR), surface analyser, thermogravimetric analysis (TGA) and back titration method which were discussed in detailed in Sections 3.6.1 to 3.5.6.

3.6.1 Surface Properties

Surface morphology of the samples was obtained by using SEM, Hitachi Model S-3400N. The image was captured at the magnification of 2000× and 5000× at 15.0 kV. The measurements of the diameter and size of pores on the surface of the sample were carried out by using the measurement tool and the scale provided on the micrographs. On the other hand, elemental composition of the samples was carried out by using EDX coupled with the SEM. The main elements on the samples are carbon (C), oxygen (O) and sulfur (S).

3.6.2 Fourier Transform Infrared Spectroscopy

FT-IR, Perkin Elmer Spectrum RX-1 was used to identify the functional groups attached on the catalyst by detecting the bonding of the elements. It was carried out by using KBr pellet technique at wavelength range of 400 – 4000 cm^{-1}. Sample pellet was prepared by pressing the mixture of small amount of the sample with KBr powder by using the hydraulic press machine. The sample pellet was then inserted into the sample holder of FT-IR to carry out analysis.

3.6.3 Surface Analysis

Surface analysis of activated and catalyst were carried out by using the surface analyser, Micrometrics, ASAP 2020. Surface area of the samples was obtained by using Bruneuer-Emmet-Teller (BET) methodology while pore size distribution and pore volume of samples was determined by using Barrett-Joyner-Halenda (BJH) method. For the analysis, about 0.1 g of samples was degassed at 90 °C for 1 hour and 200 °C for 20 hours until the static pressure was stable. N_2 adsorption analysis was carried out at -196 °C by using liquid nitrogen as coolant.

3.6.4 Thermogravimetric Analysis

TGA was carried out to study the weight loss profile of corncob and also thermal stability of the catalyst synthesised by using simultaneous thermal analyser, Perkin Elmer STA8000. In the analysis, the temperature was ramped from room temperature to 1000 ºC at the rate of 10 ºC/min under nitrogen flow. The percent weight loss of the samples was then plotted and observed.

3.6.5 Total Acid Density

Total acid density analysis of the catalyst was carried out with back titration method by using NaOH and HCl solutions. For this method, 0.1 g of catalyst was first mixed with 60 mL of 0.01 M aqueous NaOH solution and stirred at 300 rpm for 30 minutes at room temperature. The mixture was then filtered to recover the filtrate. The filtrate was then titrated with 0.02 M HCl by using phenolphthalein as pH indicator. Titration was terminated when the solution turned colourless from pink. The volume of 0.02 M HCl was recorded.

The mechanism of this method was first to neutralise the acid sites in the catalyst by using excess NaOH solution. After the catalyst had been completely neutralised, the remaining NaOH solution was titrated with HCl. The amount of HCl used to titrate the remaining NaOH would then be used to calculate the total acid density of the catalyst in mmol/g as shown in Appendix A.

3.7 Biodiesel Analysis

3.7.1 Biodiesel Product Conversion

The acid value of the feedstock, palm fatty acid distillate (PFAD) and FAME were studied by using titration method by using 0.1 N of KOH solution as titrant and phenolphthalein as pH indicator. Firstly, 10 mL of propanol was added into 1 g of sample as the solvent in a conical flask and phenolphthalein was added as pH indicator. Then, the mixture was titrated with 0.1 N KOH solution until a pink solution was formed. The volume of KOH solution used was recorded to calculate the acid value by using Equation 3.1. The conversion of FFA was calculated from acid value of oil feedstock and the biodiesel products by using Equation 3.2. Calculation of FFA % conversion was carried out by using Equation 3.3 and the sample calculation was shown in Appendix B.

$$\text{Acid Value, AV (mg KOH/ g)} = \frac{V \times N \times MW_{KOH}}{W_s} \tag{3.1}$$

$$\%\text{ conversion} = \frac{AV_{PFAD} - AV_{FAME}}{AV_{PFAD}} \times 100\% \tag{3.2}$$

$$\%\text{ conversion} = \frac{\left(\frac{V \times N \times MW_{KOH}}{W_s}\right)_{PFAD} - \left(\frac{V \times N \times MW_{KOH}}{W_s}\right)_{FAME}}{\left(\frac{V \times N \times MW_{KOH}}{W_s}\right)_{PFAD}} \times 100\% \tag{3.3}$$

Where, V is the volume of KOH solution used (mL), N is the normality of KOH solution (0.1 N), MW_{KOH} is the molecular weight of KOH (56.11 g/mol), W_s is the sample weight (1 g), AV_{PFAD} is the measured acid value of oil feedstock (mg KOH/ g) and AV_{FAME} is the measured acid value of biodiesel produced (mg KOH/ g).

3.7.2 Biodiesel Product Yield

The components present in the biodiesel was determined by using gas chromatography equipped with flame ioniser detector (GC-FID), Perkin Elmer Clarus 500. For GC analysis, the instrument was equipped with Nukol™ capillary column (30 m × 0.53 mm × 0.5 μm) and operated at helium gas flow rate 3 ml/min, injector temperature 250 °C of and detector temperature 220 °C. The initial oven temperature was set at 110 °C then increased to 220 °C at 10 °C/min. Methyl heptadecanoate was used as the internal standard. For each analysis, 1 μL of sample solution was injected into the GC column. The concentration of the components (methyl palmitate, methyl stearate, methyl oleate and methyl linoleate) present was determined by using the calibration curve as shown in Appendix C. Then, the yield of biodiesel was calculated following Equation 3.4. Sample calculation for FAME yield was attached in Appendix D.

$$Y = \frac{\sum C_{ME} \times m_{product}}{m_{PFAD}} \times 100\% \qquad (3.4)$$

Where Y is the FAME yield (%), C_{ME} is the total concentration of methyl esters $\left(\frac{\text{g ME}}{\text{g product}}\right)$, $m_{product}$ is the product mass (g product) and m_{PFAD} is the PFAD feed mass (g).

3.8 Design of Experiment

3.8.1 Quadratic Regression Modelling

Esterification reaction in the presence of the corncob derived acid catalyst to produce biodiesel was conducted according to the factorial design by using the response surface methodology (RSM) with Design Expert 7.0.0. A four factors and five levels central composite design (CCD) was employed in the design of the experiment. In this study, temperature (40 – 120 °C), time (0.5 – 8.5 hours), catalyst loading (2 – 14 wt.%) and methanol to oil molar ratio (5:1 – 37:1) were the targeted independent variables to be investigated and FAME yield (%) from the esterification reaction was the dependent variable, which is the response of the experiment. Table 3.5 shows the variables and levels of the experimental design in this study. The data obtained in this study was fitted into the second order polynomial expression as show in Equation 3.5.

$$R = \beta_0 + \sum_{i=1}^{4} \beta_i X_i + \sum_{i=1}^{4} \beta_{ii} X_i^2 + \sum_{i=1}^{4} \sum_{j=i+1}^{4} \beta_{ij} X_i X_j \qquad (3.5)$$

In Equation 3.5, R is the response factor, X_i is the independent factor, β_0 is the intercept, β_i is the linear coefficient, β_{ii} is the quadratic coefficient and β_{ij} is the cross products coefficient.

Table 3.5: Variables range and levels for response surface methodology.

Independent Variables	Symbols	Levels				
		$-\alpha$	-1	0	+1	$+\alpha$
Temperature (°C)	A	40	60	80	100	120
Time (hour)	B	0.5	2.5	4.5	6.5	8.5
Catalyst Loading (wt.%)	C	2	5	8	11	14
Methanol to oil molar ratio	D	5	13	21	29	37

3.8.2 Optimisation and Sensitivity Analysis with RSM

The optimum operating conditions of esterification reaction was obtained by using the optimisation tool of Design Expert through RSM. Then, esterification reaction was carried out following the obtained optimum conditions to verify the predicted FAME yield from RSM.

On the other hand, sensitivity analysis was carried out to investigate other possible combinations of operating condition which give comparable FAME yield with the optimised FAME yield. It was done by tuning the importance level of each of the independent variables (reaction time, reaction temperature, catalyst loading and methanol to oil molar ratio) with Design Expert.

3.9 Catalyst Reusability

The reusability of catalyst was studied by repeating biodiesel production reaction for five consecutive cycles using the same batch of catalyst. The biodiesel product obtained at each cycles was obtained for analysis. The reaction conditions of reaction temperature, reaction time, catalyst loading and methanol to oil molar ratio employed in the reaction was obtained from the optimisation analysis by using RSM. After each cycle of reaction, the catalyst was recovered by filtration and washed with hexane to remove any remaining oil on the catalyst.

3.10 Kinetics Study

3.10.1 Kinetic Model

The kinetic model of this study was built with the following assumptions:

(i) Production of biodiesel only involves esterification reaction

(ii) Non-catalytic reaction is negligible

(iii) Reaction mixture is considered as homogeneous with no mass transfer limitation with high agitation intensity and well mix of methanol with PFAD

(iv) Reverse reaction is negligible due to excess methanol added

From the assumptions, the reaction was assumed to be pseudo-homogeneous first order with only forward direction. With the stoichiometry equation of esterification in equation (3.6), the derivation of the kinetic model started from the reaction rate in equation (3.7)

$$FFA + MeOH \overset{k}{\rightarrow} FAME + H_2 \tag{3.6}$$

$$rate = -\frac{d\,[FFA]}{dt} = k[FFA][MeOH] \tag{3.7}$$

Where $[FFA]$ is the free fatty acid concentration, $[MeOH]$ is the methanol concentration and k is rate constant (min^{-1}).

By assuming this was a first order reaction, $[FFA]$ has the power of 1. On the other hand, the concentration of methanol was assumed to be constant since it was added in excess at much higher molar ratio. Therefore, Equation 3.8 and 3.9 were obtained. Then, Equation 3.9 was rearranged to obtain Equation 3.10. Equation 3.10 was then integrated to equation form. $[FFA_t]$ was then expressed in terms of $[FFA_0]$ and X_{ME} as listed in Equation 3.12 and 3.13. Equation 3.13 was then substituted into Equation 3.11 to form Equation 3.14 and rearranged into Equation 3.15 and 3.16. Finally, pseudo-first order kinetic model of esterification was obtained as Equation 3.16.

$$-\frac{d\,[FFA]}{dt} = k[FFA]^1[MeOH]^0 \tag{3.8}$$

$$-\frac{d\,[FFA]}{dt} = k[FFA] \tag{3.9}$$

$$-\int_0^t \frac{1}{[FFA]}\,d[FFA] = \int_0^t k\;dt \tag{3.10}$$

$$-\left(\ln[FFA_t] - \ln[FFA_0]\right) = kt \tag{3.11}$$

$$[FFA_t] = [FFA_0] - X[FFA_0] \tag{3.12}$$

$$[FFA_t] = [FFA_0](\,1 - X_{ME}) \tag{3.13}$$

$$-(\ln[FFA_0](\,1 - X_{ME}) - \ln[FFA_0]) = kt \tag{3.14}$$

$$-\ln\frac{[FFA_0](\,1 - X_{ME})}{[FFA_0]} = kt \tag{3.15}$$

$$- \ln(1 - X_{ME}) = kt \qquad (3.16)$$

Where $[FFA_t]$ is the concentration of free fatty acid at time t (min), $[FFA_0]$ is the initial free fatty acid concentration, X_{ME} is the FAME yield (%)

.

3.10.2 Experimental Study

Esterification reaction was carried out at temperature 40, 60, 80 and 100 ˚C, at time 15, 30, 45, 60, 75 and 90 minutes. The catalyst loading and methanol to oil molar ratio employed was obtained from the optimisation study of RSM. The biodiesel yields obtained were recorded. A linear graph of $-\ln(1 - X_{ME})$ against time, *t* was then plotted to obtain the rate constant, *k*.

3.10.3 Activation Energy

The activation energy of the reaction was obtained by following the Arrhenius Equation 3.17 which was then rearranged into Equation 3.18. A graph of ln *k* against 1/*T* was plotted to determine the activation energy of the equation.

$$k = Ae^{-E_a/RT} \qquad (3.17)$$

$$\ln k = -\frac{E_a}{RT} + \ln A \qquad (3.18)$$

CHAPTER 4

RESULTS AND DISCUSSIONS

4.1 Preliminary Studies

A preliminary study was conducted prior to starting the main study in order to screen a higher potential catalyst based on their catalytic performance in biodiesel production. In this study, two catalysts synthesised from different biomass sources were compared in terms of their total acid density and the FAME yield achieved. The first catalyst was synthesised by using wild seaweed as the biomass precursor and sulfonated through thermal decomposition of ammonium sulfate. On the other hand, the second catalyst was synthesised by using corncob as the biomass precursor and sulfonated through arylation of 4-benzenediazonium sulfonate (4-BDS). As shown in Table 4.1, at the same carbonisation temperature and reaction conditions, the FAME yield obtained by the corncob derived catalyst was higher than the seaweed based catalyst. From the comparison, the corncob catalyst had shown higher catalytic performance.

In addition, according to the total acid density obtained by both of the catalysts at different carbonisation temperatures as listed in Table 4.2, the increment of carbonisation temperature would decrease the total acid density of the seaweed based catalyst. In contrast, the total acid density of the corncob based catalyst increased with increasing carbonisation temperature. Although the total acid density of seaweed based catalyst synthesised at 200 ˚C carbonisation temperature had higher total acid density of 2.48 mmol/g compared to corn based catalyst synthesised at 200 ˚C carbonisation temperature, the FAME yield of the corncob based catalyst was still higher. This might be due to the better properties of corncob that made it more suitable to be used as catalyst.

These preliminary results had proven that corncob based catalyst has higher potential to become an efficient catalyst for biodiesel by carrying out further analysis such as further increasing the carbonisation temperature to reach the optimum point. Thereafter in this study, corncob derived catalyst was selected as the primary research material to carry out further investigation on the catalytic performance on the biodiesel production.

Table 4.1: Comparison of FAME yield from different catalysts catalysed for the biodiesel production reaction.

Biomass Source	Carbonisation Temperature (˚C)	FAME Yield (%)
Seaweed	200	23.70
Corncob	200	30.69

Reaction condition: 100 ˚C reaction temperature, 4 hours reaction time, 1: 30 methanol to oil molar ratio and 5 wt.% catalyst loading.

Table 4.2: Total acid density of different catalysts at varying carbonisation temperature.

Carbonisation Temperature (˚C)	Total Acid Density (mmol/g)	
	Seaweed Catalyst	Corncob Catalyst
200	2.48	0.91
300	1.32	1.37
400	1.24	1.45
500	0.88	1.51

4.2 Characterisation of Activated Carbon and Catalyst

4.2.1 Scanning Electron Microscopy

The observation of surface morphology of the H_3PO_4 treated raw corncob (before carbonisation), corncob derived activated carbon (after carbonisation, before sulfonation) and catalyst (after sulfonation) were carried out by using Scanning Electron Microscopy (SEM), Hitachi. Figure 4.1 (a) and (b) project the SEM micrograph of the 30v/v% H_3PO_4 treated raw corncob before being subjected to carbonisation at magnification of 500× and 2000×. They showed that the surface of the raw corncob was layered with very little pores observed. The surface structure of the raw corncob was similar with the SEM image of KOH treated raw corncob reported by Latiff et al. (2016).

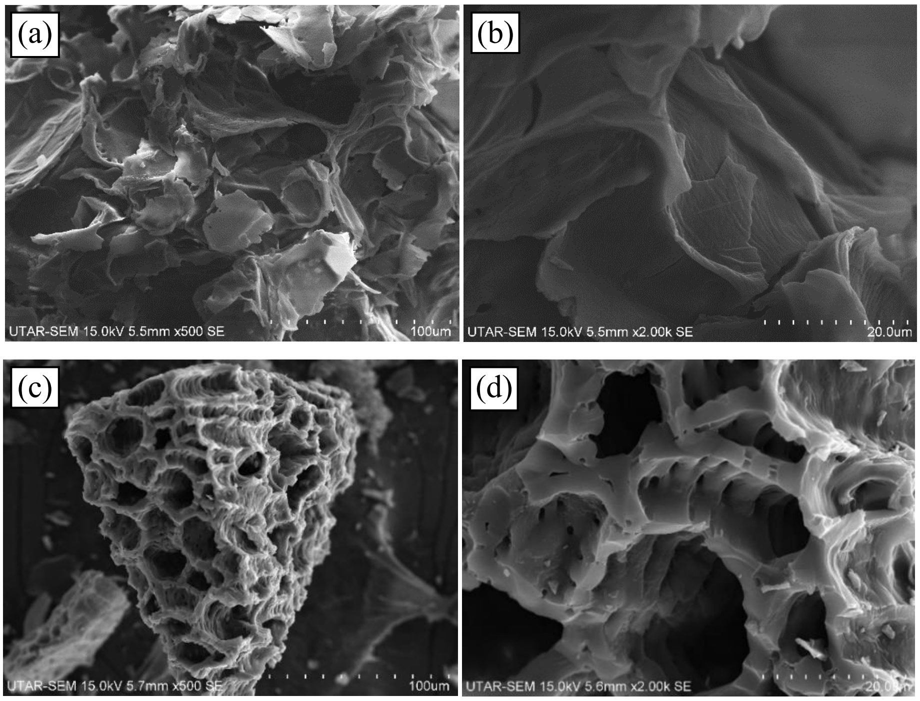

Figure 4.1: SEM image of (a) H_3PO_4 treated raw corncob at 500× (b) H_3PO_4 treated raw corncob at 2000× (c) activated carbon 500× and (d) activated carbon 2000×.

On the other hand, Figure 4.1 (c) and (d) show the micrographs of the corncob derived activated carbon after underwent carbonisation at 900 ºC for 2 hours. As compared to the H_3PO_4 treated raw corncob, the surface of the activated carbon was rougher and more uneven. The activated carbon synthesised appeared to be in a cage like material with smaller pores developed among the large pores. Good pore development was observed on the activated carbon with and the porous structure formed on the activated carbon was able to enhance the catalytic performance in esterification reaction (Konwar et al., 2015). Sun and Webley (2010) had also reported on the H_3PO_4 activated carbon derived corncob that showed similar surface morphology.

Figure 4.2 illustrates the changes of surface structure of the activated carbon produced as the carbonisation temperature was increased. As shown in Figure 4.2, the pore development improves as the carbonisation temperature increased from 600 to 1000 ºC. The surface of the activated carbon slowly transformed from an irregular shaped structure at lower carbonisation temperature to a cage-like structure with multiple porous structure formed during carbonisation. This was in accordance with Sun et al. (2008) which claimed that the increment of carbonisation temperature would enhance the pore formation of the sample. Figure 4.2 (a) and (b) show that the activated carbon produced at carbonisation temperature of 600 ºC had irregular shapes with rough and uneven surface but lesser pores structure was observed since the pores had just started to develop. As the carbonisation temperature raised to 700 ºC, the formation of pores was enhanced and a more uniform pore structure was obtained as illustrated in Figure 4.2 (c) and (d).

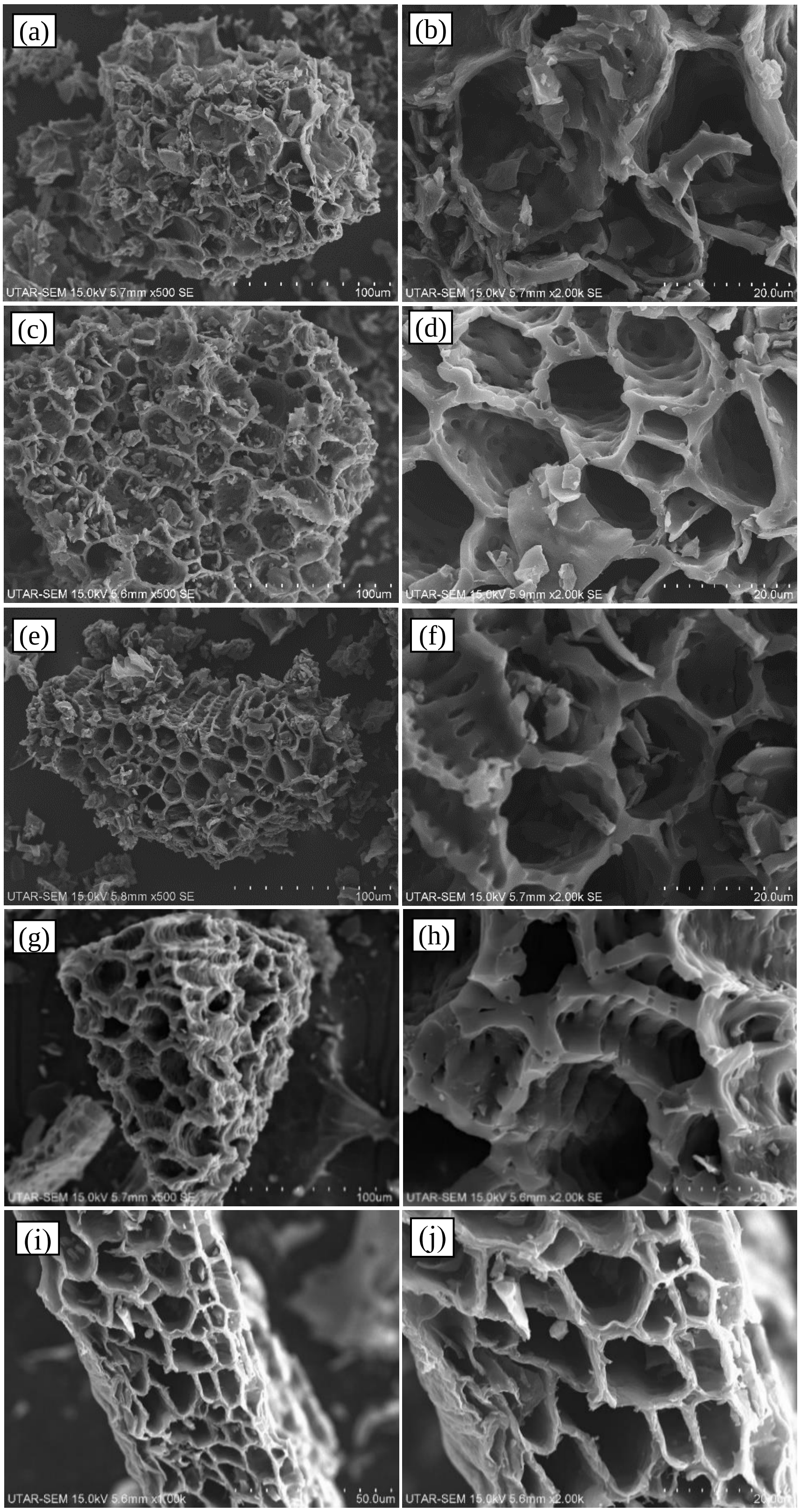

Figure 4.2: SEM images of activated carbon carbonised at (a) 600 ˚C at 500× (b) 600 ˚C at 2000× (c) 700 ˚C at 500× and (d) 700 ˚C 2000× (e) 800 ˚C at 500× (f) 800 ˚C 2000× (g) 900 ˚C at 500× and (h) 900 ˚C 2000× (i) 1000 ˚C at 500× and (j) 1000 ˚C 2000×.

According to Li et al. (2015), H_3PO_4 as the chemical activating agent would be dehydrated into phosphorus pentoxide (P_4O_{10}) and H_2O from 100 to 700 ºC. The P_4O_{10} formed will act as an oxidant to react with the carbon and releases CO_2, forming new pores structure as well as widen the current pores. Therefore, at the carbonisation temperature above 700 ºC, the pore formation was observed to be strongly enhanced.

In this context, the micrographs of activated carbon obtained from carbonisation of 800, 900 and 1000 ºC were compared in Figure 4.2 (e), (g) and (i), respectively. They show that the activated carbon formed were very porous judging from the numerous of black holes observed. The characteristics of activated carbon with high porosity in different pore sizes and shapes would provide sufficient surface area for the attachment of sulfonic groups as active sites. This showed that corncob derived activated carbon could act as a potential catalyst support material for biodiesel production (Fadhil et al., 2016).

On the other hand, Figure 4.3(a) and (b) compares the surface morphology of sample before and after sulfonation whereby sample in Figure 4.3(a) shows the corncob derived activated carbon carbonised at 900 ºC (CCAC900) before undergoing sulfonation and Figure 4.3(b) shows the corncob derived catalyst (Cat_900h) after sulfonation through arylation of 4-BDS at 1.5 hours of sulfonation time and 11: 1 sulfanilic acid to AC weight ratio. As illustrated in Figure 4.3, the surface structure of both samples showed no significant difference before and after undergoing sulfonation. This indicated that sulfonation process through arylation of 4-BDS would not alter the surface structure of the activated carbon and transform to catalyst surface morphology. Nata et al. (2017) and Okamura et al. (2006) had made similar statement that their glucose derived activated carbon showed no noticeable surface changes after sulfonation with hydroxyethylsulfonic acid and concentrated sulfuric acid, respectively.

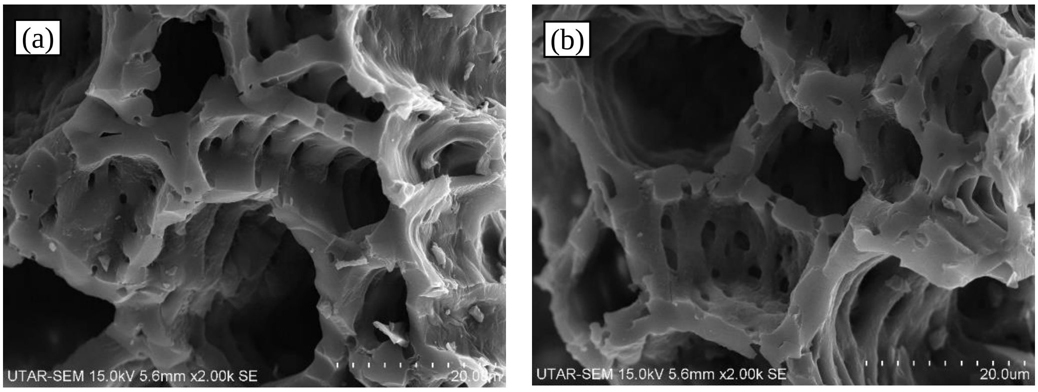

Figure 4.3: SEM images of (a) activated carbon CCAC900 and (b) Cat_900h at magnification of 2000×.

4.2.2 Energy Dispersive X-ray

Elemental composition of the samples were studied by using EDX as shown in Table 4.3. It shows that the carbon content of the corncob was increased significantly from 48.34% to 80.36% after carbonisation at 900 ˚C to form activated carbon (CCAC900) whereas the oxygen content was reduced from 50.56% to 11.65% after transforming into activated carbon. This indicated that corncob was rich in volatiles and organic matters which were released after carbonisation process at high temperature leaving compound with high carbon content for subsequent sulfonation process (Latiff et al., 2016). This enabled corncob to act as a promising raw material for activated carbon synthesis and to be utilised as the catalyst carbon precursor for biodiesel production.

Table 4.3: Elemental composition of different samples.

Sample	Element Composition (Wt. %)			
	C	O	P	S
Corncob	48.34	50.56	-	-
CCAC900	80.36	11.66	7.98	-
Cat_600	75.16	20.5	2.85	1.49
Cat_700	74.6	20.27	2.08	3.05
Cat_800	78.46	14.79	2.58	4.17
Cat_900	78	15.24	1.43	5.34
Cat_1000	81.36	13.32	1.03	4.29
Cat_900a	76.57	17.05	3.4	2.98
Cat_900b	73.02	19.6	0.95	6.43
Cat_900c	76.89	16.81	1.39	4.91
Cat_900d	79.84	14.22	1.62	4.32
Cat_900e	81.91	13.31	1.67	3.84
Cat_900f	74.18	17.73	2.2	6.07
Cat_900g	76.87	13.93	1.85	7.35
Cat_900h	71.06	15.94	3.84	9.16
Cat_900i	77.4	14.33	2.11	6.16

In addition, the activated carbon CCAC900 consisted of 80.36% of carbon (C) atom, 11.66% of oxygen (O) and 7.98% of phosphorus (P). The presence of phosphorus content in the activated carbon might be due to the remaining of phosphoric acid during the chemical activation process. No trace of sulfur (S) was observed on the activated carbon.

As compared to activated carbon, all the catalysts showed the presence of sulfur content on the surface. Figure 4.4 shows the EDX spectrum with peaks representing the C, O, P and S elements. The sulfur content on the catalyst could be associated to the presence of $–SO_3H$ functional group on the surface, indicating successful grafting of the functional group after sulfonation process which allowed the reaction to occur during biodiesel production process (Ayodele and Dawodu, 2014). On the other hand, Table 4.3 also shows that the S content of the catalyst ranged from 1.49% to 9.16% obtained at different carbonisation and sulfonation conditions. The highest S atom was achieved by Cat_900h at 900 ˚C carbonisation temperature, 1.5 hours sulfonation time and 1:11 sulfanilic acid to AC weight ratio. The result obtained was comparable with 3.79 wt.% S content found in the glucose derived carbon acid catalyst as reported by Nata et al. (2017).

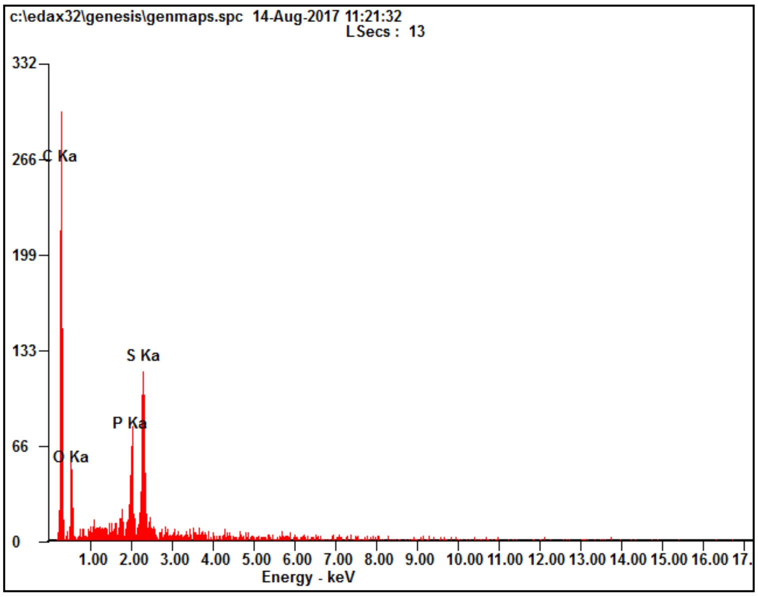

Figure 4.4: EDX spectrum of Cat_900h.

4.2.3 Fourier Transform Infrared Spectroscopy

FT-IR was carried out to identify the functional groups present in the activated carbon and catalyst synthesised. This analysis was carried out mainly to verify the presence of active site –SO_3H group on the catalyst after sulfonation process. It is crucial to ensure the successful anchoring of –SO_3H group onto the carbon support since it is playing an important role to provide a platform for the esterification reaction between PFAD and methanol to produce biodiesel.

Figure 4.5 shows the FT-IR spectra for CCAC900 and Cat_900h from wavelength of 400 to 4000 cm^{-1}. The FT-IR spectra for the activated carbon CCAC900 had peaks at wavelength of 1561 cm^{-1} representing the C=C stretching band of the poly-aromatic hydrocarbon of the activated carbon. On the other hand, there was also peak observed at wavelength of 1725 cm^{-1} from C=O band that indicated the presence of weak acid group –COOH on the carbon sample (Alves et al., 2013; Konwar et al., 2015; Haziratul et al., 2017). Peak appeared at wavelength 2377 cm^{-1} might be due to the adsorption of carbon dioxide from the atmosphere on the surface of activated carbon during carbonisation (Ngaosuwan et al., 2016).

Figure 4.5 also shows the FT-IR spectra of the catalyst Cat_900h. As compared to CCAC900, Cat_900h exhibited similar spectra. The FT-IR spectra of catalyst Cat_900h also exhibited peaks at wavelength of 1560 cm^{-1} and 1724 cm^{-1} due to the C=C stretching of poly-aromatic hydrocarbon and C=O band of weak carboxylic –COOH present, respectively. In addition, the bands at 3408 and 3349 cm^{-1} in CCAC900 and Cat900 represented the –OH stretching of the weak acid –COOH and phenolic –OH group (Ngaosuwan et al., 2016, Chen and Fang, 2011).

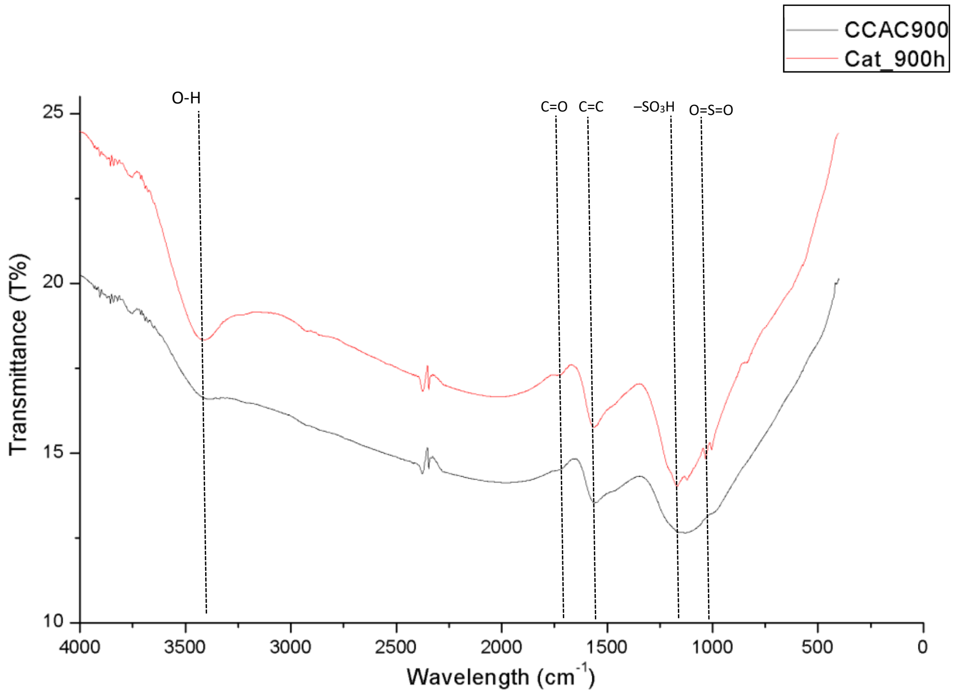

Figure 4.5: FT-IR spectra of activated carbon CCAC900 and catalyst Cat_900h.

The main difference of the spectra between Cat_900h and CCAC900 was that peaks were observed at wavelength 1167 and 1031 cm^{-1} in Cat_900h indicating O=S=O symmetric and asymmetric $–SO_3$ stretching modes, respectively. This was in accordance with the results reported by several literatures that there were also O=S=O and $–SO_3$ stretching present in their catalyst synthesised from bamboo and D-glucose (Zhou et al., 2016, Lokman et al., 2015a). The presence of the $–SO_3$ and O=S=O stretching modes had confirmed the successful attachment of sulfonic group, $–SO_3H$ onto the carbon framework as the active site for esterification reaction.

Figure 4.6 illustrated the FT-IR spectra for catalyst Cat_600, Cat_700, Cat_800, Cat_900 and Cat_1000 synthesised at varied carbonisation temperature of 600, 700, 800, 900 and 1000 ºC respectively. The FT-IR spectra of all the catalysts showed peaks that represented the C=C, C=O and –OH stretching bands on catalyst. Most importantly, the peaks that represent the $–SO_3H$ and O=S=O stretchings were present and these had confirmed the successful sulfonation process. It was observed that the peaks for $–SO_3H$ and O=S=O stretchings of CCAC600, CCAC700 and CCAC800 had lower intensity. This might be due to the lower concentration of the $–SO_3H$ group attatched on the support. A quantitative analysis on the active sites attached to the catalyst through total acid density test was discussed in Section 4.2.6.

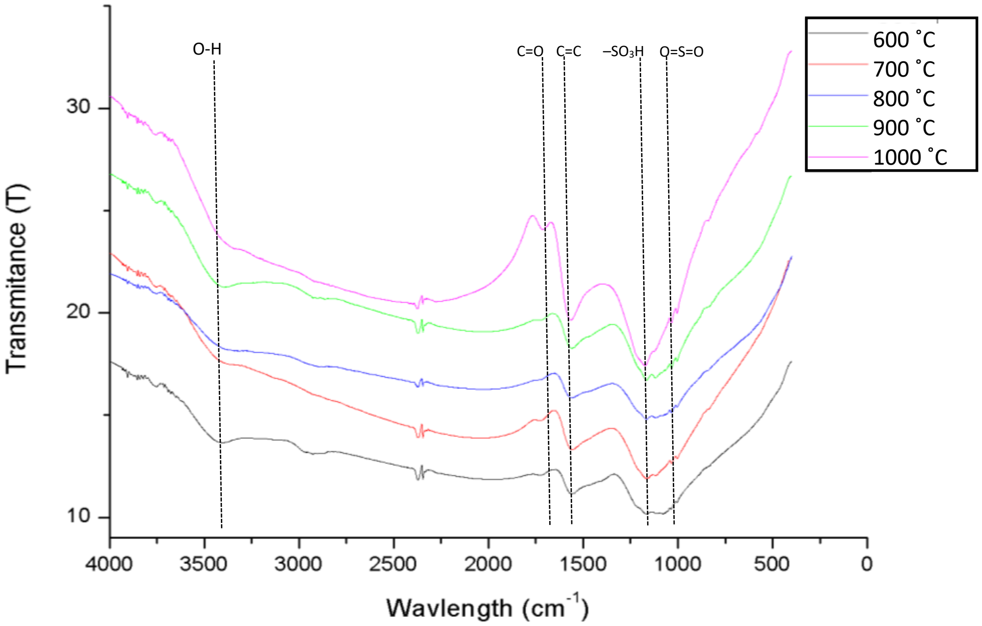

Figure 4.6: FT-IR spectra of catalyst synthesised at different carbonisation temperature.

On the other hand, Figure 4.7 and 4.8 show the FT-IR spectra for the catalyst synthesised at varying sufonation durations (0.5 to 2.5 hours) and sulfanilic acid to AC weight ratio (3: 1 to 13: 1). Similarly, the spectra of the catalysts show the presence of –SO_3H and O=S=O stretching that confirmed the successful anchoring of active site –SO_3H onto the carbon framework. In this case, the performance of the catalyst synthesised at different carbonisation and sulfonation conditions will then be evaluated through the esterification reaction of PFAD and methanol to produce biodiesel.

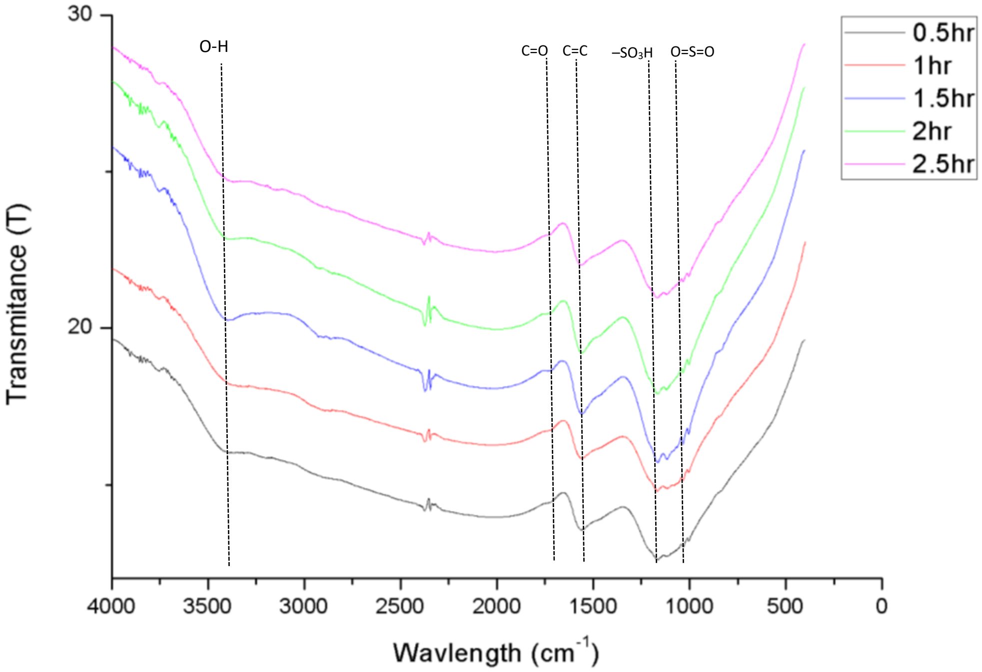

Figure 4.7: FT-IR spectra of catalyst synthesised at different sulfonation time.

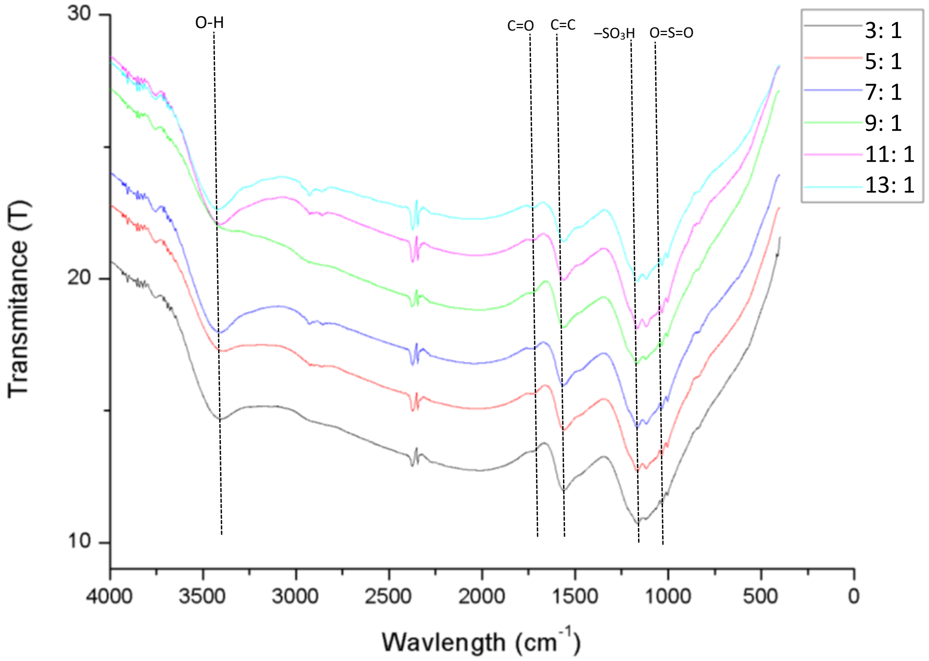

Figure 4.8: FT-IR spectra of catalyst synthesised at different sulfanilic acid to AC weight ratio.

4.2.4 Surface Analysis

Surface analysis was conducted to study the structural properties including the specific surface area, pore volume and pore size of the activated carbon and catalyst samples. The structural properties of the samples are essential as they are one of the key factors that gauge the performance of the catalyst in the reaction (Liu et al., 2008a).

Table 4.4 summarises the BET surface area, pore volume and pore diameter of the samples. It could be noticed that the BET surface area of the activated carbon increased with the carbonisation temperature from 600 to 900 ˚C and the pore volume also increased when the carbonisation temperature increased from 600 to 1000 ˚C.

Table 4.4: Surface properties of activated carbon and catalyst.

Sample	BET Surface Area (m^2/g)	Pore Volume (cm^3/g)	Average Pore Diameter (nm)
CCAC600	18.13	0.0023	6.9100
CCAC700	494.91	0.0871	2.4394
CCAC800	747.90	0.0196	2.4703
CCAC900	972.66	0.1067	2.6283
CCAC1000	929.16	0.1666	2.6743
Cat_900h	721.71	0.0654	3.7940

At higher carbonisation temperature, the activating reactions became more efficient which resulted in the formation of higher surface area and pore volume. In addition, the increment of carbonisation temperature also removed more volatiles compounds and resulted in more pores being formed on the activated carbon (Qu et al., 2015). Results showed that CCAC900 had the highest BET surface area of 972.66 m^2/g. Activated carbon with high surface area is essential in order to provide more site for the grafting of sulfonic groups onto the carbon support for esterification reaction (Lokman et al., 2015a).

The slight reduction in BET surface area when the carbonisation reached 1000 ˚C might be due to the sintering of pores within the activated carbon due to excessive heat (Nachenius et al., 2013). Thus, the surface area of the activated carbon tends to reduce due to the sintering effect between the initially separated pores and larger pore volume was formed.

In addition, it also shows that the pore diameter of the activated carbon had an increasing trend as the carbonisation temperature increased from 700 to

1000 ˚C due to the similar reasons with the increment of surface area and pore volume as mentioned previously. The pore sizes reported from most of the activated carbon formed were usually at the range of above 2 nm in order to provide access to the reactants such as FFA and triglyceride and enable the occurrence of reaction (Ngaosuwan et al., 2016). Figure 4.9 showing the N_2 sorption isotherm of CCAC900 showing the H4 hysteresis loop at p/p_0 range of about 0.4 to 1.0 similar with the isotherm of AC reported by Malins et al. (2015). This indicated that the AC was actually associated with many slit-like pores but would not be taken into account in the reaction since these small pores did not provide higher accessibility to the reactants. However, the pore diameter of CCAC600 was observed to be much larger than the other activated carbon although it was synthesised at lower carbonisation temperature. Its lower surface area rendered it not suitable to be synthesised as high performing carbon catalyst for esterification reaction.

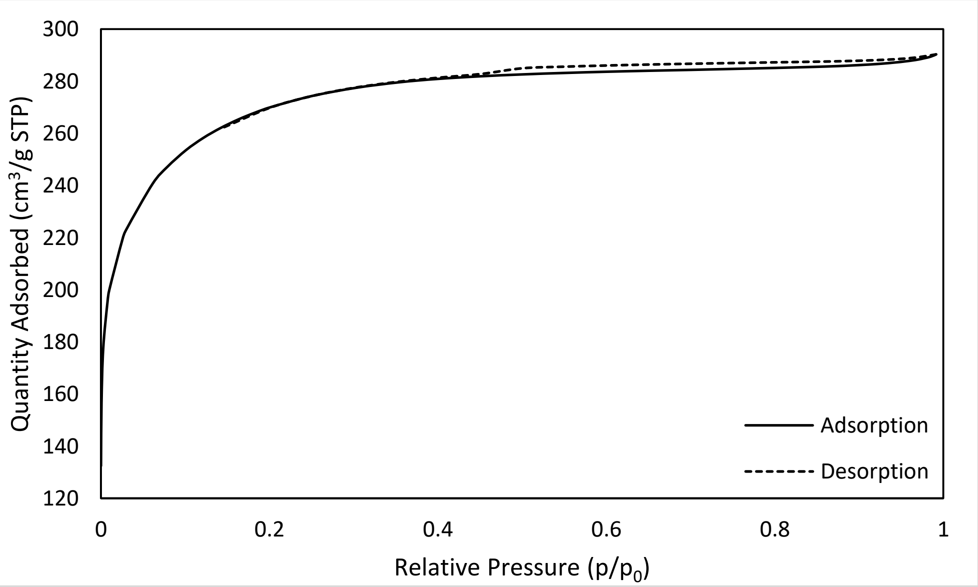

Figure 4.9: N_2 sorption isotherm of CCAC900

At temperature above 400 ˚C, the H_3PO_4 was predicted to be dehydrated to form P_4O_{10} as an oxidant to react with carbon towards the inner part of the structure to form new longitudinal pores (Li et al., 2015). On the other hand, Rodriguez et al. (2017) claimed that the biomass will first required to be completely carbonised at temperature above 600 ˚C prior to the start of activation. Therefore, at the carbonisation temperature of 600 ˚C, the corncob has not been completely carbonised and it might be only the outer surface of corncob was carbonised. Thus, the reaction of P_4O_{10} with carbon would occur sideway instead of towards the inner part, leading to the larger pore diameter formed on the surface.

Nevertheless, the surface properties of activated carbon CCAC900 was compared with catalyst Cat_900h to investigate the changes occurred after undergoing sulfonation. Result shows that the activated carbon experienced the BET surface area and pore volume reduction from 972.66 to 721.71 m^2/g and 0.1067 to 0.0654 cm^3/g, respectively due to the introduction of $-SO_3H$ groups onto the activated carbon surface during the sulfonation process which had occupied part of the vacant pores (Haziratul Mardhiah et al., 2017; Niu et al., 2018). Furthermore, the reduction of surface area and pore volume had also confirmed the successful attachments of the $-SO_3H$ groups onto the surface of activated carbon to form heterogeneous acidic catalyst for esterification reactions (Endut et al., 2017).

4.2.5 Thermogravimetric Analysis

Figure 4.10 shows the weight loss profile from thermogravimetric analysis (TGA) of H_3PO_4 treated raw corncob and Cat_900h heated from 30 to 1000 ˚C in nitrogen flow. Results showed that H_3PO_4 treated raw corncob exhibited a more significant weight loss than Cat_900h. This can be attributed to the high volatiles content found in the corncob as compared to the catalyst.

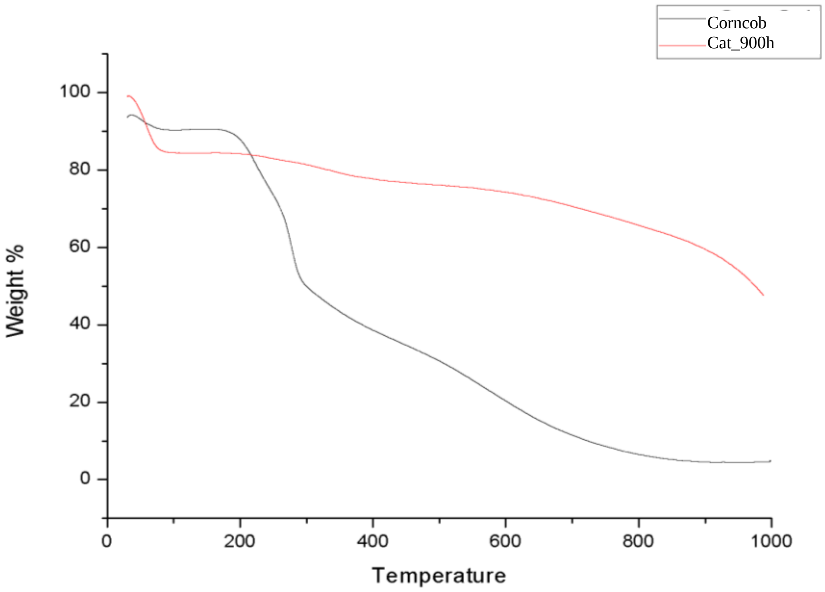

Figure 4.10: Temperature dependent mass loss curve for H_3PO_4 treated raw corncob and Cat_900h.

The weight loss of H_3PO_4 treated raw corncob can be categorised into three main stages. The first stage weight loss from initial room temperature to about 100 ˚C occurred when the physically absorbed atmospheric moisture was removed. Next, second stage of weight loss occurred at around 150 to 300 ˚C. It could be contributed by the removal of volatile components due to thermal decomposition of cellulose, hemicellulose and partial lignin. It was then followed by the weight loss at above 300 ˚C due to the further decomposition of lignin (Liu et al., 2017). The weight of the sample started to remain constant starting from the temperature of about 900 ˚C.

On the other hand, TGA has been carried out to investigate the thermal stability of catalyst. It can be studied through the weight loss profile of Cat_900h. Similarly, the weight loss from initial temperature to 100 ˚C was mainly because of the evaporation of absorbed water. As compared to H_3PO_4 treated raw corncob, it was observed that the weight loss of catalyst was more significant at this stage, this might be due to the higher amount of atmospheric moisture being physically adsorbed since catalyst had higher surface area.

Next, further weight loss at about 230 ˚C may be due to the decomposition of the functional groups such as the $–SO_3H$ group attached on the carbon (Lee, 2013). This showed that the catalyst is thermally stable until 230 ˚C where the functional groups attached onto the catalyst had started to decompose. In other words, the catalyst was thermally stable in the biodiesel production reaction up to the reaction temperature of 230 ˚C which is way beyond the temperature range for esterification reaction conducted in this study. Ayodele and Dawodu (2014) reported that the cellulose derived carbon acid catalyst had the similar thermal stability where the $–SO_3H$ groups started to decompose at 223 ˚C. In addition, Lokman et al. (2015a) also reported that the D-glucose derived catalyst experienced weight loss at 132 to 285 ˚C was attributed to the decomposition of $–SO_3H$.

4.2.6 Total Acid Density Test

Total acid density of the catalyst was obtained through back titration method. Basically, the total acid density analysis focuses on the presence of acid groups such as $–SO_3H$, –COOH and –OH attaching on the carbon structure of catalyst. The quantity of the acidic groups present in the catalyst is important since they act as the active site for reaction to occur as well as helping in the dispersion of catalyst into the reaction mixture to minimise the mass transfer limitation.

Figure 4.11 shows the total acid density of catalyst synthesised from carbonisation temperature of 600 to 1000 ºC. As shown in the figure, the total acid density of the catalyst carbonised at 600 ºC was as low as 1.55 mmol/g. The total acid density subsequently increased with the increment of carbonisation temperature from 600 to 900 ºC with the highest total acid density of 2.04 mmol/g was recorded. The total acid density showed insignificant changes when the carbonisation temperature was further increased to 1000 ºC.

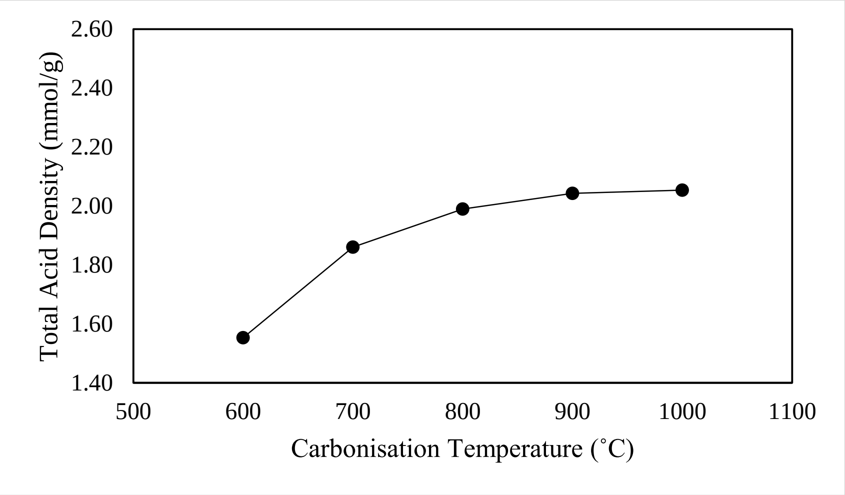

Figure 4.11: Total acid density of catalyst synthesised at different carbonisation temperature, 1 hour sulfonation time and 5:1 sulfanilic acid to AC weight ratio (Reaction conditions: 100 ˚C, 4 hours, 5 wt.% catalyst loading, 30:1 methanol to oil molar ratio).

This trend was in accordance with the surface area for activated carbon synthesised at different carbonisation temperatures from the surface analysis carried out as discussed in Section 4.2.4. Since the increment of carbonisation temperature had directly increased the surface area of carbon support until optimum, this has allowed the attachment of higher density of active groups during sulfonation.

Next, the effect of sulfonation duration on the total acid density of catalyst was also studied as shown in Figure 4.12. At the sulfonation time of 0.5 hour, the total acid density obtained by the catalyst was 2.00 mmol/g. It was then slowly increased to 2.04 and then 2.16 mmol/g when the sulfonation duration was lengthen to 1 and 1.5 hour, respectively. At the sulfonation duration above 1.5 hour, the total acid density of the catalyst showed no significant changes.

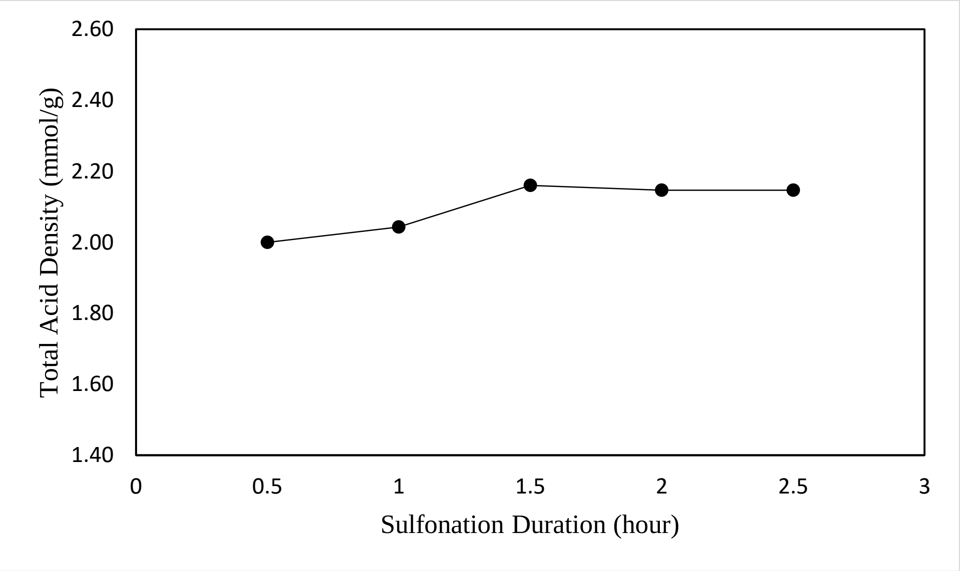

Figure 4.12: Total acid density of catalyst synthesised at different sulfonation time, carbonisation temperature of 900 ºC and 5:1 sulfanilic acid to AC weight ratio (Reaction conditions: 100 ˚C, 4 hours, 5 wt.% catalyst loading, 30:1 methanol to oil molar ratio).

These results showed that sufficient time was required in order to facilitate the attachment of maximum amount of active groups onto the carbon framework. Sulfonation process by arylation of 4-BDS typically involves several steps including the reduction of aromatic rings of 4-BDS to form radicals and then forming carbon-carbon bond with the H-terminated carbon surface of the activated carbon (Abiman et al., 2008). Therefore, longer duration is more favourable for the linkage of sulfonic group onto the carbon support. Lokman et al. (2015b) also found that the increment of duration during the sulfonation of D-glucose derived carbon had increased the total acid density of the catalyst.

Nevertheless, Figure 4.13 illustrates the effect of sulfanilic acid to AC weight ratio to the total acid density of the catalyst synthesised. In this study, the amount of activated carbon was fixed at 3 g as the basis for the varying amount of sulfanilic acid used. As the sulfanilic acid to AC weight ratio increased, the total acid density of catalyst was also increased up to an optimum point. Catalyst synthesised from weight ratio of 3: 1 had the lowest total acid density of 0.86 mmol/g and then gradually increased to 2.48 mmol/g at sulfanilic acid to weight ratio of 11: 1.

Sulfanilic acid is one of the key chemicals required for the synthesis of 4-BDS as the sulfonating agent. Therefore, it was expected that the amount of sulfanilic acid added into the 4-BDS synthesis process was a crucial factor to optimise the amount of sulfonic groups attached to the catalyst. Increasing the amount of sulfanilic acid for sulfonation was able to increase the amount of 4-BDS formed and directly increased the acid groups anchored onto the activated carbon. This could be attributed to the enhanced contact rate between the sulfonating agents with the activated carbon for successful grafting.

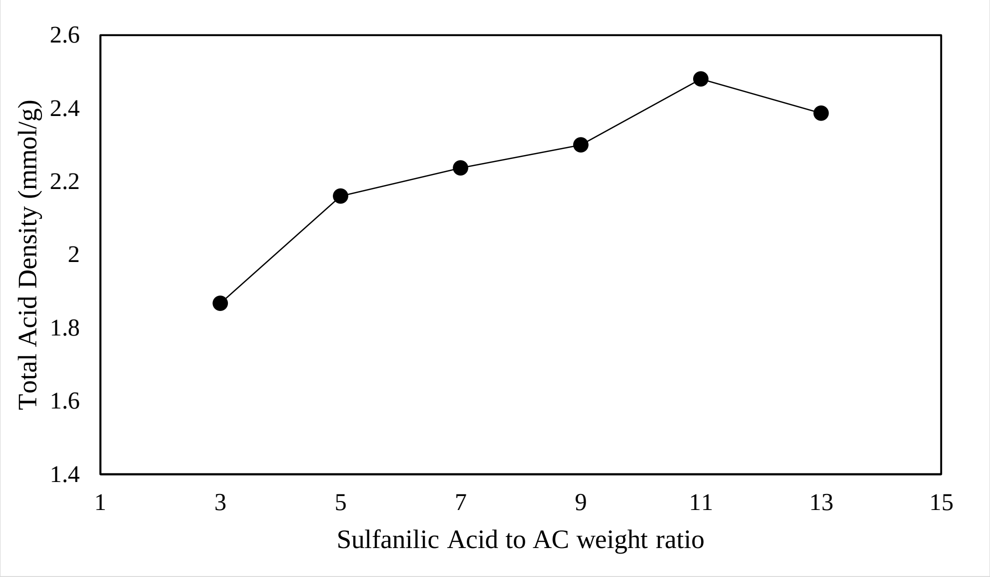

Figure 4.13: Total acid density of catalyst synthesised at different sulfanilic acid to AC weight ratio, carbonisation temperature of 900 ºC and 1.5 hour sulfonation time (Reaction conditions: 100 ˚C, 4 hours, 5 wt.% catalyst loading, 30:1 methanol to oil molar ratio).

However, a slight drop on the total acid density was recorded when the sulfanilic acid to AC weight ratio was further increased to 13: 1. This was possibly due to the excessive high amount of sulfonating agent which had increased the viscosity of the reactants and reduced the collision rate between the sulfonating agents and activated carbon. Similar trend was also reported by Malins et al. (2015) on their investigation of sulfanilic to AC weight ratio and found that the acid density of catalyst supported by AC grains increased with the increment of sulfanilic to AC weight ratio until the optimum point was reached then the acid density started to reduce when further increased the weight ratio.

4.3 Effect of Catalyst Synthesis Parameters on Biodiesel Production

The catalytic performance of the catalyst synthesised at varying conditions was determined based on the FAME yield and FFA conversion obtained from esterification reaction. The effect of carbonisation temperature, sulfonation duration and sulfanilic acid to AC weight ratio to the FAME yield and FFA conversion were studied in order to synthesise the optimum catalyst in this study.

The FFA conversion was calculated based on the difference in acid value of the feedstock and biodiesel produced. This conversion was directly related to the percentage of FFA present in PFAD being converted into FAME through esterification. On the other hand, FAME yield was determined based on the concentration of methyl esters (methyl palmitate, methyl stearate, methyl oleate and methyl linoleate) present in the final product through esterification of FFA and transesterification of triglyceride.

4.3.1 Effect of Carbonisation Temperature

Carbonisation was performed in order to transform the raw corncob into carbon material by eliminating the volatile components present through high temperature treatment. Figure 4.14 shows the FAME yield and FFA conversion by using catalyst synthesised at carbonisation temperature of 600 to 1000 ˚C.

As shown in Figure 4.14, both FAME yield and conversion exhibited positive trend as the carbonisation temperature increased. Starting from 600 ˚C, the FAME yield obtained was 45.59%, when the carbonization temperature was increased to 900 ˚C, maximum FAME yield of 59.69% was obtained and further increasing the carbonization temperature gave no significant changes to the FAME yield. As for the FAME conversion, it was raised to 59.69% when the carbonisation temperature was increased from 600 to 900 ˚C.

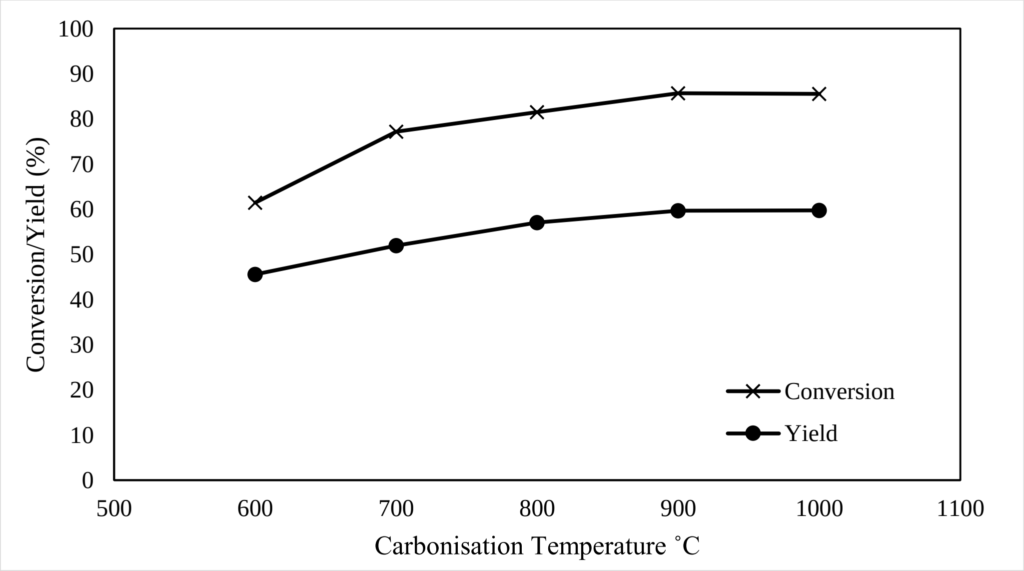

Figure 4.14: FAME yield and conversion using catalyst synthesised at different carbonisation temperature, 1.5 hour sulfonation time and 5: 1 sulfanilic acid to AC weight ratio (Reaction conditions: 100 ˚C, 4 hours, 5 wt.% catalyst loading, 30:1 methanol to oil molar ratio).

Higher carbonisation temperature can produce carbon support with higher surface area which provides a larger platform for the reaction to occur (Qu et al., 2015). On the other hand, the increase of the pore diameter along with the rise in carbonization temperature also helped to give a better access for the large reactants molecule to reach the active sites on the synthesized catalyst (Liu et al., 2008a).

It was observed that the total acid density in Figure 4.11 exhibited similar trend with the FAME yield and conversion and this has proven that total acid density of the catalyst is one of the crucial factors judging the performance of catalyst. Since the total acid density of a catalyst was contributed by the acidic sulfonic groups as the reaction active site, the increment of total acid density would also give synergistic effect to the FAME yield and conversion obtained (Zhou et al., 2016).

4.3.2 Effect of Sulfonation Time

Sulfonation is one of the essential stages in the process of synthesising a carbon acid catalyst for biodiesel production. It is the stage where the active groups –SO_3H is being grafted onto the carbon support acting as a connection bridge between the reactants in esterification reaction. Thus, the duration to allow the sulfonation to occur is important as it will directly affect the activity of the catalyst synthesised.

Figure 4.15 projects the FAME yield and FFA conversion achieved by the esterification reaction catalysed by catalyst synthesised at sulfonation duration of 0.5 to 2.5 hours. Both FAME yield and FFA conversion obtained an optimum point when the catalyst synthesised at 1.5 hours sulfonation time was used in the reaction. From sulfonation time of 0.5 to 1.5 hours, the FAME yield and FFA conversion increased from 38.8 to 66.37% and 63.66 to 89.7%, respectively.

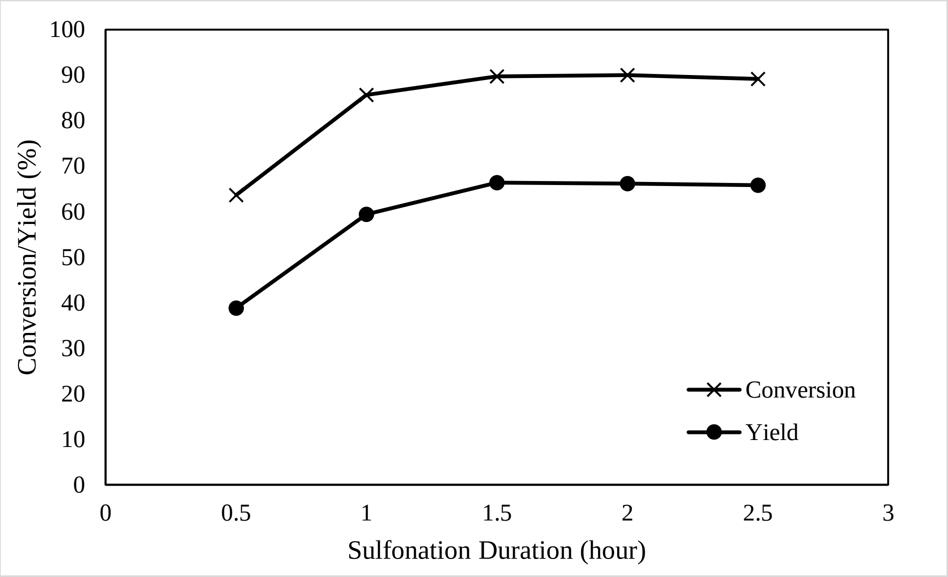

Figure 4.15: FAME yield and conversion using catalyst synthesised at different sulfonation time, carbonisation temperature of 900 ºC and 5: 1 sulfanilic acid to AC weight ratio (Reaction conditions: 100 ˚C, 4 hours, 5 wt.% catalyst loading, 30:1 methanol to oil molar ratio).

Longer reaction time was necessary to ensure sufficient time given for the grafting of active groups –SO_3H onto the activated carbon support (Niu et al., 2018). Therefore, prolonged sulfonation duration was able to enhance the density of acidic active sites on the catalyst to improve the catalytic activity in reaction. In this case, the FAME yield and conversion in Figure 4.15 also had presented the same trend with the total acid density of catalyst in Figure 4.12.

4.3.3 Effect of Sulfanilic Acid to Activated Carbon Weight Ratio

Sulfanilic acid, also known as 4-aminobenzenesulfonic acid is an important compound used for the synthesis of 4-BDS. The amount of sulfanilic acid added for the synthesis of 4-BDS is crucial as it determines the amount of 4-BDS being synthesised which will then be used in the sulfonation process with carbon catalyst as support through arylation and reduction reaction.

Figure 4.16 shows FAME yield and conversion obtained by using catalyst synthesised at sulfanilic acid to AC weight ratio of 3: 1 to 13:1. According to the figure, the FAME yield increased from 41.07 to 72.08% as the weight ratio increased from 3: 1 to 11: 1 and slightly dropped when the weight ratio was further increased to 13: 1. Similar trend was observed from the FAME conversion whereby the FAME conversion at sulfanilic acid to AC weight ratio of 3: 1 was 85.36% and further increment of the weight ratio to 11: 1 successfully raised the FAME conversion to 93.49%.

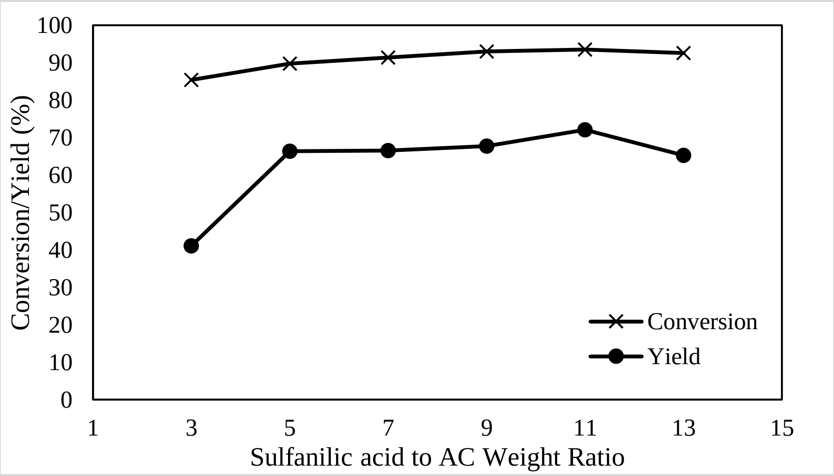

Figure 4.16: FAME yield and conversion using catalyst synthesised at different sulfanilic acid to AC weight ratio, carbonisation temperature of 900 ºC and 1.5 hours reaction time (Reaction conditions: 100 ˚C, 4 hours, 5 wt.% catalyst loading, 30:1 methanol to oil molar ratio).

The result obtained followed the trend of the total acid density of the catalyst in Figure 4.13. Since increasing the amount of sulfanilic acid added was able to increase the acid density of the catalyst, this showed that it could provide more active site to the catalyst for the esterification reaction (Malins et al., 2015). Therefore, the optimum FAME yield and conversion were obtained by using Cat_900h synthesised at 900 ˚C carbonisation temperature, 1.5 hours sulfonation time and 11: 1 sulfanilic acid to AC weight ratio. This catalyst was then used for the subsequent studies.

In overall, the FFA conversion obtained was higher than the FAME yield. Since FAME conversion involves only the conversion of FFA in PFAD while FAME yield involves the conversion of both FFA and triglyceride molecules in PFAD, it shows that the catalysts were able to effectively convert the FFA into FAME. The conversion of triglyceride was slightly more intensive as the triglyceride molecule is bulkier and may be difficult to access to the active sites of the catalyst (Ngaosuwan et al., 2016).

4.4 Optimisation Study of Reaction Parameters

The reaction optimisation study of biodiesel production was done by using the response surface methodology (RSM) with a four factors and five levels central composite design (CCD). The reaction parameters studied include reaction temperature (60 – 100 ˚C), reaction time (2.5 – 6.5 hours), catalyst loading (5-11 wt.%) and methanol to oil molar ratio (13: 1 to 29:1) with FAME yield (%) as the response. The statistical analysis was performed by using the software Design Expert 7.0 and optimisation study was completed via analysis of variance (ANOVA) with a quadratic regression model.

4.4.1 Quadratic Regression Model

Table 4.5 illustrated the actual and predicted biodiesel yield obtained based on the independent variables of 30 experimental runs. As shown in the table, the FAME yield obtained falls in the range of 49.59 - 85.58 %. The highest FAME yield was achieved at experiment run 9 with reaction conditions of reaction temperature 80 ˚C, reaction time of 4.5 hours, catalyst loading of 14 wt.% and methanol to oil molar ratio of 21: 1. The response (FAME yield) was calculated from the quadratic regression equation as shown in Equation 4.1.

$$\begin{aligned} Y \;=\; & 76.41 + 4.03A + 5.69B + 3.59 + 1.94D - 0.52AB - 0.20AC - 1.44AD \\ & - 1.18BC - 0.51BD - 0.44CD - 3.41A^2 - 2.13B^2 + 1.01C^2 - 1.43D^2 \qquad (4.1) \end{aligned}$$

In Equation 4.1, Y is the biodiesel yield, A, B, C and D represent the temperature (˚C), time (hour), catalyst loading (wt.%) and methanol to oil molar ratio, respectively. According to the regression, all four factors A, B, C and D gave positive effect towards the biodiesel yield where increasing the temperature, time, catalyst loading and methanol to oil molar ratio would actually increase the biodiesel yield until an optimum point.

Table 4.5: Actual and predicted response at difference combinations of reaction variables.

Run no.	A Temperature (˚C)	B Time (hour)	C Catalyst Loading (wt.%)	D Methanol to oil molar ratio	Actual Yield (%)	Predicted Yield (%)
1	80	4.5	8	37	73.59	74.58
2	60	2.5	5	13	50.94	50.92
3	80	4.5	8	21	74.33	76.41
4	60	6.5	5	29	77.43	73.35
5	80	8.5	8	21	78.71	79.27
6	100	2.5	11	29	73.99	74.47
7	100	6.5	5	29	76.62	77.86
8	60	2.5	11	13	63.38	61.73
9	80	4.5	14	21	85.58	87.65
10	100	2.5	5	13	65.51	63.30
11	100	6.5	11	13	84.01	82.32
12	80	4.5	8	5	66.85	66.80
13	60	2.5	5	29	58.32	59.59
14	80	4.5	8	21	75.06	76.41
15	80	4.5	8	21	73.64	76.41
16	100	6.5	5	13	72.71	77.00
17	100	2.5	5	29	64.52	66.20
18	80	4.5	8	21	79.21	76.41
19	80	4.5	8	21	77.45	76.41
20	120	4.5	8	21	74.71	70.84
21	40	4.5	8	21	49.89	54.72
22	80	4.5	2	21	74.40	73.28
23	100	2.5	11	13	69.79	73.33
24	60	6.5	11	29	75.90	77.69
25	100	6.5	11	29	81.93	81.42
26	60	6.5	5	13	67.60	66.71
27	80	0.5	8	21	56.12	56.52
28	60	6.5	11	13	75.04	72.82
29	60	2.5	11	29	73.46	68.64
30	80	4.5	8	21	78.76	76.41

Table 4.6 shows the analysis of variance (ANOVA) obtained from RSM. ANOVA was performed to study the statistical significance and fitness of the regression model. In addition, the significance and interaction effects of the individual terms on the response were also investigated. According to the results obtained from ANOVA, the F value of the regression model obtained was high at 13.43 with the small p-value of less than 0.0001 and this had indicated that the model was highly significant at 95% confidence level (Anwar et al., 2018).

In this case, when p-value is less than 0.05, it indicated that the model terms were significant. In contrast, when p- value of the model term was greater than 0.1, it indicated that the term is insignificant at 95% confidence level (Dharma et al., 2016). Therefore, the terms of A (temperature), B (time), C (catalyst loading), D (methanol to oil molar ratio), A^2 (quadratic effect of temperature), B^2 (quadratic effect of time) and D^2 (quadratic effect of methanol to oil molar ratio) showed significant effect towards the biodiesel yield.

Lack of fit in the ANOVA indicates that the model is insufficient to describe the relationship between the independent variables and dependant variables. In this study, F value and p-value obtained were 2.51 and 0.1608, respectively which indicated that the lack of fit was insignificant. In other words, it means there was appropriate fitting between the experimental data and regression model. It was noted that the R-squared (R^2) of the model is 0.9260 indicated that 92.6% of the variation could be explained by the model. However, the difference between Predicted R-Squared of 0.6273 and the Adjusted R-Squared of 0.8571 is slightly larger than 0.2 which may indicate a large block effect. Figure 4.17 shows the graph of predicted response versus the actual response, indicating quite a good fit of the collected experimental data with the regression model.

Table 4.6: Results for analysis of variance of quadratic regression.

Source	Sum of Squares	Degree of freedom	Mean Square	F Value	p-value Prob > F	Remarks
Model	2135.68	14	152.55	13.43	< 0.0001	significant
A: Temperature	389.49	1	389.49	34.28	< 0.0001	significant
B: Time	776.33	1	776.33	68.32	< 0.0001	significant
C: Catalyst Loading	309.76	1	309.76	27.26	0.0001	significant
D: Molar Ratio	90.77	1	90.77	7.99	0.0128	significant
AB	4.40	1	4.40	0.39	0.5429	
AC	0.61	1	0.61	0.05	0.8199	
AD	33.35	1	33.35	2.93	0.1073	
BC	22.11	1	22.11	1.95	0.1833	
BD	4.14	1	4.14	0.36	0.5550	
CD	3.12	1	3.12	0.27	0.6079	
A^2	318.51	1	318.51	28.03	< 0.0001	significant
B^2	124.31	1	124.31	10.94	0.0048	significant
C^2	28.24	1	28.24	2.49	0.1358	
D^2	56.01	1	56.01	4.93	0.0422	significant
Residual	170.44	15	11.36			
Lack of Fit	142.12	10	14.21	2.51	0.1608	insignificant
Pure Error	28.32	5	5.66			
Cor Total	2306.12	29				
Mean	71.64954			Adj R-Squared	0.857109	
C.V. %	4.70469			Pred R-Squared	0.627333	
R-Squared	0.926091			Adeq Precision	15.41283	

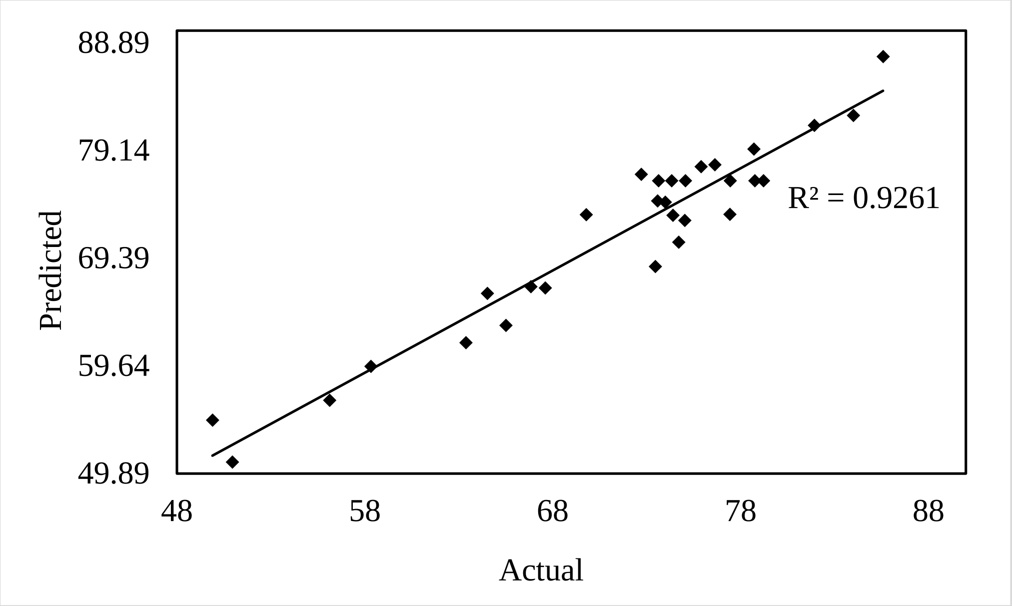

Figure 4.17: Graph of predicted versus actual FAME yield (%).

4.4.2 Response Surface Study

The three dimensional surface response curves were plotted to study the effect of the reaction parameters (reaction temperature, reaction time, catalyst loading and methanol to oil molar ratio) towards the response and their interaction effects. The surface plots of the response (FAME yield) calculated from Equation 4.1 are shown in Figure 4.18 to 4.23.

4.4.2.1 Effect of Reaction Temperature and Methanol to Oil Molar Ratio

The response surface plot of reaction temperature, methanol to oil molar ratio and FAME yield at constant reaction time of 4.5 hours and 8.0 wt.% catalyst loading is as shown in Figure 4.18. According to the response surface plot, at the methanol to oil molar ratio of 29: 1 and at 90 ˚C reaction temperature, FAME yield of about 76% was recorded. FAME yield slightly decreased when the reaction temperature was further increased to 100 ˚C. In addition, at the reaction temperture of 100 ˚C, the FAME yield showed positive effect when the methanol to oil molar ratio increased to 21: 1 and then started to decline when the molar ratio further increased. However, when the reaction temperature was at 60 ˚C, the highest FAME yield was only recorded at 73% at methanol to oil molar ratio of 29: 1.

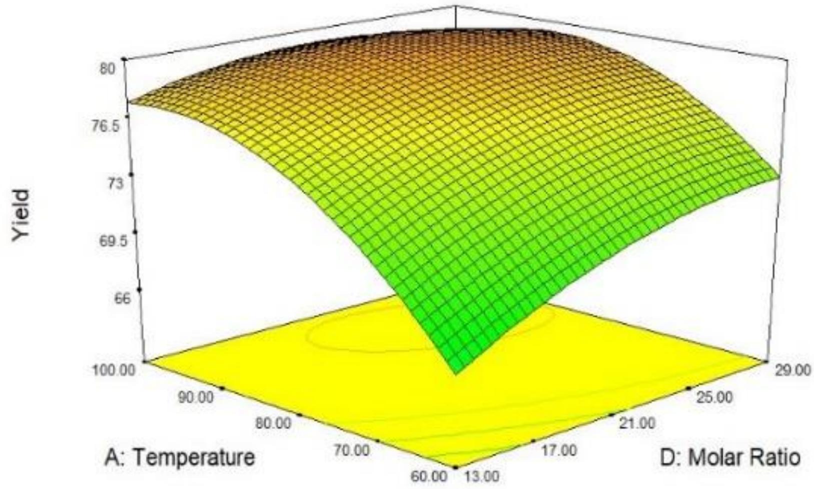

Figure 4.18: Three dimension surface response plot of FAME yield, temperature (˚C) and methanol to oil molar ratio at 4.5 hours reaction time and catalyst loading of 8.0 wt.%.

In this case, the optimum FAME yield of about 78% was achieved at reaction temperature of 90 ˚C and methanol to oil molar ratio of 21: 1. There were several researches which reported similar optimum methanol to oil molar ratio at around 20: 1 with differet catalyst. Konwar et al. (2015) had achieved FAME conversionof 97% at methanol to oil molar ratio of 20: 1, 10 hour reaction time, 70 ˚C reaction temperature and 1.2 wt.% catalyst loading by using catalyst derived from de-oiled waste cake in the esterification reaction of oleic acid and methanol. Further more, Zhang et al. (2015) had also reported on the optimum methanol to oil molar ratio of 24: 1 in the reaction between *jatropha* oil and methanol with glucose derived catalyst, which is also close to the current finding.

The increment of methanol to oil molar ratio gave positive effect to the reaction since adding methanol in excess helped to drive the equilibrium of reversible reaction towards the product side. However, excessive addition of methanol would lead to the negative effect to the esterfication reaction leading to the reduction of FAME yield. This was due to higher volume of methanol added would dilute the reaction system and reduce the collision rate of reactants with the catalyst resulting in lower amount of FAME formed (Ezebor et al., 2014b; Zhou et al., 2016).

4.4.2.2 Effect of Reaction Temperature and Reaction Time

Figure 4.19 shows the response surface plot of reaction temperature, reaction time and FAME yield at constant methanol to oil molar ratio of 21: 1 and 8.0 wt.% catalyst loading. Both the effects of reaction temperature and reaction time gave similar positive trends towards the FAME yield. The maximum FAME yield of about 80% was obtained at the temperature of about 90 ˚C and reaction time of 6.3 hours. Longer reaction time was necessary to provide sufficient time for a good mass transfer between the reactants and catalyst and to ensure that the reaction was able to react completely on the catalyst active sites (Dawodu et al., 2014; Zhou et al., 2016)

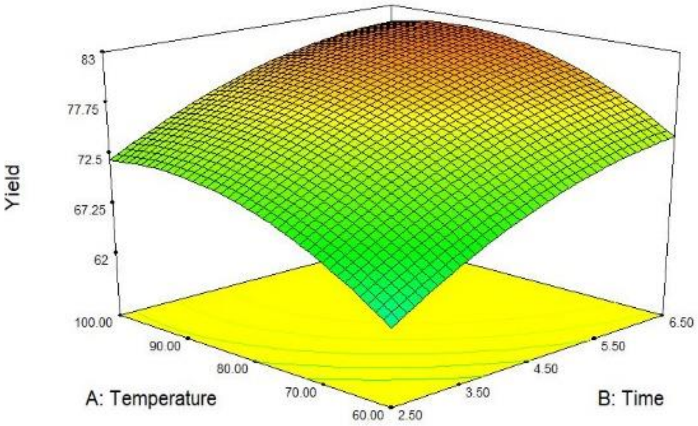

Figure 4.19: Three dimension surface response plot of FAME yield, temperature (˚C) and reaction time (hour) at methanol to oil molar ratio of 21: 1 and 8.0 wt.% catalyst loading.

As shown in the surface response plot in Figure 4.19, at the reaction time range of 2.5 to 6.5 hours, the optimum reaction temperature of was always at 90 ˚C. On the other hand, the reaction time of 6.5 hours was always the optimum reaction duration regardless the change of reaction temperature. Therefore, it shows that the change of reaction time would not affect the optimum reaction temperature and vice versa. This might be due to the less interaction effect between both of these reaction parameters.

4.4.2.3 Effect of Reaction Temperature and Catalyst Loading

From the surface response plot as shown in Figure 4.20, it shows the plot of reaction temperature, catalyst loading and FAME yield at the constant reaction time of 4.5 hours and methanol to oil molar ratio of 21: 1. At the catalyst loading of 11 wt.%, the FAME yield increased when reaction temperature increased and reached the optimum yield at reaction temperature of about 90 ˚C with the maximised FAME yield of about 75%.

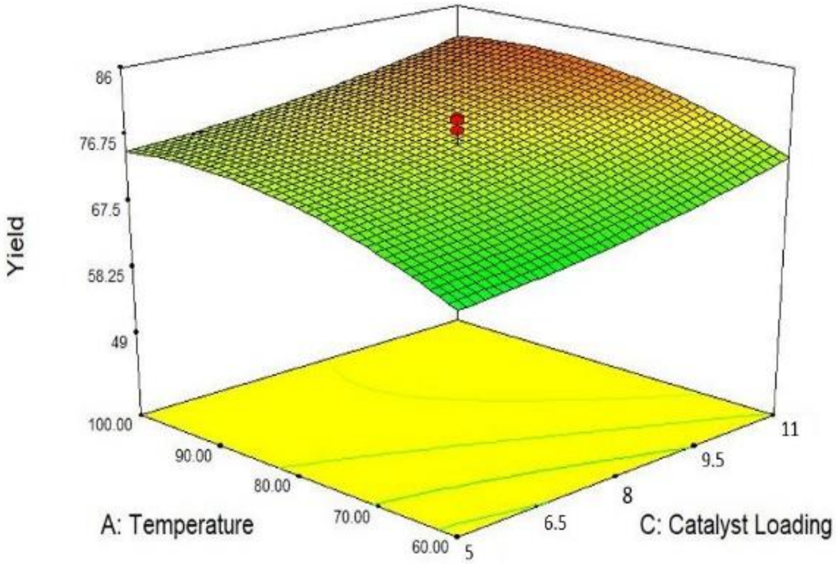

Figure 4.20: Three dimension surface response plot of FAME yield, temperature (˚C) and catalyst loading (wt.%) at 4.5 hours reaction time and methanol to oil molar ratio of 21: 1.

The optimum reaction temperature of 90˚C in this case was in accordance with the studies as reported by Zhou et al. (2016) that had recorded the optimum reaction temperature of 90 ˚C in the esterification reaction of oleic acid and methanol with bamboo derived carbon catalyst. The increment of reaction temperature was able to push the reaction equilibrium towards the right that favors the product formation. In addition, a sufficiently high temperature is also necessary in order to promote the protonation of acid catalyst to start a reaction (Ayodele and Dawodu, 2014; Zhou et al., 2016).

According to the ANOVA analysis, the reaction temperature and catalyst loading showed the least interaction effect between each other. This is similar the literature reported by Regalado et al. (2017) where the reaction temperature and catalyst loading has only moderate interaction in the transesterification reaction of oil and methanol with NaOH as catalyst.

4.4.2.4 Effect of Reaction Time and Catalyst Loading

Figure 4.21 shows the surface response plot of reaction time, catalyst loading and FAME yield at constant reaction temperature of 80 ˚C and 21: 1 methanol to oil molar ratio. As shown in the figure, the maximum FAME yield of about 83% was obtained at reaction time of 6.4 hours and 11 wt.% catalyst loading.

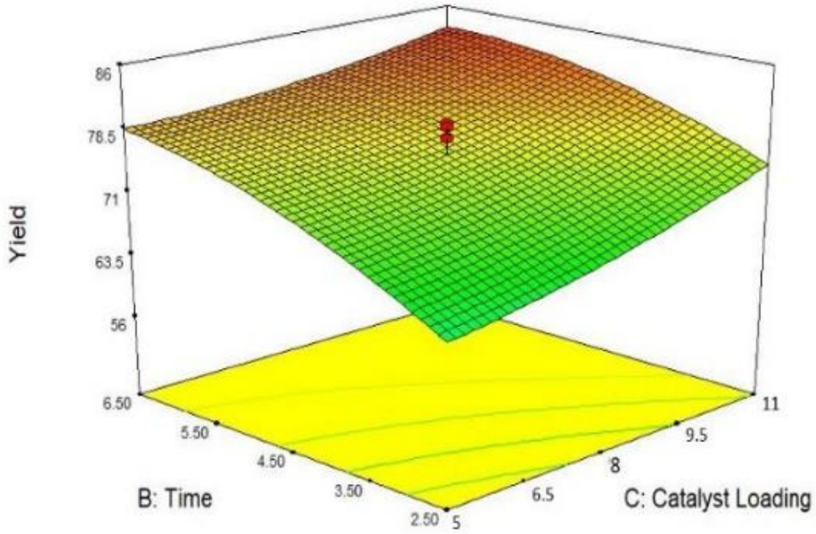

Figure 4.21: Three dimension surface response plot of FAME yield, reaction time (hour) and catalyst loading (wt.%) at reaction temperature of 80 ˚C and methanol to oil molar ratio of 21: 1.

As shown in the surface response plot, the increment of reaction time will lead to the increment FAME yield and this trend was observed in the investigation reported by Shu et al. (2009) in the reaction of cottonseed oil and methanol with vegetable asphalt derived catalyst. On the other hand, it was also observed that at shorter reaction time of 2.5 hours, the effect of catalyst loading was more obvious as compared to the longer reaction time of 6.5 hours.

The increment of catalyst loading has led to the increment of FAME yield as well. This was understandable since catalyst is playing an important role in a reaction whereby it helps to lower down the activation energy in order for the reaction to occur.

4.4.2.5 Effect of Reaction Time and Methanol to Oil Molar Ratio

The surface response plot of reaction time, methanol to oil molar ratio and FAME yield at constant temperature of 80 ˚C and 8.0 wt.% catalyst loading is shown in Figure 4.22. It was observed that the maximum FAME yield of about 80% was obtained at reaction time of 6.5 hours and 22: 1 methanol to oil molar ratio.

In the plot, it shows that the effect of reaction time at either higher or lower molar ratio demonstrated no significant difference. Similarly, the effect of methanol to oil molar ratio also had no significant difference at longer or shorter reaction time. In overall, the reaction time and methanol to oil molar ratio had very less interaction effects with each other similar to the outcome reported by Regaldo et al. (2017) in the transesterification reaction of oil and methanol with NaOH as catalyst.

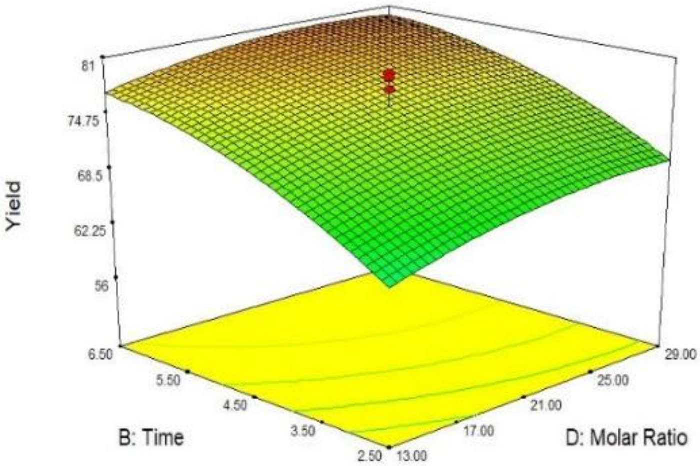

Figure 4.22: Three dimension surface response plot of FAME yield, reaction time (hour) and methanol to oil molar ratio at reaction temperature of 80 ˚C and catalyst loading of 8.0 wt.%.

4.4.2.6 Effect of Catalyst Loading and Methanol to Oil Molar Ratio

Figure 4.23 shows the surface response plot for the effect of catalyst loading, methanol to oil molar ratio on the FAME yield at constant reaction temperature of 80 ˚C and 4.5 hours reaction time. The varying catalyst loading gave a very obvious effect to the FAME yield at constant reaction temperature and reaction time in which the FAME yield significantly increased with the addition of higher of catalyst loading. At the lower catalyst loading of 5 wt.%, the optimum methanol to oil molar ratio was maximised at about 25: 1. When the catalyst loading had increased to 11 wt.%, the optimum molar ratio was lowered slightly to 21 :1. In this case, the maximum FAME yield was obtained at methanol to oil molar ratio of about 21: 1 and catalyst loading of 11 wt.%.

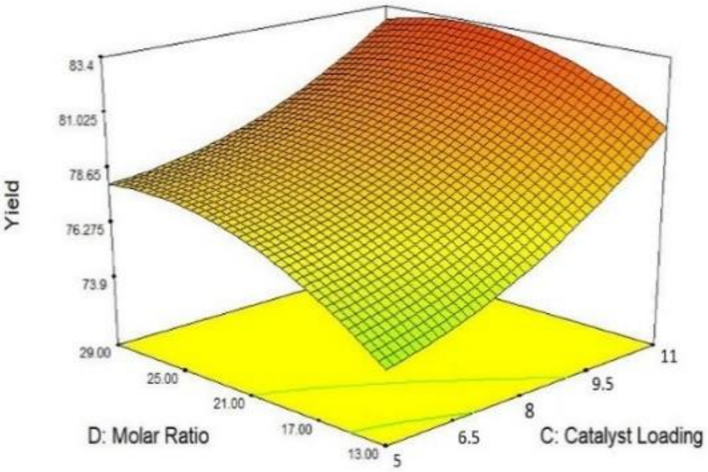

Figure 4.23: Three dimension surface response plot of FAME yield, methanol to oil molar ratio and catalyst loading (wt.%) at reaction temperature of 80 ˚C and 4.5 hours reaction time.

4.4.2.7 Reaction Optimisation through RSM Model

The optimisation of reaction parameters was carried out through the response surface methodology model. It is important to obtain the optimum point of the parameters in order to reach the maximum FAME yield with the minimal cost incurred in the process operation. The optimum reaction conditions of the biodiesel production reaction was investigated by using the optimisation tool in Design Expert software.

Table 4.7 summarised the optimum reaction conditions as obtained from the optimisation study. It was predicted that a maximum FAME yield of 85.94% could be achieved at the reaction temperature of 89.24 ˚C, reaction time of 6.48 hours, 11 wt.% catalyst loading and 21.94 methanol to oil (PFAD) molar ratio.

Table 4.7: Optimum reaction conditions obtained from optimisation study.

Reaction Parameters	Optimum Reaction Conditions
Reaction temperature	89.24 ˚C
Reaction time	6.48 hours
Catalyst Loading	11 wt.%
Methanol to oil (PFAD) molar ratio	21.94: 1

Next, three experiments run was conducted at the optimum conditions obtained through the optimisation study to verify the validity of the predicted optimum conditions and FAME yield. As shown in Table 4.8, FAME yield of 84.38, 80.41 and 85.64 % were achieved at the first, second and third run conducted respectively. An average FAME yield of 83.48% was obtained, which was close to the predicted FAME yield of 85.94%. The variation of actual FAME yield from the theoretical FAME yield was at the percentage error of 2.86%, which was considered low.

Table 4.8: Predicted and actual FAME yield of biodiesel production reaction.

Response	Predicted	Actual				Error (%)
		1	2	3	Average	
FAME yield (%)	85.94	84.38	80.41	85.64	83.48	2.86

Table 4.9 compared the esterification reaction of this study with other literatures. The maximum FAME yield of 83.48% obtained by using the corncob derived heterogeneous catalyst was similar with the 83.2% FAME yield obtained by sugarcane bagasse derived carbon acid catalyst but corncob derived catalyst required milder reaction temperature to achieve the FAME yield. Although the

FAME yield obtained in this study was lower than the coconut meal residue derived catalyst, the reaction time required for corncob based catalyst was much lower. In addition, the sulfonation method for the coconut meal residue derived catalyst still involved the usage of corrosive concentrated H_2SO_4 which might create handling problem. Compared to the de-oiled waste cake derived catalyst synthesised through arylation reaction, corncob derived catalyst synthesised with the similar sulfonation method might showed slightly lower catalytic performance. However, the corncob derived catalyst required shorter reaction time to achieve the maximum FAME yield of 83.48%.

Compared to HPA supported on zirconia, which is a non-biomass based catalyst, corncob derived catalyst had shown a slightly lower FAME yield. However, corncob derived catalyst still contributed to several advantages over HPA catalyst since corncob derived catalyst required much lower catalyst loading and methanol to oil molar ratio. Further, corncob derived catalyst also incurred lower raw material cost since corncob can be obtained at very low cost. As a whole, the corncob derived heterogeneous acid catalyst synthesised through arylation with 4-BDS showed comparable performance with the biomass derived catalyst reported by other researchers with potential to be commercialised in the biodiesel industry.

Table 4.9: Comparison of esterification reactions.

Catalyst	Sulfonation method/ agent	Reaction Conditions					FAME Yield (%)	Ref.
		Feedstock	Reaction Temperature (˚C)	Reaction Time (hour)	Catalyst Loading (wt.%)	Methanol to Oil Molar Ratio		
Sugarcane bagasse	Direct Sulfonation/ Conc. H_2SO_4	Waste oil	130	4	12	1.17 mL/min	83.2	(Ezebor et al., 2014a)
Coconut meal residue	Direct Sulfonation/ Conc. H_2SO_4	Waste palm oil	65-70	10	5	12: 1	92.7	(Thushari and Babel, 2018)
De-oiled waste cake	Arylation/ 4-BDS	Oleic acid	64	10	3	20: 1	Conversion = 97	(Konwar et al., 2015)
HPA supported on zirconia	-	Palmitic acid	60	6	30	94.9: 1	90	(Alcañiz-Monge et al., 2018)
Corncob	Arylation/ 4-BDS	PFAD	89.24	6.48	11	21.94	83.48	Current study

4.4.2.8 Sensitivity Study

Sensitivity study was carried out to determine several other combinations of milder reaction conditions as compared to the optimum conditions to achieve a slightly lower FAME yield that was still reasonably close to the optimum value. The combinations of reaction conditions was determined by varying the importance of the reaction parameters by using the RSM model generated.

Five different possible combinations were obtained as shown in Table 4.10. For combination 1, the reaction time was significantly reduced to 3.42 hours to obtained FAME yield as high as 79.35% by just slightly increasing the methanol to oil molar ratio. Next, combination 2 offered to reduce the catalyst loading to 5 wt.% and increased the methanol to oil molar ratio to 24.35: 1 in order to achieve FAME yield of 79.8.

Table 4.10: Different combinations of reaction conditions with predicted FAME yield.

No	Reaction Temperature (˚C)	Reaction Time (hour)	Catalyst Loading (wt.%)	Methanol to oil molar ratio	FAME Yield (%)
1	90.6	3.42	11	23.83	79.35
2	89.11	6.5	5	24.35	79.80
3	93.68	6.49	11	13	82.63
4	63.19	6.5	11	27.23	79.06
5	90	4.5	8	24.44	77.83

Furthermore, combination 3 shows that reducing the methanol to oil molar ratio to 13:1 and slightly increase the reaction temperature to 93.68% from 89.24% was able to obtain FAME yield of 79.06%. In addition, combination 4 shows that lowering the reaction temperature to 63.19 ˚C while simultaneously raise the methanol to oil molar ratio was able to give FAME yield of 79.06%.

Lastly, combination 5 demonstrated the reduction of two dominant parameters including the catalyst loading and reaction time was still able to give a relatively high FAME yield by just slightly increasing the methanol to oil molar ratio. Out of the five combinations listed, combination 3 could be considered as the most reasonable reaction condition given because the predicted FAME yield of 82.63% was still very close to the original maximised FAME yield of 83.48% but the methanol to oil molar ratio was significantly reduced. However, the selection of these combination of reaction conditions is still mainly dependent on the choice of resources to be conserved in the production process.

4.5 Catalyst Reusability Study

Catalyst reusability test was carried out to investigate the ability of the catalyst to be maintained for several cycles of reaction. The reusability study of Cat_900h was carried out by running five consecutive cycles of reaction using the same batch of catalyst. The catalyst was rinsed with hexane to get rid of the remaining reactant attached on the catalyst after each cycle of reaction before being reused.

Figure 4.24 shows the FAME yield obtained at each cycles of reactions. The FAME yield remained relatively high at the first and second cycle at 84.48% and 79.76% respectively. Then, the FAME yield started to reduce to 65.84% at the third cycles and continued to decrease to 57.16% at the fourth cycle. Finally at the fifth cycles, the catalyst was only able to sustain FAME yield at only 47.52%. The drop of FAME yield from first to fifth cycle had attributed to 43.75% of reduction. The reduction of the FAME yield was reasonable as compared to Zhou et al. (2016) reported a 66.63% drop of esterification efficiency after fifth cycle reaction using bamboo derived acid catalyst.

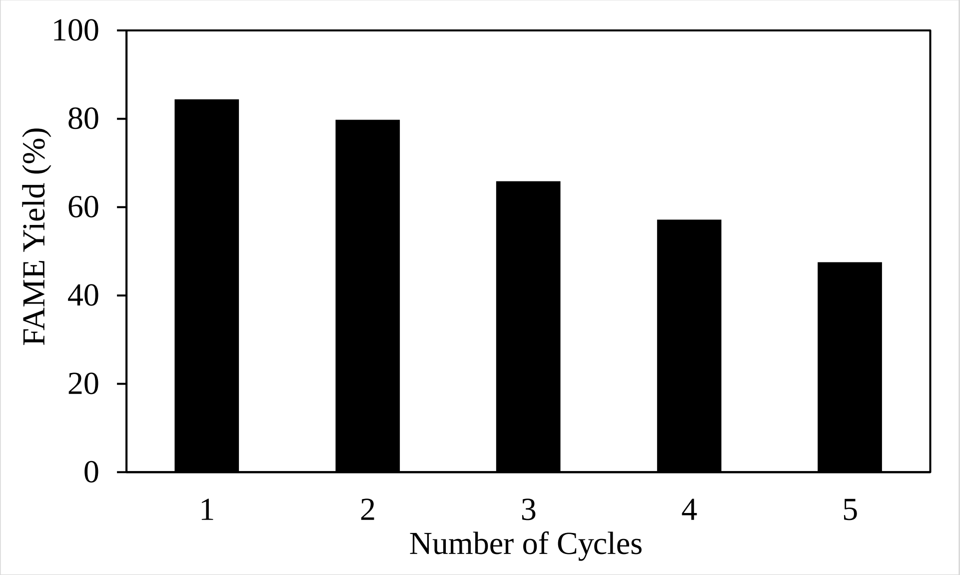

Figure 4.24: FAME yield obtained by Cat_900h at five consecutive cycles of reaction at reaction temperature 89.24 ˚C, reaction time of 6.48 hours, 21.94: 1 methanol to oil molar ratio and 11 wt.% of catalyst loading.

The total acid density of the catalyst after the fifth cycle was tested to be only 1.48 mmol/g, which had decreased from original total acid density of 2.43 mmol/g as a fresh catalyst. This had indicated that the drop of FAME yield across the reaction cycles might be due to the leaching of $–SO_3H$ active groups from the catalyst (Niu et al., 2018). The reduction of $–SO_3H$ active site density from the catalyst had directly reduced the catalyst efficiency to promote the esterification reaction.

4.6 Reaction Kinetics Study

Reaction kinetics study was carried out to determine the reaction kinetic model as one of the preparatory steps for a scale up process. In this study, an irreversible pseudo-homogeneous first order kinetic model was proposed for the esterification reaction. In the process of developing the kinetic model, several assumptions were made as explained in Section 3.9.1. The kinetic equation proposed was as shown in Equation 3.16

Figure 4.25 shows the pseudo-homogeneous kinetic model plot of exponential trend of FAME yield against reaction time. The esterification reaction was carried out at varying reaction temperatures of 40, 60, 80 and 100 ˚C from reaction time of 0 to 90 minutes at constant catalyst loading of 11 wt.% and 21.94: 1 methanol to oil molar ratio.

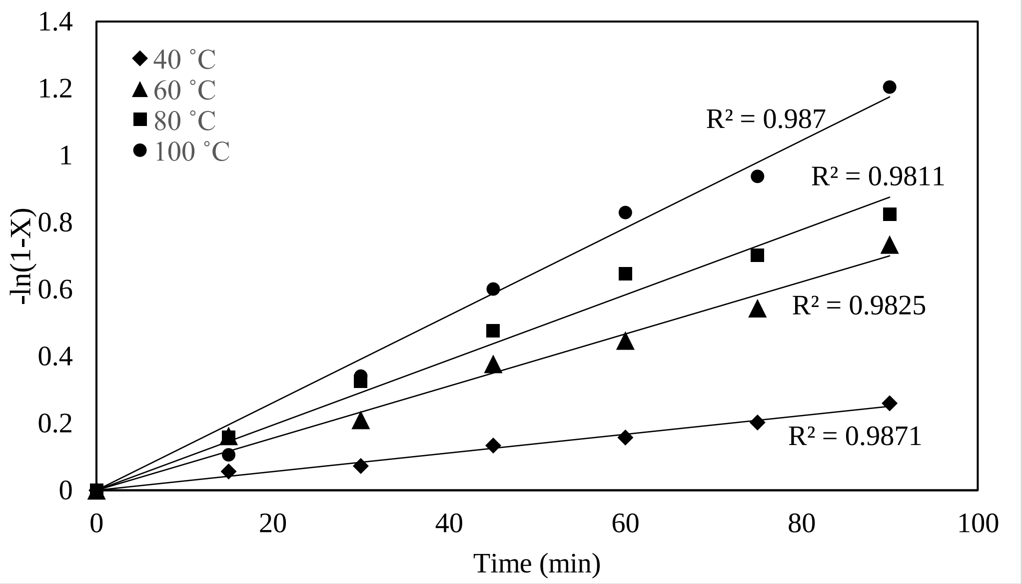

Figure 4.25: Kinetic modelling curve of esterification reaction at different time for different reaction temperature (reaction conditions: 21.94: 1 methanol to oil molar ratio and 11 wt.% catalyst loading).

As shown in the kinetic plot, four best fit line using linear regression was plotted according to the FAME yield obtained. The kinetic plots for all temperatures exhibited R-squared values of above 98%, the good fit of experimental results data to the kinetic model through linear regression proved that the esterification reaction of PFAD and methanol catalysed by corncob derived heterogeneous acid catalyst followed the homogeneous pseudo-first order reaction kinetic as proposed. Fadhil et al. (2016) had also reported on the application of irreversible pseudo-homogeneous first order reaction kinetics for the esterification reaction of *Silybum Marianum* seed oil and methanol catalysed by polyethylene terephthalate waste bottle derived carbon acid catalyst.

In addition, Table 4.11 shows the calculated reaction rate constant at different reaction temperatures. The rate constant, *k* was obtained from the gradient of the straight line plotted in the kinetic modelling as shown in Figure 4.25. Since this is an endothermic reaction, it shows that the reaction rate actually increased from 0.0029 to 0.0131 min^{-1} with the increment of reaction temperature. Therefore, the highest reaction rate of 0.0131 min^{-1} was achieved at the reaction temperature of 100 ˚C. Fadhil et al. (2016) had also reported on the reaction rate of 0.01484 min^{-1}.

Table 4.11: Reaction rate constant at different reaction temperatures.

Reaction Temperature, T (˚C)	**Reaction Temperature, T (K)**	**Rate Constant, *k* (min^{-1})**	**1/T × 10^{3} (K^{-1})**	**ln k**
40	313	0.0029	3.1949	-5.8430
60	333	0.0078	3.0030	-4.8536
80	353	0.0097	2.8329	-4.6356
100	373	0.0131	2.6810	-4.3351

The reaction rate constant was then related with the reaction temperature to form the Arrhenius equation as shown in Equation 3.17 and rearranged to Equation 3.18 to determine the activation energy of the reaction system catalysed by corncob based heterogeneous acid catalyst.

Figure 4.26 shows the Arrhenius plot with best fit line of ln *k* against 1/*T* according to the data tabulated in Table 4.11. It was found that the activation energy of the reaction was at 23.36 kJ/mol. The activation energy required was slightly lower as compared to the reaction catalysed by conventional catalyst H_2SO_4 and composite catalytic membrane at 36.62 kJ/mol and 35.97 kJ/mol (Shi et al., 2013; Neumann et al., 2016). The ability of heterogeneous acid to achieve lower activation energy required might be due to the high surface area that allow the reaction to occur at which the catalyst synthesised in this study had the BET surface area of 721.71m^2/g. Besides that, homogeneous catalyst required higher activation energy since it is immiscible with the oil feedstock and the reaction was only limited to the contact surface of the two immiscible layers.

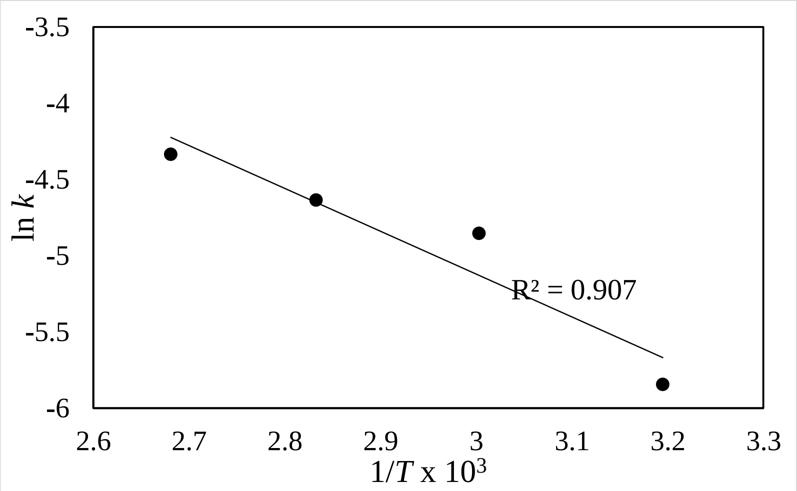

Figure 4.26: Arrhenius plot for the reaction at reciprocal temperature (reaction conditions: 21.94 methanol to oil molar ratio and 11 wt.% catalyst loading).

CHAPTER 5

CONCLUSION AND RECOMMENDATIONS

5.1 Conclusion

Corncob based carbon acid catalyst was successfully synthesised through arylation of 4-BDS sulfonation method. The catalyst synthesised had successfully catalysed the esterification reaction of PFAD and methanol to produce FAME. In this research, the research objective was achieved to draw the following conclusions.

The porous structure of the activated carbon produced from carbonisation of corncob was observed under the SEM micrographs. EDX showed that S content was observed on the catalyst after sulfonation process. Besides that, FT-IR spectrum showed peak for the O=S=O and $–SO_3H$ stretching on the catalyst after sulfonation. In addition, the reduction of BET surface area of the sample from 972.66 m^2/g to 721.71 m^2/g after sulfonation had also confirmed the successful grafting of $–SO_3H$ groups onto the activated carbon. TGA result shows that the catalyst is thermally stable up to the temperature of 230 ˚C which is far above the esterification reaction temperature employed in this study. The total acid density of the catalyst synthesised from optimum condition was 2.48 mmol/g.

On the other hand, in the process of synthesising catalyst, the increment of carbonisation temperature, sulfonation time and sulfanilic acid to AC weight ratio had gave positive trend towards the FAME yield. Cat_900h with the optimum catalyst synthesis condition of 900 ˚C carbonisation temperature, 1.5 hour sulfonation time and 11:1 sulfanilic acid to AC ratio had obtained FAME yield of 72.09% and conversion of 93.49%.

In the esterification reaction study, result shows that the increment of esterification parameters including the reaction temperature, reaction time, catalyst lading and methanol to oil molar ratio were able to give positive effect towards the FAME yield. The optimum esterification condition obtained from the RSM study was at reaction temperature 89.24 ˚C, reaction time of 6.48 hours, 11 wt.% catalyst loading and 21.94:1 methanol to oil molar ratio with maximum FAME yield of 83.48%.

Nevertheless, the catalyst reusability study showed that FAME yield decreased from 83.48% at the first cycle to 47.52% at the fifth cycle due to leaching of active site. Esterification reaction of PFAD and methanol catalysed by carbon acid catalyst followed the pseudo-first order reaction kinetic model with activation energy of 23.36 kJ/mol.

In conclusion, all the objectives in this study were fulfilled. Corncob based heterogeneous carbon acid catalyst was successfully synthesised through arylation of 4-BDS and gave promising catalytic performance in the esterification reaction of PFAD and methanol. Some areas of this research can be improved in the future studies as one of the preparatory steps for the commercialisation of this catalyst in biodiesel production industry.

5.2 Recommendations

Upon the completion of the current research work, several recommendations was made for the future studies:

i. The raw materials should be sufficiently prepared in a single batch and obtained from the same source to ensure the consistency of the data obtained.
ii. The properties of biodiesel produced such as flash point, cloud point, viscosity, *etc*. should be studied to ensure that they met the standard specifications for biodiesel in diesel engine.
iii. The methanol used in the esterification reaction could be recovered and reused for next reaction.
iv. Deactivated catalyst should be regenerated again through sulfonation.
v. The reaction should be carried out in a pressurised reactor to evaluate the scaled up parameters.

REFERENCES

Abiman, P., Wildgoose, G.G. and Compton, R.G., 2008. A mechanistic investigation into the covalent chemical derivatisation of graphite and glassy carbon surfaces using aryldiazonium salts. *Journal of Physical Organic Chemistry*, 21, pp. 433 – 439.

Akinfalabi, S.I., Rashid, U., Yunus, R. and Taufiq-Yap, Y.H., 2017. Synthesis of biodiesel from palm fatty acid distillate using sulfonated palm seed cake catalyst. Renewable Energy, 111, pp. 611 – 619.

Alaswad, A., Dassisti, M., Prescott, T. and Olabi, A.G., 2015. Technologies and developments of third generation biofuel production. Renewable and Sustainable Energy Reviews, 51, pp. 1446 – 1460.

Alcañiz, M.J., Bakkali, B.E., Trautwein, G. and Reinoso, S. 2018. Zirconia-supported tungstophosphoric heteropolyacid as heterogeneous acid catalyst for biodiesel production. Applied Catalysis B: Environmental, 224, pp. 194 – 203.

Ali, C.H. et al., 2017. Biodiesel production from waste cooking oil using onsite produced purified lipase from Pseudomonas aeruginosa FW_SH-1: Central composite design approach. Renewable Energy, 109, pp. 93 – 100.

Alves, C., Franca, A. and Oliveira, L., 2013. Evaluation of an Adsorbent Based on Agricultural Waste (Corn Cobs) for Removal of Tyrosine and Phenylalanine from Aqueous Solutions. BioMed Research International, 2013, p. 1 – 8.

Anand, M.D., Vijay A.S., Jackson, D. and Prabhu, N., 2016. Investigation of Biodiesel Production from High Free Fatty Acid through RSM. Indian Journal of Science and Technology. 9, pp. 1 – 11.

Anis, D. et al., 2014. Production of Rubber Seed Pericarp Based Activated Carbon Using Microwave-Induced Different Chemical Activating Agent. International Journal of Scientific and Research Publications, 4, pp. 1 – 7.

Anwar, M., Rasul, M.G. and Ashwath, N., 2018. Production optimization and quality assessment of papaya (Carica papaya) biodiesel with response surface methodology. Energy Conversion and Management, 156, pp. 103 – 112.

Arpornpong, N., Attaphong, C., Charoensaeng, A., Sabatini, D.A. and Khaodhiar, S., 2014. Ethanol-in-palm oil/diesel microemulsion-based biofuel: Phase behavior, viscosity, and droplet size. Fuel, 132, pp. 101 – 106.

Ayodele, O.O. and Dawodu, F.A., 2014. Production of biodiesel from Calophyllum inophyllum oil using a cellulose-derived catalyst. Biomass and Bioenergy, 70, pp. 239 – 248.

Bilgen, S., 2014. Structure and environmental impact of global energy consumption. Renewable and Sustainable Energy Reviews, 38, pp. 890 – 902.

Bioenergy, I., 2008. From 1st to 2nd Generation Biofuel Technologies. International Energy Agency [online]. Available at: https://www.iea.org/publications/freepublications/publication/2nd_Biofuel_Gen.pdf [Accessed: 23 January 2018]

Bora, P., Boro, J., Konwar, L.J. and Deka, D., 2016. Formulation of microemulsion based hybrid biofuel from waste cooking oil – A comparative study with biodiesel. Journal of the Energy Institute, 89, pp. 560 – 568.

Boro, J., Konwar, L.J., Thakur, A.J. and Deka, D., 2014. Ba doped CaO derived from waste shells of T striatula (TS-CaO) as heterogeneous catalyst for biodiesel production. Fuel, 129, pp. 182 – 187.

BP, 2017. BP Statistical Review of World Energy June 2017. [online]. Available at: https://www.bp.com/content/dam/bp/en/corporate/pdf/energy-economics/statistical-review-2017/bp-statistical-review-of-world-energy-2017-full-report.pdf [Accessed: 23 January 2018]

Buasri, A., Chaiyut, N., Loryuenyong, V., Rodlum, C., Chaiwan,T. and Kumphan, N., 2012. Continuous Process for Biodiesel Production in Packed Bed Reactor from Waste Frying Oil Using Potassium Hydroxide Supported on Jatropha curcas Fruit Shell as Solid Catalyst. Applied Sciences, 2, pp. 641 – 653.

Carvalho, A.K.F., Daconceição, L.R.V., Silva, J.P.V., Perez, V.H. and Castro, D.H.F., 2017. Biodiesel production from Mucor circinelloides using ethanol and heteropolyacid in one and two-step transesterification. Fuel, 202, pp. 503 – 511.

Chen, G. and Fang, B., 2011. Preparation of solid acid catalyst from glucose–starch mixture for biodiesel production. Bioresource Technology, 102, pp. 2635 – 2640.

Chen, G.Y., Shan, R., Shi, J.F. and Yan, B.B., 2015. Transesterification of palm oil to biodiesel using rice husk ash-based catalysts. Fuel Processing Technology, 133, pp. 8 – 13.

Czitrom, V., 1999. One-Factor-at-a-Time versus Designed Experiments. The American Statistician, 53, pp. 126 – 131.

Dawodu, F.A., Ayodele, O.O., Xin, J., Zhang, S. and Yan, D., 2014. Effective conversion of non-edible oil with high free fatty acid into biodiesel by sulphonated carbon catalyst. Applied Energy, 114, pp. 819 – 826.

De, S., Balu, A.M., Waal, J.C.V.D. and Luque, R., 2015. Biomass-Derived Porous Carbon Materials: Synthesis and Catalytic Applications. ChemCatChem, 7, pp. 1608 – 1629.

Dehkhoda, A.M. and Ellis, N., 2013. Biochar-based catalyst for simultaneous reactions of esterification and transesterification. Catalysis Today, 207, pp. 86 – 92.

Dharma, S. et al., 2016. Optimization of biodiesel production process for mixed Jatropha curcas–Ceiba pentandra biodiesel using response surface methodology. Energy Conversion and Management, 115, pp. 178 – 190.

Dhawane, S.H., Kumar, T. and Halder, G., 2016. Biodiesel synthesis from Hevea brasiliensis oil employing carbon supported heterogeneous catalyst: Optimization by Taguchi method. Renewable Energy, 89, pp. 506 – 514.

Dutta, K., Daverey, A. and Lin, J.G., 2014. Evolution retrospective for alternative fuels: First to fourth generation. Renewable Energy, 69, pp. 114 – 122.

EIA, U.S., 2017a. International Energy Outlook 2017 [online]. Available at: https://www.eia.gov/outlooks/ieo/pdf/0484(2017).pdf [Accessed: 23 January 2018]

EIA, U.S., 2017b. Monthly Energy Review November 2017 [online]. Available at: https://www.eia.gov/totalenergy/data/monthly/ [Accessed: 23 January 2018]

Endut, A., Abdullah, S.H.Y.S., Hanapi, N.H.M., Hamid, S.H.A., Lananan, F., Kamarudin, M.K.A., Umar, P., Juahir, H. and Khatoon, H., 2017. Optimization of biodiesel production by solid acid catalyst derived from coconut shell via response surface methodology. International Biodeterioration & Biodegradation, 124, pp. 250 – 257.

Ezebor, F., Khairuddean, M., Abdullah, A.Z. and Boey, P.L., 2014a. Esterification of oily-FFA and transesterification of high FFA waste oils using novel palm trunk and bagasse-derived catalysts. Energy Conversion and Management, 88, pp. 1143-1150.

Ezebor, F., Khairuddean, M., Abdullah, A.Z. and Boey, P.L., 2014b. Oil palm trunk and sugarcane bagasse derived heterogeneous acid catalysts for production of fatty acid methyl esters. Energy, 70, pp. 493 – 503.

Fadhil, A.B., Aziz, A.M. and Al-Tamer, M.H., 2016. Biodiesel production from Silybum marianum L. seed oil with high FFA content using sulfonated carbon catalyst for esterification and base catalyst for transesterification. Energy Conversion and Management, 108, pp. 255 – 265.

Ferreira, S.L.C., Bruns, R.E., Silva, E.G.P., Santos, W.M.L., Quintella, C.M., David, J.M., Andrade, J.B., Breitkreitz, M.C., Jardim, I.C.S.F. and Neto, B.B.,

2007. Statistical designs and response surface techniques for the optimization of chromatographic systems. Journal of Chromatography A, 1158, pp. 2 – 14.

Fu, J., Chen, L., LV, P., Yang, L. and Yuan, Z. 2015. Free fatty acids esterification for biodiesel production using self-synthesized macroporous cation exchange resin as solid acid catalyst. Fuel, 154, pp. 1 – 8.
Fu, X., Li, D., Chen, J., Zhang, Y., Huang, W., Zhu, Y., Yang, J. and Zhang,C., 2013. A microalgae residue based carbon solid acid catalyst for biodiesel production. Bioresource Technology, 146, pp. 767 – 770.

Gashaw, A., Getachew, T. and Mohammed, A., 2015. A review on biodiesel production as alternative fuel. Journl of Forest Products & Industries, 4, pp. 80 – 85.

Guldhe, A., Singh, B., Rawat, I., Permaul, K. and Bux, F., 2015. Biocatalytic conversion of lipids from microalgae Scenedesmus obliquus to biodiesel using Pseudomonas fluorescens lipase. Fuel, 147, pp. 117-124.

Guo, F. and Fang, Z., 2011. Biodiesel production with solid catalysts. In: Stoytcheva, M. and Montero, G. (eds) Biodiesel-feedstocks and processing technologies. London: InTech pp. 339 – 358.

Hara, M., 2010. Biodiesel Production by Amorphous Carbon Bearing SO3H, COOH and Phenolic OH Groups, a Solid Brønsted Acid Catalyst. Topics in Catalysis, 53, pp. 805 – 810.

Haziratul M.H., Ong, H.C., Masjuki, H.H., Lim, S. and Pang, Y., 2017. Investigation of carbon-based solid acid catalyst from Jatropha curcas biomass in biodiesel production. Energy Conversion and Management, 144, pp. 10 – 17.

Hill, J., Nelson, E., Tilman, D., Polasky, S. and Tiffany, D., 2006. Environmental, economic, and energetic costs and benefits of biodiesel and ethanol biofuels. Proceedings of the National Academy of Sciences, 103, pp. 11206 – 11210.

Huang, J., Xia, J., Jiang, W., Li, Y. and Li, J., 2015. Biodiesel production from microalgae oil catalyzed by a recombinant lipase. Bioresource Technology, 180, pp. 47 – 53.

Härmas, M., Thomberg, T., Kurig, H., Romann, T., Jänes,A. and Lust, E., 2016. Microporous–mesoporous carbons for energy storage synthesized by activation of carbonaceous material by zinc chloride, potassium hydroxide or mixture of them. Journal of Power Sources, 326, pp. 624 – 634.

Iqbaldin, M.N.M., Khudzir, I., Azlan, M.M., Zaidi, A.G., Surani,B. and Zubri,Z., 2013. Properties Of Coconut Shell Activated Carbon. Journal of Tropical Forest Science, 25, pp. 497 – 503.

Jain, A., Balasubramanian, R. amd Srinivasan, M.P., 2015. Production of high surface area mesoporous activated carbons from waste biomass using hydrogen peroxide-mediated hydrothermal treatment for adsorption applications. Chemical Engineering Journal, 273, pp. 622 – 629.

Janaun, J., Abang, S. and Anwar, A.M., 2013. Synthesis and characterization of carbon-based catalyst derived from seaweed. IEEE Conference of Clean Energy and Technology. 18 – 20 November 2013 Langkawi, Malaysia. Langkawi: IEEE, pp. 19 – 22.

Janaun, J. and Ellis, N., 2011. Role of silica template in the preparation of sulfonated mesoporous carbon catalysts. Applied Catalysis A: General, 394, pp. 25 – 31.

Kastner, J.R., Miller, J., Geller, D.P., Lockln, J., Keith, L.H. and Johnson, T., 2012. Catalytic esterification of fatty acids using solid acid catalysts generated from biochar and activated carbon. Catalysis Today, 190, pp. 122 – 132.

Knothe, G. and Razon, L.F., 2017. Biodiesel fuels. Progress in Energy and Combustion Science, 58, pp. 36 – 59.

Konwar, L.J., Mäki-Arvela, P., Salminen, E., Kumar, N., Thakur, A.J., Mikkola, J. and Deka, D., 2015. Towards carbon efficient biorefining: Multifunctional mesoporous solid acids obtained from biodiesel production wastes for biomass conversion. Applied Catalysis B: Environmental, 176–177, pp. 20 – 35.

Latiff, M., Abustan, I., Ahmad, M.A., Yahaya, N. and Khalid, A.M., 2016. Effect of preparation conditions of activated carbon prepared from corncob by CO2 activation for removal of Cu (II) from aqueous solution. AIP Publishing, 1774, pp. 1 – 13.

Lee, D., 2013. Preparation of a sulfonated carbonaceous material from lignosulfonate and its usefulness as an esterification catalyst. Molecules, 18, pp. 8168 – 8180.

Li, Y., Zhang, X., Yang, R., Li, G. and Hu, C., 2015. The role of H3PO4 in the preparation of activated carbon from NaOH-treated rice husk residue. RSC Advances, 5, pp. 32626 – 32636.

Lien, Y.S., Hsieh, L.S. and Wu, J.C.S., 2010. Biodiesel Synthesis by Simultaneous Esterification and Transesterification Using Oleophilic Acid Catalyst. Industrial & Engineering Chemistry Research, 49, pp. 2118 – 2121.

Liu, R.L., Liu, Y., Zhou, X., Zhang, Z., Zhang, J. and Dang, F., 2014. Biomass-derived highly porous functional carbon fabricated by using a free-standing template for efficient removal of methylene blue. Bioresource Technology, 154, pp. pp. 138 – 147.

Liu, R., Wang, X., Zhao, X. and Feng, P., 2008a. Sulfonated ordered mesoporous carbon for catalytic preparation of biodiesel. Carbon, 46, pp. 1664 – 1669.

Liu, T., Li, Z., Li, W., Shi, C. and Wang, Y., 2013a. Preparation and characterization of biomass carbon-based solid acid catalyst for the esterification of oleic acid with methanol. Bioresource Technology, 133, pp. 618 – 621.

Liu, X., He, H., Wang, Y., Zhu, S. and Piao, X., 2008b. Transesterification of soybean oil to biodiesel using CaO as a solid base catalyst. Fuel, 87, pp. 216 – 221.

Liu, X., Zhang, L., Sun, W., Zhang, M. and Yu, S., 2017. One-step preparation of sulfonated carbon-based solid acid from distillers' grain for esterification. Research on Chemical Intermediates, 43, pp. 5917 – 5932.

Liu, X.Y., Huang, M., Ma, H.L., Zhang, Z.Q., Gao, J.M., Zhu, Y.L., Han, X.J. and Guo, X.Y., 2010. Preparation of a Carbon-Based Solid Acid Catalyst by Sulfonating Activated Carbon in a Chemical Reduction Process. Molecules, 15, pp. 7188 – 7196.

Liu, Z., Quek, A., Kent, H.S. and Balasubramanian, R., 2013b. Production of solid biochar fuel from waste biomass by hydrothermal carbonization. Fuel, 103, pp. 943 – 949.

Lokman, I.M., Rashid, U. and Taufiq-Yap, Y.H., 2015a. Production of biodiesel from palm fatty acid distillate using sulfonated-glucose solid acid catalyst: Characterization and optimization. Chinese Journal of Chemical Engineering, 23, pp. 1857 – 1864.

Lokman, I.M., Rashid, U., Taufiq-Yap, Y.H. and Yunus, R., 2015b. Methyl ester production from palm fatty acid distillate using sulfonated glucose-derived acid catalyst. Renewable Energy, 81, pp. 347 – 354.

Lotero, E., Liu, Y., Lopez, D.E., Suwannakarn, K., Bruce, D.A. and Goodwin, J.G., 2005. Synthesis of Biodiesel via Acid Catalysis. Industrial & Engineering Chemistry Research, 44, pp. 5353 – 5363.

Malins, K., Kampars, V., Brinks, J., Neibolte, I. and Murnieks, R., 2015. Synthesis of activated carbon based heterogenous acid catalyst for biodiesel preparation. Applied Catalysis B: Environmental, 176–177, pp. 553 – 558.

Maneerung, T., Liew, J., Dai, Y., Kawi, S., Chong, C. and Wang, C., 2016. Activated carbon derived from carbon residue from biomass gasification and its application for dye adsorption: Kinetics, isotherms and thermodynamic studies. Bioresource Technology, 200, pp. 350 – 359.

Mansir, N., Teo, S.H., Rashid, U. and Taufiq-Yap, Y.H., 2018. Efficient waste Gallus domesticus shell derived calcium-based catalyst for biodiesel production. Fuel, 211, pp. 67 – 75.

Mardhiah, H.H., Ong, H.C., Masjuki, H.H., Lim, S. and Lee, H.V., 2017. A review on latest developments and future prospects of heterogeneous catalyst in biodiesel production from non-edible oils. Renewable and Sustainable Energy Reviews, 67, pp. 1225 – 1236.

Mohamad, N.N., Lau, L.C., Lee, K.T. and Mohamed, A.R., 2013. Synthesis of activated carbon from lignocellulosic biomass and its applications in air pollution control—a review. Journal of Environmental Chemical Engineering, 1, pp. 658 – 666.

Mohd, A.S.H., Abdulla, R., Jambo, S.A., Marbawi, H., Gansau, J.A., Fail, A.A.M. and Rodigues, K.F., 2017. Yeasts in sustainable bioethanol production: A review. Biochemistry and Biophysics Reports, 10, pp. 52 – 61.

Muciño, G.G., Romero, R., Ramírez,A., Martínez,S.L., Baeza-Jiménez,R. and Natividad, R., 2014. Biodiesel production from used cooking oil and sea sand as heterogeneous catalyst. Fuel, 138, pp. 143 – 148.

Nachenius, R.W., Ronsse, F., Venderbosch, R.H. and Prins, W., 2013. Chapter Two - Biomass Pyrolysis. In: Murzin, D. Y. (ed.). Advances in Chemical Engineering. Burlington: Academic Press, pp. 75 – 130.

Nata, I.F., Putra, M.D., Irawan, C. and Lee, C.K., 2017. Catalytic performance of sulfonated carbon-based solid acid catalyst on esterification of waste cooking oil for biodiesel production. Journal of Environmental Chemical Engineering, 5, pp. 2171 – 2175.

Navarro, L.E. et al., 2016. Biodiesel production from Nannochloropsis gaditana lipids through transesterification catalyzed by Rhizopus oryzae lipase. Bioresource Technology, 203, pp. 236 – 244.

Nelson, L.A., Foglia, T.A. and Marmer, W.N., 1996. Lipase-catalyzed production of biodiesel. Journal of the American Oil Chemists' Society, 73, pp. 1191 – 1195.

Ngaosuwan, K., Goodwin J.J.G. and Prasertdham, P., 2016. A green sulfonated carbon-based catalyst derived from coffee residue for esterification. Renewable Energy, 86, pp. 262 – 269.

Niu, S., Ning, Y., Lu, C., Han, K., Yu, H. and Zhou,Y., 2018. Esterification of oleic acid to produce biodiesel catalyzed by sulfonated activated carbon from bamboo. Energy Conversion and Management, 163, pp. 59 – 65.

Okamura, M., Takagaki, A., Toda, M., Konda, J.N., Domen, K., Tatsumi,T., Hara, M. and Hayashi,S., 2006. Acid-Catalyzed Reactions on Flexible Polycyclic Aromatic Carbon in Amorphous Carbon. Chemistry of Materials, 18, pp. 3039 – 3045.

Paiva, A.L., Balcão, V.M. and Malcata, F.X., 2000. Kinetics and mechanisms of reactions catalyzed by immobilized lipases. Enzyme and Microbial Technology, 27, pp. 187 – 204.

Prado, C.M.R. and Antoniosi, F.N.R., 2009. Production and characterization of the biofuels obtained by thermal cracking and thermal catalytic cracking of vegetable oils. Journal of Analytical and Applied Pyrolysis, 86, pp. 338 - 347.

Prauchner, M.J. and Rodríguez, R.F., 2012. Chemical versus physical activation of coconut shell: A comparative study. Microporous and Mesoporous Materials, 152, pp. 163 – 171.

Qu, W.H., Xu, Y.Y., Lu, A.H., Zhang, X.Q. and Li, W.C. 2015. Converting biowaste corncob residue into high value added porous carbon for supercapacitor electrodes. Bioresource Technology, 189, pp. 285 – 291.

Regalado, A. et al., 2017. Biodiesel Production from Jatropha oaxacana Oil by Reactive Vacuum Distillation: Optimization by Response Surface Methodology. Key Engineering Material, 737, pp. 385 – 392.

REN21, 2016. Renewables 2016 Global Status Report. Renewable Energy Policy Network for the 21st Century [online]. Available at: http://www.ren21.net/wp-content/uploads/2016/05/GSR_2016_Full_Report_lowres.pdf [Accessed: 23 January 2018]

Reza, M.T., Uddin, M.H., Lynam, J.G., Hoekman, S.K. and Coronella, C.J., 2014. Hydrothermal carbonization of loblolly pine: reaction chemistry and water balance. Biomass Conversion and Biorefinery, 4, pp. 311 – 321.

Robles, A., Gonzalez, P.A., Esteban, L and Molina, E., 2009. Biocatalysis: Towards ever greener biodiesel production. Biotechnology Advances, 27, pp. 398-408.

Rodriguez, C.C., Otto, T. and Kruse, A., 2017. Influence of the biomass components on the pore formation of activated carbon. Biomass and Bioenergy, 97, pp. 53 – 64.

Sadaka, S., Sharara, M.A., Ashworth, A., Keyser, P., Allen, F. and Wright, A., 2014. Characterization of Biochar from Switchgrass Carbonization. Energies, 7, pp. 548 – 567.

Sahira, J., Mandira, A., Prasad, P.B. and Ram, P.R., 2013. Effects of Activating Agents on the Activated Carbons Prepared from Lapsi Seed Stone. Research Journal of Chemical Sciences, 3, pp. 19 – 24.

Saluja, R.K., Kumar, V. and Sham, R., 2016. Stability of biodiesel – A review. Renewable and Sustainable Energy Reviews, 62, pp. 866 – 881.

Saravanan, K., Tyagi, B., Shukla, R.S. and Bajaj, H.C., 2016. Solvent free synthesis of methyl palmitate over sulfated zirconia solid acid catalyst. Fuel, 165, pp. 298 – 305.

Shi, W., He, B., Cao, Y., Li, J., Yan, F., Cui, Z., Zou, Z., Guo, S. and Qian, X., 2013. Continuous esterification to produce biodiesel by SPES/PES/NWF composite catalytic membrane in flow-through membrane reactor: Experimental and kinetic studies. Bioresource Technology, 129, pp. 100 – 107.

Shu, Q. et al., 2009. Synthesis of biodiesel from cottonseed oil and methanol using a carbon-based solid acid catalyst. Fuel Processing Technology, 90, pp. 1002 – 1008.

Shuit, S.H. and Tan, S.H., 2014. Feasibility study of various sulphonation methods for transforming carbon nanotubes into catalysts for the esterification of palm fatty acid distillate. Energy Conversion and Management, 88, pp. 1283 – 1289.

Sims, R.E.H., Mabee, W., Saddler, J.N. and Taylor, M., 2010. An overview of second generation biofuel technologies. Bioresource Technology, 101, pp. 1570 – 1580.

Smets, K. et al., 2016. Rapeseed and Raspberry Seed Cakes as Inexpensive Raw Materials in the Production of Activated Carbon by Physical Activation: Effect of Activation Conditions on Textural and Phenol Adsorption Characteristics. Materials, 9, pp. 1 – 19.

Smith, A.M. and Ross, A.B., 2016. Production of bio-coal, bio-methane and fertilizer from seaweed via hydrothermal carbonisation. Algal Research, 16, pp. 1 – 11.

Somasundaram, S., Sekar, K., Gupta, V.K. and Ganesan, S., 2013. Synthesis and characterization of mesoporous activated carbon from rice husk for adsorption of glycine from alcohol-aqueous mixture. Journal of Molecular Liquids, 177, pp. 416 – 425.

Sun, Y., Li, H., Li, G., Gao, B., Yue, Q. and Li, X., 2016. Characterization and ciprofloxacin adsorption properties of activated carbons prepared from biomass wastes by H3PO4 activation. Bioresource Technology, 217, pp. 239 – 244.

Sun, Y. and Webley, P.A., 2010. Preparation of activated carbons from corncob with large specific surface area by a variety of chemical activators and their application in gas storage. Chemical Engineering Journal, 162, pp. 883 – 892.

Sun, Z.X., Zheng, T.T., Bo, Q.B., Du, M. and Forsling, W., 2008. Effects of calcination temperature on the pore size and wall crystalline structure of mesoporous alumina. Journal of Colloid and Interface Science, 319, pp. 247 – 251.

Suwanwong, M., Ratanawilai, S.B. and Meyer, P., 2008. Application of ferric sulfate loaded on activated carbon as solid catalyst for biodiesel production. 15th

Regional Symposium on Chemical Engineering – 22nd Symposium of Malaysian Chemical Engineering, 2 – 3 December 2008 Kuala Lumpur, Malaysia. Kuala Lumpur: UKM, pp. 531 – 536.

Tao, M.L., Guan, H.Y., Wang, X.H., Liu, Y.C. and Louh, R.F., 2015. Fabrication of sulfonated carbon catalyst from biomass waste and its use for glycerol esterification. Fuel Processing Technology, 138, pp. 355 – 360.

Taufiq-Yap, Y.H., Lee, H.V., Hussein, M.Z. and Yunus, R., 2011. Calcium-based mixed oxide catalysts for methanolysis of Jatropha curcas oil to biodiesel. Biomass and Bioenergy, 35, pp. 827 – 834.

Taufiq-Yap, Y.H., Teo, S.H., Rashid, U., Islam, A., Hussien, M.Z. and Lee, K.T., 2014. Transesterification of Jatropha curcas crude oil to biodiesel on calcium lanthanum mixed oxide catalyst: Effect of stoichiometric composition. Energy Conversion and Management, 88, pp. 1290 – 1296.

Thushari, I. and Babel, S., 2018. Sustainable utilization of waste palm oil and sulfonated carbon catalyst derived from coconut meal residue for biodiesel production. Bioresource Technology, 248, pp. 199 – 203.

Toda, M., Takagaki, A., Okamura, M., Kondo, J.N., Hayashi, S., Domen, K. and Hara, M., 2005. Green chemistry: Biodiesel made with sugar catalyst. Nature, 438, pp. 178 – 178.

Tran, D.T., Chen, C.L. and Chang, J.S., 2016. Continuous biodiesel conversion via enzymatic transesterification catalyzed by immobilized Burkholderia lipase in a packed-bed bioreactor. Applied Energy, 168, pp. 340 – 350.

Wahab, A.G., 2016. Malaysia Biofuels Annual 2016 Global Agricultural Infromation [online]. Available at: https://gain.fas.usda.gov/Recent%20GAIN%20Publications/Biofuels%20Annual_Kuala%20Lumpur_Malaysia_7-27-2016.pdf [Accessed: 23 January 2018]

Wang, C., Hu, Y., Chen, Q., Lv, C. and Jia, S., 2013. Bio-oil upgrading by reactive distillation using p-toluene sulfonic acid catalyst loaded on biomass activated carbon. Biomass and Bioenergy, 56, pp. 405 – 411.

Wang, X., Liu, R., Waje, M.M., Chen, Z., Yan, Y., Bozhilov, K.N. and Feng, P., 2007. Sulfonated Ordered Mesoporous Carbon as a Stable and Highly Active Protonic Acid Catalyst. Chemistry of Materials, 19, pp. 2395 – 2397.

Xie, A., Dai, J., Chen, X., Ma, P., He, J., Li, C., Zhou, Z. and Yan, Y., 2016. Ultrahigh adsorption of typical antibiotics onto novel hierarchical porous carbons derived from renewable lignin via halloysite nanotubes-template and in-situ activation. Chemical Engineering Journal, 304, pp. 609 – 620.

Yacob, A.R., Azmi, A. and Amat, M.M.K.A., 2015. Physical and Chemical Activation Effect on Activated Carbon Prepared from Local Pineapple Waste. Applied Mechanics and Materials, 699, pp. 87 – 92.

Yoo, S.J., Lee, H., Veriansyah, B., Km, J., Kim, J. and Lee, Y., 2010. Synthesis of biodiesel from rapeseed oil using supercritical methanol with metal oxide catalysts. Bioresource Technology, 101, pp. 8686 – 8689.

Zhang, F., Fang, Z. and Wang, Y.T., 2015. Biodiesel production direct from high acid value oil with a novel magnetic carbonaceous acid. Applied Energy, 155, pp. 637 – 647.

Zhou, Y., Niu, S. and Li, J., 2016. Activity of the carbon-based heterogeneous acid catalyst derived from bamboo in esterification of oleic acid with ethanol. Energy Conversion and Management, 114, pp. 188 – 196.

Zhu, H. et al., 2006. Preparation of Biodiesel Catalyzed by Solid Super Base of Calcium Oxide and Its Refining Process. Chinese Journal of Catalysis, 27, pp. 391 – 396.

Zuo, D. et al., 2013. Sulfonic acid functionalized mesoporous SBA-15 catalysts for biodiesel production. Applied Catalysis B: Environmental, 129, pp. 342 – 350.

Appendix A

Calculation for Total Acid Density

The sample calculation of catalyst total acid density will be demonstrated by using the result obtained from **Cat_900h**.

Volume of 0.02 M HCl used = 17.55 mL

Number of mol of HCl used $= 17.55\ mL \times \frac{0.02\ mol}{L} \times \frac{1\ L}{1000\ mL}$

= 0.000351 mol

60 mL of NaOH in excess will be reacted with 0.1 g of acid catalyst and the amount of NaOH used to react with 0.1 g of acid catalyst will be calculated.

Number of mol of 60 mL 0.01 M NaOH $= 60\ mL \times \frac{0.01\ mol}{L} \times \frac{1\ L}{1000\ mL}$

= 0.000600 mol

Since 1 mol of HCl reacts with 1 mol of NaOH,

0.000351 mol of HCl had reacted with 0.000351 mol of remaining NaOH

Number of mol of NaOH reacted with 0.1 g of acid catalyst

= number of mol of 60 mL 0.01 M NaOH − number mol of remaining NaOH

= 0.000600 mol − 0.000351 mol

= 0.000249 mol

Therefore, the number of mol of acid present in the catalyst $=\frac{0.000249\ mol}{0.1\ g\ catalyst}$

= **2.49 mmol/g**

The back titration was repeated for three times and the average total acid density was calculated.

Average total acid density $= \frac{2.49+2.56+2.39}{3}$

= **2.48 mmol/g**

Appendix B

Calculation for Biodiesel Conversion

The sample calculation of FAME conversion was demonstrated by using the result obtained from Cat_900h. Table B.1 shows the results obtained from titration by using 0.1 N KOH as titrant. The calculation of FAME conversion was carried out following Equation 3.3.

Table B.1: Results obtained from titration of PFAD and FAME samples.

Sample	**Initial (mL)**	**Final (mL)**	**KOH used (mL)**
PFAD	37.6	77.0	39.4
Cat_900h	88.4	91.4	3.0

$$\%\ \text{conversion} = \frac{\left(\frac{\mathrm{V}\times \mathrm{N}\times \mathrm{MW_{KOH}}}{\mathrm{W_S}}\right)_{\mathrm{PFAD}} - \left(\frac{\mathrm{V}\times \mathrm{N}\times \mathrm{MW_{KOH}}}{\mathrm{W_S}}\right)_{\mathrm{FAME}}}{\left(\frac{\mathrm{V}\times \mathrm{N}\times \mathrm{MW_{KOH}}}{\mathrm{W_S}}\right)_{\mathrm{PFAD}}} \times 100\%$$

$$= \frac{\frac{39.4\ \mathrm{mL} \times 0.1\ \frac{\mathrm{mol}}{L} \times 56.11 \frac{\mathrm{g}}{mol}}{1\ g} - \frac{3.0\ \mathrm{mL} \times 0.1\ \frac{\mathrm{mol}}{L} \times 56.11 \frac{\mathrm{g}}{mol}}{1\ \mathrm{g}}}{\frac{39.4\ \mathrm{mL} \times 0.1\ \frac{\mathrm{mol}}{L} \times 56.11 \frac{\mathrm{g}}{mol}}{1\ g}} \times 100\%$$

= 92.38%

The titration was repeated for three times and the average FAME % conversion was calculated.

$$\text{Average \% conversion} = \frac{92.38 + 94.59 + 93.5}{3}$$

= **93.49 %**

Appendix C

Calibration Curve for Gas Chromatography Analysis

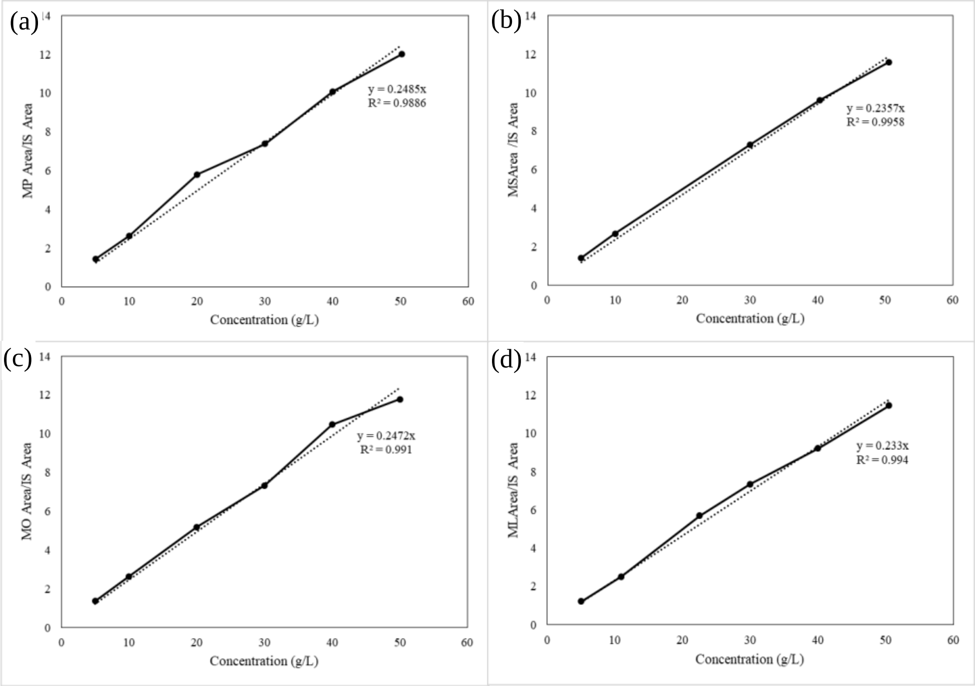

Figure C.1: Calibration curve for (a) Methyl Palmitate (MP), (b) Methyl Stearate (MS), (c) Methyl Oleate (MO) and (d) Methyl Linoleate (ML).

Appendix D

Calculation for Biodiesel Yield

The sample calculation of FAME yield was demonstrated by using the result obtained from Cat_900h. Table D.1 recorded the retention time and area of the components in biodiesel product obtained from GC. In addition, the GC Chromatogram of Cat_900h is shown in Figure D.1. The concentration of MP, MS, MO and ML in product was first calculated individually.

Table D.1: Retention time and area of Cat_900h from GC result.

Cat_900h	Methyl Heptadecanoate (IS Area)	Methyl Palmitate (MP Area)	Methyl Stearate (MS Area)	Methyl Oleate (MO Area)	Methyl Linoleate (ML Area)
Retention Time (min)	13.281	12.184	14.634	15.043	15.843
Area (μV·s)	2258.88	12799.7	949.32	8275.4	1864.8

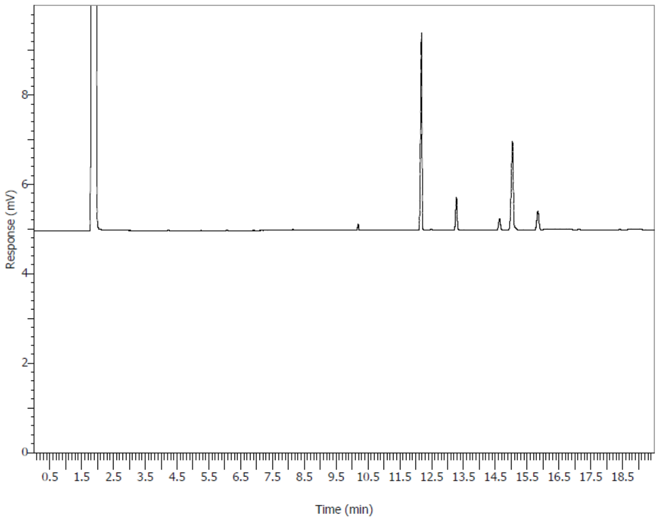

Figure D.1: GC Chromatogram of Cat_900h.

Methyl Palmitate (MP)

To calculate the concentration of MP in the sample solution prepare:

At MP Area 12799.7 µV·s,

MP Area/ IS Area $= \frac{12799.7}{2258.88}$

$= 5.6664$

At MP Area/ IS Area = 5.6664,

Concentration of MP in sample solution $= 22.8024\ \frac{\text{g MP}}{\text{L solution}}$

To calculate the concentration of MP in the product:

Concentration of product in sample solution $= 53.5\ \frac{\text{g product}}{\text{L solution}}$ solution

Concentration of MP in product

$$= \frac{\text{Concentration of MP in sample solution } (\frac{\text{g MP}}{\text{L solution}})}{\text{Concentration of product in sample solution } (\frac{\text{g product}}{\text{L solution}})}$$

$$= \frac{22.8024\ (\frac{\text{g MP}}{\text{L solution}})}{53.5(\frac{\text{g product}}{\text{L solution}})}$$

$$= \mathbf{0.4262}\ \frac{\textbf{g MP}}{\textbf{g product}}$$

Methyl Stearate (MS)

To calculate the concentration of MS in the sample solution prepare:

At MS Area 949.32 µV·s,

MS Area/ IS Area $= \frac{949.32}{2258.88}$

$= 0.4208$

At MS Area/ IS Area = 0.420864,

Concentration of MS in sample solution $= 1.7854\ \frac{\text{g MS}}{\text{L solution}}$

To calculate the concentration of MS in the product:

Concentration of product in sample solution $= 53.5\ \frac{\text{g product}}{\text{L solution}}$ solution

Concentration of MS in product

$$= \frac{\text{Concentration of MS in sample solution } (\frac{\text{g MS}}{\text{L solution}})}{\text{Concentration of product in sample solution } (\frac{\text{g product}}{\text{L solution}})}$$

$$= \frac{1.7854\ (\frac{\text{g MS}}{\text{L solution}})}{53.5(\frac{\text{g product}}{\text{L solution}})}$$

$$= \mathbf{0.0334}\ \frac{\textbf{g MS}}{\textbf{g product}}$$

Methyl Oleate (MO)

To calculate the concentration of MO in the sample solution prepare:

At MO Area 8275.4 μV·s,

MO Area/ IS Area $= \frac{8275.4}{2258.88}$

$= 3.6645$

At MO Area/ IS Area = 3.6645,

MO in sample solution $= 14.82 \frac{\text{g MO}}{\text{L solution}}$

To calculate the concentration of MO in the product:

Concentration of product in sample solution $= 53.5 \frac{\text{g product}}{\text{L solution}}$ solution

Concentration of MO in product

$$= \frac{\text{Concentration of MP in sample solution } (\frac{\text{g MO}}{\text{L solution}})}{\text{Concentration of product in sample solution } (\frac{\text{g product}}{\text{L solution}})}$$

$$= \frac{14.82\ (\frac{\text{g MO}}{\text{L solution}})}{53.5(\frac{\text{g product}}{\text{L solution}})}$$

$$= \mathbf{0.2770}\ \frac{\textbf{g MO}}{\textbf{g product}}$$

Methyl Linoleate (ML)

To calculate the concentration of ML in the sample solution prepare:

At ML Area 1864.8 μV·s,

ML Area/ IS Area $= \frac{1864.8}{2258.88}$

$= 0.8255$

At ML Area/ IS Area = 0.8255,

Concentration of ML in sample solution $= 3.5431 \frac{\text{g MS}}{\text{L solution}}$

To calculate the concentration of ML in the product:

Concentration of product in sample solution $= 53.5 \frac{\text{g product}}{\text{L solution}}$ solution

Concentration of ML in product

$$= \frac{\text{Concentration of ML in sample solution } (\frac{\text{g ML}}{\text{L solution}})}{\text{Concentration of product in sample solution } (\frac{\text{g product}}{\text{L solution}})}$$

$$= \frac{3.5431\ (\frac{\text{g ML}}{\text{L solution}})}{53.5(\frac{\text{g product}}{\text{L solution}})}$$

$$= \mathbf{0.06623}\ \frac{\textbf{g ML}}{\textbf{g product}}$$

Total concentration of ME in product, $\sum \mathrm{C_{ME}}$

= Concentration of (MP + MS + MO + ML)

= $0.4262 + 0.0334 + 0.2770 + 0.06623$

= $0.80283 \ \frac{\mathrm{g\ ME}}{\mathrm{g\ product}}$

According to Equation 3.4,

FAME Yield $= \frac{\sum \mathrm{C_{ME}} \times \mathrm{m_{product}}}{\mathrm{m_{PFAD}}} \times 100\%$

$= \frac{0.80363 \frac{\mathrm{g\ ME}}{\mathrm{g\ product}} \times 8.98\ \mathrm{g\ product}}{10\ \mathrm{g\ PFAD}} \times 100\%$

$= \mathbf{72.08}\ \%$

LIST OF PUBLICATIONS

Tang, Z.E., Lim, S., Pang, Y.L., Wong, K.H. and Ong, H.C., 2017. Synthesis of seaweed based carbon acid catalyst by thermal decomposition of ammonium sulfate for biodiesel production. Proceedings of International Symposium on Green & Sustainable Technology. 10 – 13 January 2017 Perak, Malaysia. New York: AIP Publishing, pp. 020009.

Tang, Z.E., Lim, S., Pang, Y.L., Ong, H.C. and Lee, K.T., 2018. Synthesis of biomass as heterogeneous catalyst for application in biodiesel production: State of the art and fundamental review. Renewable and Sustainable Energy Reviews, 92, pp. 235 – 253.

Tang, Z.E., Lim, S., Pang, Y.L. and Ong, H.C., 2018. Optimisation of corncob based heterogeneous acid catalysed biodiesel synthesis using response surface methodology. Proceedings of International Conference on Process Engineering and Advanced Materials. 13-14 August 2018 Kuala Lumpur, Malaysia. IOP Conference Series: Materials Science and Engineering, pp. 012082.